

# Numerical Methods for Dynamical Low-Rank Approximations of Stochastic Differential Equations

## Part I: Time discretization

Yoshihito Kazashi<sup>1</sup>, Fabio Nobile<sup>2</sup>, and Fabio Zoccolan<sup>2</sup>

<sup>1</sup>Department of Mathematics, The University of Manchester, Oxford Road, Manchester, M13 9PL, UK. email: y.kazashi@manchester.ac.uk

<sup>2</sup>Institute de Mathématiques, École Polytechnique Fédérale de Lausanne, 1015 Lausanne, Switzerland. email: fabio.nobile@epfl.ch, fabio.zoccolan@epfl.ch

### Abstract

In this work (Part I), we study three time-discretization procedures of the Dynamical Low-Rank Approximation (DLRA) of high-dimensional stochastic differential equations (SDEs). Specifically, we consider the Dynamically Orthogonal (DO) method for DLRA proposed and analyzed in [18], which consists of a linear combination of products between deterministic orthonormal modes and stochastic modes, both time-dependent. The first strategy we consider for numerical time-integration is very standard, consisting in a forward discretization in time of both deterministic and stochastic components. Its convergence is proven subject to a time-step restriction dependent on the smallest singular value of the Gram matrix associated to the stochastic modes. Under the same condition on the time-step, this smallest singular value is shown to be always positive, provided that the SDE under study is driven by a non-degenerate noise. The second and the third algorithms, on the other hand, are staggered ones, in which we alternately update the deterministic and the stochastic modes in half steps. These approaches are shown to be more stable than the first one and allow us to obtain convergence results without the aforementioned restriction on the time-step. Computational experiments support theoretical results. In this work we do not consider the discretization in probability, which will be the topic of Part II.

## 1 Introduction

Many models used in engineering applications or to model natural phenomena are described by stochastic differential equations (SDEs) [1, Chapter 5], [23, Chapter 7], [41, Chapter 5], [28]. In various situations, due to the high dimensionality of the studied physical system, their numerical simulations are computationally prohibitive. A possible solution to lower the computational burden is to exploit model order reduction (MOR) techniques.

These techniques aim to build a surrogate system of low dimensionality that is numerically inexpensive to solve. MOR methods have witnessed success when applied to problems with high nominal dimensions, yet their most relevant features evolve in a subspace of lower dimension [11, 12, 13, 34, 37, 39, 42].

Among various possible applications for SDEs, MOR techniques can be suitable in machine learning problems, such as simulations of particle dynamics for adaptive sampling of concentrated measures [43], in climate modeling [11], in stochastic models in finance, for example considering a huge basket of options described by an Heston model [34], or, more generally, in data assimilation and filtering procedures [26].

However, when applied to a given problem, not all MOR approaches can necessarily show good numerical performance a priori, and, hence, one has to also carefully choose the surrogate technique based on the known properties of the analyzed system. For instance, in the aforementioned SDE examples, fixed reduced basis methods might not always be the

best approximation strategy, as the roughness of the system can rapidly change, making it challenging to capture the behavior of the time-dependent solution with a single, fixed subspace over time.

For this reason, here we consider a Dynamical Low-Rank Approximation (DLRA) framework for SDEs [18]. In contrast with the majority of reduced order models for uncertainty quantification, DLRA aims to construct a numerical surrogate which is spanned by time-varying basis, in both the deterministic and stochastic domains. The first rigorous formalization of DLRA was proposed in [24], where its evolution was described through constraining the time derivative of the dynamics into the tangent space of a low-rank manifold. Despite being a quite new topic, DLRA has been intensively studied for ordinary differential equations [4, 24, 27, 21, 22], deterministic [3, 8, 9, 33], and random partial differential equations (rPDEs) [16, 17, 25], while in the SDE context this is still a novelty and its potential has not been fully discovered yet [18].

In general, there are several ways to instantiate the DLRA equations. One possibility is through the Dynamical Orthogonal (DO) framework, which was first proposed in [38] for rPDEs and was used in [18] to obtain a well-posed mathematical setting in the SDEs framework. Here, we propose methods for discretizing these DO equations rigorously derived in [18] to achieve an exploitable DLRA numerical solution.

The DO approach consists in building an approximation composed by two components, a deterministic basis and a stochastic one, both allowed to evolve in time and to be computed on the fly. More precisely, we are seeking a solution  $X$  made by the following linear combination of  $k$  members for any random realization  $\omega$

$$X(t, \omega) = \sum_{i=1}^k U^i(t) Y^i(t, \omega), \quad t \geq 0, \quad (1)$$

where  $\{U^i\}_{i=1,\dots,k}$  is the time-dependent deterministic modes, orthonormal according to a fixed scalar product, and  $\{Y^i\}_{i=1,\dots,k}$  is the stochastic one. One can derive a system of coupled equations for the deterministic modes and the stochastic modes from (1). This decomposition in two coupled equations is beneficial, as we can discretize both of them to obtain the DLRA via their product at every time step. Under the assumptions that will be considered in this article, well-posedness of the DO equations for SDEs is provided in [18].

The presented work on discretization for DLRA of SDEs consists in two parts. In this paper, we consider studying the approximation in time of the aforementioned setting, where all the involved stochastic quantities will be taken with respect to the measure induced by the continuous DLRA, and, hence, not approximated. We point out that employing a stochastic discretization that allows us to exactly compute the expectation of quantities of interest applies to this case, too. We refer to the second part of this work, i.e. [19], for analyzing the error introduced by an approximation of the stochastic space.

Here we will propose three algorithms for the time discretization of DLRA for SDEs. It will be shown that their numerical solutions converge over time to the continuous DLRA; hence these frameworks can be used to approximate the aforementioned phenomena. Moreover, under some conditions, their discretizations of (1) are proven to be always composed of  $k$  non-trivial components over time. This is certainly not a standard behavior in the DLRA framework for deterministic and rPDEs, where the numerical solution can blow up in finite time.

Specifically, the system of equations derived from (1) expressing the deterministic and stochastic modes is characterized by the presence of the inverse of the Gramian of  $Y(t)$ , i.e. the matrix  $C_{Y(t)} = \mathbb{E}[Y(t)Y(t)^\top]$ . This inverse is well-defined if  $Y(t)$  consists of  $k$  non-trivial components, namely if  $Y(t)$  has rank  $k$ . *If it is the case, all the singular values of  $C_{Y(t)}$  are strictly positive and we will say that also  $C_{Y(t)}$  is of rank  $k$ .* If one of these singular values was zero at a certain instant of time  $t$ , then the approximation (1) would not be well-defined in  $t$  as some of the components in (1) would be redundant. As one will see in this article, this problem is reflected in the discretization framework, too, where we need to assure that  $C_{Y_n}$ , i.e. the discretization of  $C_{Y(t)}$  at the mesh point  $t_n$ , is always of rank  $k$  for all  $n$ .

The first numerical algorithm that we propose is the *DLR Euler-Maruyama*. This consists in first discretizing the equation of the stochastic modes with a Euler-Maruyama and the one of the deterministic modes with a Forward Euler method. This method is not a direct

Euler–Maruyama discretization of the DLRA equations. Indeed, such a naive discretization would break the orthogonality of the spatial modes, which is enforced in the continuous DO equations. To preserve this property, we perform a QR decomposition at each time step to restore orthogonality, making the analysis non-standard. Nevertheless, the DLR-Euler Maruyama (DLR-EM) turns out to be convergent in time with the same rate as the standard Euler-Maruyama for SDEs. However, due to its explicit nature, a condition on the time step  $\Delta t$ , dependent on the smallest singular value of  $C_{Y_n}$ , is needed to reach this goal.

On the contrary, the other two schemes differ from the former in the update of the deterministic modes: these are calculated using the pre-orthonormalized stochastic modes just computed in the same step. What differentiates these two methods is the implementation of both drift and diffusion to compute the pre-orthogonal deterministic modes. Indeed, the second scheme uses both drift and diffusion increments to compute the deterministic modes. It turns out that this scheme can be interpreted as a projector-splitting type scheme, according to the same philosophy of what was proposed for matrix differential equations [27, 6, 5, 21] and for random PDEs [17]. For this reason, we will refer to this algorithm as *DLR Projector Splitting for Euler-Maruyama*. At every discretized time  $t_n$ , this method acts as a projection of the right-hand side of the discretized SDE into the tangent space of random vectors of rank  $k$  computed in the product between the deterministic mode and just pre-orthonormalized stochastic modes. We prove that this construction is very stable, as similar results to the ones obtained with the DLR Euler-Maruyama are still valid here without any condition on the time step. Specifically, this algorithm is not affected by the smallest singular value of the Gramian for quantifying the norm of the approximation and its convergence in time to the true solution.

Concerning the last scheme, only the drift increment is employed in the computation of the deterministic modes. The whole method resembles a piece-by-piece discretization of the SDE satisfied by the DLRA ([18, Equation (2.17)]). Indeed, the aforementioned projector into the tangent space of the intermediate point of the update is applied to the drift increment only, whereas solely a deterministic one is employed in the diffusion term. From this perspective, we call this method as the *DLR Projector Splitting for SDEs*. Similar results to the ones of the DLR Projector Splitting for Euler-Maruyama can be proven. The main difference between the two approaches concerns their stochastic discretization and it will be under study in the second part of this work [19].

Throughout this article, we will always assume a full-rank setting, i.e. our DO approximation in (1) always has to be described by at least  $k$  components over time and, hence, its Gramian always has to admit a proper inverse. It is worth mentioning that asking only for a Gramian  $C_{Y_n}$  of full-rank  $k$  does not prevent ill-conditioned discretizations a priori. Indeed, the smallest singular value of  $C_{Y_n}$  can theoretically be very close to the zero machine even if it is positive, accumulating machine errors in the computations of the deterministic and stochastic modes. Therefore, that is why it is interesting to find conditions that assure the Gramian to be strictly lower-bounded by a known positive constant. Such questions will also be investigated in this paper.

In Section 2, we illustrate the general framework needed to obtain the well-posedness of DLRA for SDEs, which is the same setting that we will consider throughout this work. In Section 3, the two discretization algorithms will be introduced. Sections 4, 5 and 6 are centred at demonstrating properties of convergence in time of the three schemes; more specifically, mean-square stability, non-degeneracy of the Gramian under non-degenerate diffusion, and convergence in time. These results will be confirmed via numerical experiments in Section 7. Finally, we will draw the conclusion in Section 8.

## 2 General Setting of DLRA for SDEs

In this section, we will briefly introduce the general theoretical framework for continuous DLRA for SDEs. More precisely, we will state the DO equations for DLRA of SDEs as derived in [18] and recall sufficient conditions that ensure the existence and uniqueness of a DO solution. Under these constraints, it is worth studying numerical time discretization schemes to find approximate solutions of the DO equations.

Let  $(\Omega, \mathcal{F}, \mathbb{P}, (\mathcal{F}_t)_{t \geq 0})$  be a filtered complete probability space with the usual conditions [40, Remark 6.24]. We denote by  $W$  a real  $m$ -dimensional  $(\mathcal{F}_t)$ -Brownian motion, i.e.,

$W(t) = (W_1(t), \dots, W_m(t))^\top$ . We want to approximate SDEs taking values in  $\mathbb{R}^d$  of the following type

$$dX^{\text{true}}(t) = a(t, X^{\text{true}}(t))dt + b(t, X^{\text{true}}(t))dW_t, \quad \text{for all } t \in [0, T], \quad X^{\text{true}}(0) = X_0^{\text{true}}, \quad (2)$$

where  $T > 0$ . The solution of (2) is a random vector  $X^{\text{true}}(t) = (X_1^{\text{true}}(t), \dots, X_d^{\text{true}}(t))^\top$ . We work under the following assumptions.

**Assumption 1** (Lipschitz coefficients). *The drift  $a: [0, \infty) \times \mathbb{R}^d \rightarrow \mathbb{R}^d$  and the diffusion  $b: [0, \infty) \times \mathbb{R}^d \rightarrow \mathbb{R}^{d \times m}$  are measurable between the Borel fields  $([0, \infty) \times \mathbb{R}^d; \mathcal{B}([0, \infty) \times \mathbb{R}^d))$  and  $(\mathbb{R}^d; \mathcal{B}(\mathbb{R}^d)), (\mathbb{R}^{d \times m}; \mathcal{B}(\mathbb{R}^{d \times m}))$ , respectively, and Lipschitz continuous with respect to the second variable, uniformly in the first one:*

$$\begin{cases} |a(s, x) - a(s, y)| \leq C_{\text{Lip}}|x - y|, & \text{for all } x, y \in \mathbb{R}^d, s \in [0, \infty), \\ \|b(s, x) - b(s, y)\|_{\text{F}} \leq C_{\text{Lip}}|x - y|, & \text{for all } x, y \in \mathbb{R}^d, s \in [0, \infty), \end{cases} \quad (3)$$

for some constant  $C_{\text{Lip}} > 0$ , where  $|\cdot|$  and  $\|\cdot\|_{\text{F}}$  are the usual Euclidean norm on  $\mathbb{R}^d$  and the Frobenius one on  $\mathbb{R}^{d \times m}$ , respectively.

**Assumption 2** (Linear growth bound). *The drift  $a$  and the diffusion  $b$  fulfil the following linear-growth bound condition:*

$$|a(s, x)|^2 + \|b(s, x)\|_{\text{F}}^2 \leq C_{\text{lgb}}(1 + |x|^2), \quad \text{for all } x \in \mathbb{R}^d, s \in [0, \infty) \quad (4)$$

for some constant  $C_{\text{lgb}} > 0$ .

Furthermore, we assume that the initial condition  $X_0^{\text{true}}$  in (2) satisfies the following:

**Assumption 3** (Square integrable initial condition).

$$X_0^{\text{true}} \text{ is } \mathcal{F}_0\text{-measurable and satisfies } \mathbb{E}[|X_0^{\text{true}}|^2] < +\infty. \quad (5)$$

Under Assumptions 1-3, equation (2) has a unique strong solution; see for example [40, Theorem 21.13].

In what follows, we say that a process  $\{X(t)\}_{t \in [0, T]}$  is of rank  $k$  if the matrix  $\mathbb{E}[X(t)X(t)^\top]$  is of rank  $k$  for all  $t \in [0, T]$ . In order to ensure that the DLRA provides an effective way of approximating the stochastic dynamics described by (2), we suppose further that (2) exhibits a nearly low-rank structure at each time instant.

As discussed in [18], approximating  $X^{\text{true}}$  with a rank- $k$  DO approximation  $X$  consists of finding a pair  $(U, Y)$  satisfying the following conditions. The function  $U: [0, T] \rightarrow \mathbb{R}^{k \times d}$  is a deterministic absolutely continuous matrix-valued function such that  $U_0U_0^\top = I_{k \times k}$  and  $U(t)\dot{U}(t)^\top = 0$  for all  $t$  (which implies that  $U(t)U(t)^\top = I_{k \times k}$  for all  $t$ ), and  $Y: [0, T] \rightarrow L^2(\Omega; \mathbb{R}^k)$  is an adapted stochastic process of almost surely continuous paths with  $Y^1(t), \dots, Y^k(t)$  linearly independent in  $L^2(\Omega)$ . The rank- $k$  DO approximation is then  $X(t) = U(t)^\top Y(t)$  for all  $t$ . The  $(U, Y)$  pair satisfies the following system, called the DO equations [18, 38],

$$\begin{aligned} C_{Y(t)}\dot{U}(t) &= \mathbb{E}[Y(t)a(t, U(t)^\top Y(t))^\top] \left( I_{d \times d} - P_{U(t)}^{\text{row}} \right), \\ Y(t) &= Y_0 + \int_0^t U(s)a(s, U(s)^\top Y(s))ds + \int_0^t U(s)b(s, U(s)^\top Y(s))dW_s, \end{aligned} \quad (6)$$

where  $C_{Y(t)} := \mathbb{E}[Y(t)Y(t)^\top]$  is the Gramian associated to  $Y^1, \dots, Y^k$ ,  $P_{U(t)}^{\text{row}} := U(t)^\top U(t)$  is the projector-matrix onto the vector space  $\text{span}\{U^1(t), \dots, U^k(t)\} \subset \mathbb{R}^d$ , with  $U^i(t)$  the  $i$ -th row of  $U(t)$ , and  $U_0^\top Y_0$  is a suitable rank- $k$  approximation of  $X_0^{\text{true}}$ . Under Assumptions 1-3, equation (6) admits a unique strong DO solution  $(U, Y)$ , at least for short times, if  $X_0^{\text{true}}$  has rank greater than or equal to  $k$  [18]. See [18] for more details on such DLR approximation.

## 2.1 General Notation

For the sake of clarity, we list here the most used notation throughout the document. Consider a vector  $v \in \mathbb{R}^m$ , then  $|v|$  denotes the Euclidean norm of  $v$ . Consider a matrix  $A \in \mathbb{R}^{m \times n}$ , then  $|A|$  and  $\|A\|_F$  denote its spectral and Frobenius norm, respectively. Henceforth, the notation  $A \succ B$  (respectively  $A \succeq B$ ) with  $A, B$  square matrices means that  $A - B$  is positive definite (respectively positive semi-definite). Moreover,  $\{\sigma_i(A)\}_{i \geq 1}^{\min\{n,m\}}$  denote the largest singular values of the matrix  $A$ , whereas  $\{\lambda_i(A)\}_{i \geq 1}$  denotes the eigenvalues of  $A$ , whenever  $A$  is a squared matrix, whereas  $\lambda_{\max}(A)$  and  $\sigma_{\max}(A)$  denote the largest eigenvalue and singular value, respectively. Finally, we will say that a process  $Z \in L^2(\Omega, \mathbb{R}^d)$  is of rank  $k$  if  $\text{rank}(\mathbb{E}[ZZ^\top]) = k$  (for more details see e.g. [18, Section 2.2]).

## 3 Time integration schemes

In this section, we introduce three time-integration schemes to compute the DLRA solution  $X(t) = U^\top(t)Y(t)$ . Concretely, considering a partition  $\Delta := \{t_n : 0 = t_0 < t_1 < \dots < t_{N-1} < t_N = T\}$  of  $[0, T]$ , we seek suitable approximations  $(U_n)_n$ ,  $(Y_n)_n$  of  $(U(t_n))_n$  and  $(Y(t_n))_n$ , respectively, and reconstruct afterwards an approximate DLRA solution  $X_n = U_n^\top Y_n \approx X(t_n)$ .

In Section 3.1 we present the DLR Euler–Maruyama algorithm, which employs a forward discretization of both  $U$  and  $Y$ , whereas in Section 3.2 and in Section 3.3 we proposed two extensions to the SDE setting of the DLR projector splitting scheme [27, 17], which updates  $U$  and  $Y$  in a staggered way.

### 3.1 DLR Euler–Maruyama discretization

The DO equations (6) are a system of stochastic differential equations. In this section, we consider the most basic discretization method for such equations: the Euler–Maruyama scheme, which reads: given  $(U_n, Y_n)$ ,

$$\text{find } C_{Y_n} \tilde{U}_{n+1} = C_{Y_n} U_n + \mathbb{E}[Y_n a(t_n, U_n^\top Y_n)^\top] (I_{d \times d} - P_{U_n}^{\text{row}}) \Delta t_n, \quad (7)$$

$$\tilde{Y}_{n+1} = Y_n + U_n a(t_n, U_n^\top Y_n) \Delta t_n + U_n b(t_n, U_n^\top Y_n) \Delta W_n, \quad (8)$$

$$\text{compute } (U_{n+1}, Y_{n+1}) : \tilde{U}_{n+1}^\top \tilde{Y}_{n+1} = U_{n+1}^\top Y_{n+1}, \quad U_{n+1} U_{n+1}^\top = I_{d \times d}. \quad (9)$$

with  $C_{Y_n} := \mathbb{E}[Y_n Y_n^\top]$ ,  $\Delta t_n := t_{n+1} - t_n$ ,  $\Delta W_n := W(t_{n+1}) - W(t_n) \sim \mathcal{N}(0, \Delta t_n I_{m \times m})$ , and  $\mathbb{E}[\Delta W_n | \mathcal{F}_{t_n}] = 0$  for all  $n$ . In the continuous DO framework of equations (6) the deterministic modes  $U(t)$  have orthogonal rows for all  $t \in [0, T]$ . To be consistent with this continuous setting, in (9) we orthonormalize the computed deterministic modes  $\tilde{U}_{n+1}$  through a QR decomposition. We summarize the whole discretization procedure in Algorithm 1. We point out that in Algorithm 1, as well as in the other algorithms of this paper, the QR decomposition works as follows: for all rectangular matrices  $A \in \mathbb{R}^{n \times k}$  one has  $(Q, R) = \text{QR}(A)$  with  $Q \in \mathbb{R}^{n \times k}$  with orthogonal columns and  $R \in \mathbb{R}^{k \times k}$ .

We assume hereafter that  $C_{Y_n}$  remains of full rank for all  $n$ . Sufficient conditions for this assumption are discussed in Section 4. Then, the scheme (7) can be rewritten as

$$\begin{aligned} \tilde{U}_{n+1} &= U_n + C_{Y_n}^{-1} \mathbb{E}[Y_n a(t_n, U_n^\top Y_n)^\top] (I_{d \times d} - P_{U_n}^{\text{row}}) \Delta t_n, \\ \tilde{Y}_{n+1} &= Y_n + U_n a(t_n, U_n^\top Y_n) \Delta t_n + U_n b(t_n, U_n^\top Y_n) \Delta W_n. \end{aligned} \quad (10)$$

**Remark 3.1** (Well posedness of equation (7)). *Observe that the system (7) has a solution even if  $C_{Y_n}$  is singular, since the right-hand side is always in the range of  $C_{Y_n}$ , which includes the span $\{Y_n(\omega), \omega \in \Omega\} \subset \mathbb{R}^k$ . Indeed, the stochastic basis can be rewritten as  $Y_n(\omega) = C_{Y_n}^{\frac{1}{2}} \tilde{Y}_n(\omega)$ , with  $\mathbb{E}[\tilde{Y}_n \tilde{Y}_n^\top] = \text{diag}(\tilde{\sigma}_n^i)$  with  $\tilde{\sigma}_n^i = 1$  or  $0$ , and, hence,  $\text{span}\{Y_n(\omega), \omega \in \Omega\} \subseteq \text{Ran}(C_{Y_n})$ .*

In view of Remark (3.1), a numerical solution, for instance that of minimal norm, can be defined also if  $C_{Y_n}$  is singular. However, our error analysis indicates that constants in the error estimate may deteriorate when the smallest eigenvalue of  $C_{Y_n}$  tends to zero. For non-degenerate noise we will show that a stringent condition on the time step assures  $C_{Y_n}$  to remain full-rank for all time steps, although, the constant in the error estimate may still be

---

**Algorithm 1** DLR Euler–Maruyama approximation for SDEs

---

**Input:** initial data  $U_0, Y_0$ .  
**Output:** approximation  $\{X_n = U_n^\top Y_n\}_{n=0,\dots,N}$ .

```

1: for all  $n \in \{0, \dots, N-1\}$  do
2:   Generate a Brownian increment  $\Delta W_n \sim \mathcal{N}(0, \Delta t_n I_{m \times m})$ 
3:   Assemble  $C_{Y_n} = \mathbb{E}[Y_n Y_n^\top]$ 
4:   Compute  $\tilde{Y}_{n+1} = Y_n + U_n a(t_n, U_n^\top Y_n) \Delta t_n + U_n b(t_n, U_n^\top Y_n) \Delta W_n$ 
5:   Compute  $C_{Y_n} \tilde{U}_{n+1} = C_{Y_n} U_n + \mathbb{E}[Y_n a(t_n, U_n^\top Y_n)^\top] (I_{d \times d} - P_{U_n}^{\text{row}}) \Delta t_n$ 
6:   Reorthonormalize the deterministic modes: find  $(U_{n+1}, Y_{n+1})$  such that:

```

$$U_{n+1}^\top Y_{n+1} = \tilde{U}_{n+1}^\top \tilde{Y}_{n+1}, \quad U_{n+1} U_{n+1}^\top = I_{d \times d}.$$

with  $(U_{n+1}^\top, R) = \text{QR}(\tilde{U}_{n+1}^\top)$  and  $Y_{n+1} = R \tilde{Y}_{n+1}$ .

```
7: end for
```

---

very large for small singular values. In Section 4, we will analyze the numerical properties of this algorithm in detail.

The main interests of this method are the ease of implementation and low computational cost. For instance, in the case of a linear deterministic drift  $a(t, x) = A(t)x$ , which appears in various practical applications including the Kalman-Bucy Filter [26] or the Heston model [34], the algorithm significantly simplifies. Indeed, since in this case the inverse Gramian matrix  $C_{Y_n}^{-1}$  can be simplified in (10), the update of the deterministic modes becomes simply

$$\tilde{U}_{n+1} = U_n + U_n^\top A^\top(t_n) (I_{d \times d} - P_{U_n}^{\text{row}}) \Delta t_n. \quad (11)$$

This also means that a possible ill-conditioning of  $C_{Y_n}$  does not affect the numerical scheme. Moreover, the deterministic modes can be evolved completely independently of the stochastic modes, leading to parallelization opportunities.

### 3.2 DLR Projector Splitting for Euler-Maruyama (EM)

Here we present a numerical method for DLRA that is as cheap to compute as Algorithm 1, yet whose accuracy and stability are less sensitive to the smallest singular value of the Gramian of  $Y_n$  than Algorithm 1. This algorithm (as well as Algorithm 3) can be reinterpreted as a projector splitting approximation, similar to the one proposed for rPDEs (see [17, Section 4.4] for more details), which itself was inspired by the procedure presented in [27]. The name of the scheme is motivated by this reason.

The idea of the projector splitting scheme in [17] is to sequentially perform the projections onto the spaces spanned by the deterministic and stochastic modes: first, the stochastic modes are updated at step  $n$  projecting the equations on the deterministic modes  $U_n$ , and then the deterministic modes are updated projecting the equations on the newly computed stochastic modes. In both steps, we still approximate the drift and diffusion in a forward-Euler way. We remark that in [17] other approximations of implicit or semi-implicit type are considered as well.

This procedure leads to the same update as in Algorithm 1 for the stochastic modes  $\tilde{Y}_{n+1}$

$$\tilde{Y}_{n+1} = Y_n + U_n a(t_n, U_n^\top Y_n) \Delta t_n + U_n b(t_n, U_n^\top Y_n) \Delta W_n. \quad (12)$$

while providing an alternative update for the deterministic modes  $\tilde{U}_{n+1}$ :

$$C_{\tilde{Y}_{n+1}} \tilde{U}_{n+1} = C_{\tilde{Y}_{n+1}} U_n + \mathbb{E} \left[ \tilde{Y}_{n+1} (a(t_n, U_n^\top Y_n)^\top \Delta t_n + (\Delta W_n)^\top b(t_n, U_n^\top Y_n)^\top) \right] (I_{d \times d} - P_{U_n}^{\text{row}}). \quad (13)$$

Then the final update  $(U_{n+1}, Y_{n+1})$  at the  $n$ -th step is obtained by QR orthonormalization. Notice the presence of the diffusion term inside the expectation in (13) which does not appear in Algorithm 1, where the projection is done with respect to the old modes  $Y_n$ , causing that term to vanish. The final projector-splitting scheme that we consider is summarized in Algorithm 2.

---

**Algorithm 2** DLR Projector Splitting for Euler-Maruyama approximation for SDEs

---

**Input:** initial data  $U_0, Y_0$ .

**Output:** approximation  $\{X_n = U_n^\top Y_n\}_{n=0,\dots,N}$ .

1: **for all**  $n \in \{0, \dots, N-1\}$  **do**

2:    Generate a Brownian increment  $\Delta W_n \sim \mathcal{N}(0, \Delta t_n I_{m \times m})$ .

3:    Compute  $\tilde{Y}_{n+1} = Y_n + U_n a(t_n, U_n^\top Y_n) \Delta t_n + U_n b(t_n, U_n^\top Y_n) \Delta W_n$

4:    Assemble  $C_{\tilde{Y}_{n+1}} = \mathbb{E}[\tilde{Y}_{n+1} \tilde{Y}_{n+1}^\top]$

5:    Compute  $\tilde{U}_{n+1}$ :

$$C_{\tilde{Y}_{n+1}} \tilde{U}_{n+1} = C_{\tilde{Y}_{n+1}} U_n + \mathbb{E} \left[ \tilde{Y}_{n+1} (a(t_n, U_n^\top Y_n)^\top \Delta t_n + (\Delta W_n)^\top b(t_n, U_n^\top Y_n)^\top) \right] (I_{d \times d} - P_{U_n}^{\text{row}})$$

6:    Reorthonormalize the deterministic modes: find  $(U_{n+1}, Y_{n+1})$  such that:

$$U_{n+1}^\top Y_{n+1} = \tilde{U}_{n+1}^\top \tilde{Y}_{n+1}, \quad U_{n+1} U_{n+1}^\top = I_{d \times d}.$$

with  $(U_{n+1}^\top, R) = \text{QR}(\tilde{U}_{n+1}^\top)$  and  $Y_{n+1} = R \tilde{Y}_{n+1}$ .

7: **end for**

---

This procedure indeed yields a projected scheme. To see this, first define the following orthogonal projectors  $P_{U_n}^{\text{row}}[\cdot] = U_n^\top U_n \cdot$  and  $P_{\tilde{Y}_{n+1}}[\cdot] = \mathbb{E}[\cdot \tilde{Y}_{n+1}^\top] C_{\tilde{Y}_{n+1}}^{-1} \tilde{Y}_{n+1}$ , which project, respectively, onto the span of the rows of  $U_n$  and onto the span of the components of  $\tilde{Y}_{n+1}$ . Then we can define the operator  $P_{U_n^\top \tilde{Y}_{n+1}} : L^2(\Omega; \mathbb{R}^d) \rightarrow L^2(\Omega; \mathbb{R}^d)$  as the following:

$$P_{U_n^\top \tilde{Y}_{n+1}}[\cdot] = (I_{d \times d} - P_{U_n}^{\text{row}}) P_{\tilde{Y}_{n+1}}[\cdot] + P_{U_n}^{\text{row}}[\cdot]. \quad (14)$$

It is easy to see that (14) is a linear, idempotent and symmetric operator, as such  $P_{U_n^\top \tilde{Y}_{n+1}}$  is an orthogonal projector. If we multiply (13) by (12), we obtain

$$\begin{aligned} X_{n+1} &= U_{n+1}^\top Y_{n+1} = \tilde{U}_{n+1}^\top \tilde{Y}_{n+1} \\ &= \left( U_n + C_{\tilde{Y}_{n+1}}^{-1} \mathbb{E} \left[ \tilde{Y}_{n+1} (a(t_n, U_n^\top Y_n)^\top \Delta t_n + (\Delta W_n)^\top b(t_n, U_n^\top Y_n)^\top) \right] (I_{d \times d} - P_{U_n}^{\text{row}}) \right)^\top. \\ &= (Y_n + U_n a(t_n, U_n^\top Y_n) \Delta t_n + U_n b(t_n, U_n^\top Y_n) \Delta W_n) \\ &= X_n + (I_{d \times d} - P_{U_n}^{\text{row}}) \mathbb{E} \left[ (a(t_n, U_n^\top Y_n) \Delta t_n + b(t_n, U_n^\top Y_n) \Delta W_n) \tilde{Y}_{n+1}^\top \right] C_{\tilde{Y}_{n+1}}^{-1} \tilde{Y}_{n+1} \\ &\quad + U_n^\top U_n a(t_n, U_n^\top Y_n) \Delta t_n + U_n^\top U_n b(t_n, U_n^\top Y_n) \Delta W_n \\ &= X_n + (I_{d \times d} - P_{U_n}^{\text{row}}) \mathbb{E} \left[ (a_n \Delta t_n + b_n \Delta W_n) \tilde{Y}_{n+1}^\top \right] C_{\tilde{Y}_{n+1}}^{-1} \tilde{Y}_{n+1} + U_n^\top U_n a_n \Delta t_n + U_n^\top U_n b_n \Delta W_n \\ &= X_n + \underbrace{\left( (I_{d \times d} - P_{U_n}^{\text{row}}) P_{\tilde{Y}_{n+1}} + P_{U_n}^{\text{row}} \right)}_{P_{U_n^\top \tilde{Y}_{n+1}}} [a_n \Delta t_n + b_n \Delta W_n] \\ &= X_n + P_{U_n^\top \tilde{Y}_{n+1}} [a_n \Delta t_n + b_n \Delta W_n], \end{aligned} \quad (15)$$

where we have used the shorthand notation  $a_n = a(t_n, U_n^\top Y_n)$ ,  $b_n = b(t_n, U_n^\top Y_n)$ . Consider the forward Euler approximation of the original SDE

$$X_{n+1}^{\text{FE}} = X_n^{\text{FE}} + a(t_n, X_n^{\text{FE}}) \Delta t_n + b(t_n, X_n^{\text{FE}}) \Delta W_n. \quad (16)$$

Then, the update of the projector splitting method in Algorithm 2 is given by projecting the Euler-Maruyama increment  $a(t_n, X_n) \Delta t_n + b(t_n, X_n) \Delta W_n$  of the studied SDE, i.e. equation (16) using the projector  $P_{U_n^\top \tilde{Y}_{n+1}}$  and adding it to the initial point  $X_n$ .

This nature of projected scheme will turn out to be favorable for numerical properties, as we will see in Section 5. More precisely, the operator  $P_{U_n^\top \tilde{Y}_{n+1}}$  corresponds to the orthogonal projector onto the tangent space of the manifold of rank- $k$  random vectors at the

intermediate point  $U_n^\top \tilde{Y}_{n+1}$ , see e.g. [10, 31] for more details on the topic. Thanks to its projected structure, the error estimates do not depend on the smallest singular values of the Gramian, unlike the DLR Euler-Maruyama.

To conclude this section, we provide a technical lemma that will be useful for later computations.

**Lemma 3.2** (Auxiliary result for DLR PS EM computations). *Let  $X_n = U_n^\top Y_n$ ,  $n = 0, \dots, N$  be the solution produced by Algorithm 2 with an arbitrary step-size  $\Delta t_n$  such that  $\sum_{n=1}^N \Delta t_n = T$ . Then, the following relations hold:*

$$\mathbb{E}[|X_{n+1}|^2] \leq \mathbb{E}[|X_n|^2] + 2\mathbb{E}[X_n^\top a_n] \Delta t_n + \mathbb{E}[|a_n|^2] (\Delta t_n)^2 + \mathbb{E}[|b_n|^2] \Delta t$$

and

$$\mathbb{E}[|X_{n+1} - X_n|^2] \leq \mathbb{E}[|a_n|^2] (\Delta t_n)^2 + \mathbb{E}[|b_n|^2] \Delta t.$$

*Proof.* First, let us recall that  $P_{U_n^\top \tilde{Y}_{n+1}} : L^2(\Omega, \mathbb{R}^d) \rightarrow L^2(\Omega, \mathbb{R}^d)$ , defined in (15), is an orthogonal projector for all  $n$ . Via expression (15), one has that

$$\begin{aligned} X_{n+1} &= X_n + P_{U_n^\top \tilde{Y}_{n+1}}[a_n \Delta t_n + b_n \Delta W_n] \\ &= X_n + (I_{d \times d} - P_{U_n}^{\text{row}}) \mathbb{E}[(a_n \Delta t_n + b_n \Delta W_n) \tilde{Y}_{n+1}^\top] C_{\tilde{Y}_{n+1}}^{-1} \tilde{Y}_{n+1} \\ &\quad + P_{U_n}^{\text{row}} a_n \Delta t_n + P_{U_n}^{\text{row}} b_n \Delta W_n. \end{aligned}$$

Therefore the second moment of  $X_n$  reads as

$$\begin{aligned} \mathbb{E}[|X_{n+1}|^2] &= \mathbb{E}[|X_n + (I_{d \times d} - P_{U_n}^{\text{row}}) \mathbb{E}[(a_n \Delta t_n + b_n \Delta W_n) \tilde{Y}_{n+1}^\top] C_{\tilde{Y}_{n+1}}^{-1} \tilde{Y}_{n+1} + P_{U_n}^{\text{row}} a_n \Delta t_n + P_{U_n}^{\text{row}} b_n \Delta W_n|^2] \\ &= \mathbb{E}[|X_n|^2] + 2\mathbb{E}[X_n^\top a_n] \Delta t_n + 2\mathbb{E}[X_n^\top b_n \Delta W_n] + \mathbb{E}[|P_{U_n^\top \tilde{Y}_{n+1}}[a_n \Delta t_n + b_n \Delta W_n]|^2] \\ &= \mathbb{E}[|X_n|^2] + 2\mathbb{E}[X_n^\top a_n] \Delta t_n + \mathbb{E}[|P_{U_n^\top \tilde{Y}_{n+1}}[a_n \Delta t_n + b_n \Delta W_n]|^2], \end{aligned}$$

where in the second line we used the orthonormality of the columns of  $U_n$  and in the last line we exploited the properties of Brownian increments.

Using the property of the orthogonal projector of  $P_{U_n^\top \tilde{Y}_{n+1}}$  in  $L^2(\Omega, \mathbb{R}^d)$  and the properties of Brownian increments, finally one has

$$\mathbb{E}[|X_{n+1}|^2] \leq \mathbb{E}[|X_n|^2] + 2\mathbb{E}[X_n^\top a_n] \Delta t_n + \mathbb{E}[|a_n|^2] (\Delta t_n)^2 + \mathbb{E}[|b_n|^2] \Delta t.$$

Concerning the second bound, likewise one has that

$$\begin{aligned} \mathbb{E}[|X_{n+1} - X_n|^2] &= \mathbb{E}[|P_{U_n^\top \tilde{Y}_{n+1}}[(a_n \Delta t_n + b_n \Delta W_n)]|^2] \\ &\leq \mathbb{E}[|a_n|^2] (\Delta t_n)^2 + \mathbb{E}[|b_n|^2] \Delta t. \end{aligned}$$

□

### 3.3 DLR Projector Splitting for SDEs

Similarly to what was done in Section 3.2, here we first update the stochastic modes using the deterministic modes  $U_n$ , and then we build the new deterministic mode using the newly computed stochastic modes. However, here the expectation present in the equation of the  $U_n$  involves only the drift terms. Then, this strategy applied to (6) leads to the scheme

$$\begin{aligned} \tilde{Y}_{n+1} &= Y_n + U_n a(t_n, U_n^\top Y_n) \Delta t_n + U_n b(t_n, U_n^\top Y_n) \Delta W_n \\ C_{\tilde{Y}_{n+1}} \tilde{U}_{n+1} &= C_{\tilde{Y}_{n+1}} U_n + \mathbb{E}[\tilde{Y}_{n+1} a(t_n, U_n^\top Y_n)^\top \Delta t_n] (I_{d \times d} - P_{U_n}^{\text{row}}) \end{aligned} \tag{17}$$

Recall that the DLR Projector Splitting for EM algorithm discussed in the previous section can be viewed as a projected method; see (15). Following a similar line of reasoning,

(17) can also be interpreted as a projected method:

$$\begin{aligned}
X_{n+1} &= U_{n+1}^\top Y_{n+1} \\
&= \tilde{U}_{n+1}^\top \tilde{Y}_{n+1} = X_n + \left( (I_{d \times d} - P_{U_n}^{\text{row}}) P_{\tilde{Y}_{n+1}} + P_{U_n}^{\text{row}} \right) [a_n] + \Delta t_n + P_{U_n}^{\text{row}} [b_n] \Delta W_n \\
&= X_n + P_{U_n^\top \tilde{Y}_{n+1}} [a_n] \Delta t_n + P_{U_n}^{\text{row}} [b_n] \Delta W_n.
\end{aligned} \tag{18}$$

This form mirrors the continuous DLRA formulation for SDEs (see equation (6) and [18, Equation (2.17)]); where, the diffusion term  $b$  is projected only onto the subspace spanned by the deterministic modes, unlike (15). Algorithm 3 summarizes the whole procedure.

---

**Algorithm 3** DLR Projector Splitting for SDEs

---

**Input:** initial data  $U_0, Y_0$ .

**Output:** approximation  $\{X_n = U_n^\top Y_n\}_{n=0,\dots,N}$ .

- 1: **for all**  $n \in \{0, \dots, N-1\}$  **do**
- 2:   Generate a Brownian increment  $\Delta W_n \sim \mathcal{N}(0, \Delta t_n I_{m \times m})$ .
- 3:   Compute  $\tilde{Y}_{n+1} = Y_n + U_n a(t_n, U_n^\top Y_n) \Delta t_n + U_n b(t_n, U_n^\top Y_n) \Delta W_n$
- 4:   Assemble  $C_{\tilde{Y}_{n+1}} = \mathbb{E}[\tilde{Y}_{n+1} \tilde{Y}_{n+1}^\top]$
- 5:   Compute  $\tilde{U}_{n+1}$ :

$$C_{\tilde{Y}_{n+1}} \tilde{U}_{n+1} = C_{\tilde{Y}_{n+1}} U_n + \mathbb{E} \left[ \tilde{Y}_{n+1} (a(t_n, U_n^\top Y_n)^\top) \right] (I_{d \times d} - P_{U_n}^{\text{row}}) \Delta t_n$$

- 6:   Reorthonormalize the deterministic modes: find  $(U_{n+1}, Y_{n+1})$  such that:

$$U_{n+1}^\top Y_{n+1} = \tilde{U}_{n+1}^\top \tilde{Y}_{n+1}, \quad U_{n+1} U_{n+1}^\top = I_{d \times d}.$$

with  $(U_{n+1}^\top, R) = \text{QR}(\tilde{U}_{n+1}^\top)$  and  $Y_{n+1} = R \tilde{Y}_{n+1}$ .

- 7: **end for**

---

Using the fact that it is a projected scheme, all the numerical results concerning Algorithm 3 presented here can be derived in a similar way to those described for Algorithm 2. Indeed, this procedure will present similar stability of Algorithm 2 and we will manage to derive a slightly better theoretical accuracy result independent of  $\sigma_k$  than Algorithm 2 in the framework of time discretization. However, the main difference between the two projected schemes will arise when dealing with the discretization of the stochastic space (see [19] for more details). In this light, in Section 6, we will briefly present only the statements of the corresponding results.

**Remark 3.3** (Independence of the choice of solution for Projector Splitting schemes). *As previously pointed out, the equation for the deterministic basis  $\tilde{U}_{n+1}$  in equations (8), (13), and (18) does always have a solution, even when dealing with a singular Gramian, by choosing, for instance, the one of minimal norm. In the case of the two Projector Splitting algorithms, this choice does not change the ambient solution  $X_n$ . Indeed, in (13), and (18), any possible deterministic basis solution is of the type*

$$\hat{\tilde{U}}_{n+1} = \tilde{U}_{n+1} + N,$$

where  $\hat{\tilde{U}}_{n+1}$  is the minimal norm solution obtained, e.g. for the DLR Projector Splitting for SDEs, through the equation

$$\tilde{U}_{n+1} = U_n + C_{\tilde{Y}_{n+1}}^\dagger \mathbb{E} \left[ \tilde{Y}_{n+1} (a(t_n, U_n^\top Y_n)^\top) \right] (I_{d \times d} - P_{U_n}^{\text{row}}) \Delta t_n,$$

where  $C_{\tilde{Y}_{n+1}}^\dagger$  is the pseudoinverse of  $C_{\tilde{Y}_{n+1}}$ , and  $N \in \mathbb{R}^{k \times d}$  is a matrix whose range belongs to the null space of  $C_{\tilde{Y}_{n+1}}$ . Since,  $C_{\tilde{Y}_{n+1}}$  is symmetric, then one has

$$\hat{\tilde{U}}_{n+1}^\top \tilde{Y}_{n+1} = \tilde{U}_{n+1}^\top \tilde{Y}_{n+1} + N^\top \tilde{Y}_{n+1} = \tilde{U}_{n+1}^\top \tilde{Y}_{n+1} = X_{n+1},$$

which implies that  $X_{n+1}$  is independent of the choice of  $N$ . This is not the case for Algorithm 1, as any deterministic basis is of the type  $\widehat{\tilde{U}}_{n+1} = \tilde{U}_{n+1} + N$ , with  $N \in \mathbb{R}^{k \times d}$  in the null space of  $C_{Y_n}$ , and,

$$\widehat{\tilde{U}}_{n+1}^\top \tilde{Y}_{n+1} = \tilde{U}_{n+1}^\top \tilde{Y}_{n+1} + N^\top \tilde{Y}_{n+1} \neq \tilde{U}_{n+1}^\top \tilde{Y}_{n+1}.$$

## 4 Convergence of the DLR Euler-Maruyama

We now derive error estimates. We begin with the DLR Euler-Maruyama scheme described in Algorithm 1 and defer the analysis of the DLR Projector Splitting for EM scheme (Algorithm 2) and of the DLR Projector Splitting for SDEs (Algorithm 3), to Section 5 and 6, respectively. The main results of this section are Theorems 4.7 and 4.10.

Our convergence analysis relies on the formulation (10) for the update of the deterministic modes, for which we need to ensure that the Gramian of the stochastic modes  $C_{Y_n}$  is invertible at each time step. For this purpose, we first assume invertibility of the Gramian associated to the initial condition.

**Assumption 4** (Invertibility of  $C_{Y_0}$ ). *Given  $Y_0 \in L^2(\Omega, \mathbb{R}^k)$ , we have that  $\sigma_0 := \min_{i=1,\dots,k} \sigma_i(C_{Y_0}) > 0$ , where  $C_{Y_0} = \mathbb{E}[Y_0 Y_0^\top]$ .*

Assumption (4) will be considered to hold from now on. In this case, we trivially have  $C_{Y_0} = \mathbb{E}[Y_0 Y_0^\top] \succeq \sigma_0 \cdot I_{k \times k} \succ 0$ .

A first ingredient we need for convergence analysis is given by Proposition 4.1, which shows invertibility of  $C_{Y_n}$  for all  $n$  without any condition on the time step, provided the noise satisfies uniform ellipticity (see Assumption 5 below). Such an assumption is often considered in literature and, for instance, it guarantees the existence of a transition density of the associated SDE [32, 40].

Another ingredient in proving convergence is a bound on the second moment of the DLR Euler-Maruyama solution. We can establish such a bound, even though the algorithm includes a QR decomposition at the end of each time step  $n$ , provided that a certain condition on  $\Delta t_n = t_{n+1} - t_n$  is satisfied; see Lemma 4.2. This second-moment bound also yields a lower bound on  $C_{Y_n}$ , as shown in Proposition 4.5. This bound is identical in form to the one holding in the continuous case for uniformly elliptic noise, as shown in [18, Proposition 4.5].

**Assumption 5** (Non-degenerate diffusion). *There exists a positive constant  $\sigma_B$  such that*

$$b(t, x)b(t, x)^\top \succeq \sigma_B \cdot I_{d \times d} \succ 0,$$

for all  $t \in \mathbb{R}$  and for all  $x \in \mathbb{R}^d$ .

**Proposition 4.1.** *If Assumptions 4 and 5 hold, then for any sequence  $\{\Delta t_n\}_n$  with  $\Delta t_n = t_{n+1} - t_n$ , the Gramian of the DLR-EM solution  $\{U_n, Y_n\}_n$  of Algorithm 1 satisfies*

$$C_{Y_{n+1}} \succeq \sigma_B \Delta t_n \cdot I_{k \times k}. \quad (19)$$

*Proof.* We prove the proposition by induction on  $n$ . For the sake of notation, hereafter we write  $a_n := a(t_n, U_n^\top Y_n)$  and  $b_n := b(t_n, U_n^\top Y_n)$ .

By hypothesis,  $C_{Y_0}$  has full-rank and therefore the solution  $(U_1, Y_1)$  is well (and uniquely) defined through (10). The calculations below show that  $C_{Y_1}$  has full rank. We assume then that  $C_{Y_n}$  is full-rank and  $\{U_\ell, Y_\ell\}_{\ell=1}^n$  exist up to  $n$ , so that  $\{U_{n+1}, Y_{n+1}\}$  is well-defined through (10), and we derive a lower bound on the smallest singular eigenvalue of  $C_{Y_{n+1}}$ .

Using (10), we get

$$\begin{aligned}
C_{Y_{n+1}} &= \mathbb{E}[Y_{n+1}Y_{n+1}^\top] = R\mathbb{E}[\tilde{Y}_{n+1}\tilde{Y}_{n+1}^\top]R^\top \\
&= R\mathbb{E}[Y_nY_n^\top]R^\top + R\mathbb{E}[Y_n(U_n a_n \Delta t_n)^\top]R^\top + R\mathbb{E}[Y_n(U_n b_n \Delta W_n)^\top]R^\top \\
&\quad + R\mathbb{E}[(U_n a_n \Delta t_n)Y_n^\top]R^\top + R\mathbb{E}[(U_n b_n \Delta W_n)Y_n^\top]R^\top \\
&\quad + R\mathbb{E}[(U_n a_n \Delta t_n)(U_n a_n \Delta t_n)^\top]R^\top + R\mathbb{E}[(U_n a_n \Delta t_n)(U_n b_n \Delta W_n)^\top]R^\top \\
&\quad + R\mathbb{E}[(U_n b_n \Delta W_n)(U_n a_n \Delta t_n)^\top]R^\top + R\mathbb{E}[(U_n b_n \Delta W_n)(U_n b_n \Delta W_n)^\top]R^\top \\
&= R\mathbb{E}[Y_nY_n^\top]R^\top + R\mathbb{E}[Y_n(U_n a_n \Delta t_n)^\top]R^\top + R\mathbb{E}[(U_n a_n \Delta t_n)Y_n^\top]R^\top \\
&\quad + R\mathbb{E}[(U_n a_n \Delta t_n)(U_n a_n \Delta t_n)^\top]R^\top + R\mathbb{E}[(U_n b_n \Delta W_n)(U_n b_n \Delta W_n)^\top]R^\top,
\end{aligned} \tag{20}$$

where  $R$  is the square matrix obtained by the QR decomposition, denoted by  $\text{QR}$  in Algorithm 1. To derive the last equality, we have exploited the fact that all the terms linear in  $\Delta W_n$  vanish since  $\Delta W_n$  is independent of  $\{U_\ell, Y_\ell\}_{\ell=0}^n$  and have zero-mean.

We can now find an estimate on the smallest eigenvalue of  $\mathbb{E}[Y_{n+1}Y_{n+1}^\top]$  through the Rayleigh-quotient. Let us take a unit vector  $v \in \mathbb{R}^d$  and consider the following:

$$\begin{aligned}
v^\top \mathbb{E}[Y_{n+1}Y_{n+1}^\top]v &= v^\top R\mathbb{E}[Y_nY_n^\top]R^\top v + 2v^\top R\mathbb{E}[Y_n(U_n a_n \Delta t_n)^\top]R^\top v \\
&\quad + v^\top R\mathbb{E}[(U_n a_n \Delta t_n)(U_n a_n \Delta t_n)^\top]R^\top v + v^\top R\mathbb{E}[(U_n b_n \Delta W_n)(U_n b_n \Delta W_n)^\top]R^\top v.
\end{aligned} \tag{21}$$

Now the goal is to take the infimum over  $v$  on both sides of (21) and to lower bound the right-hand side by a positive quantity. This will imply that the Rayleigh quotient  $\inf_{\|v\|=1, v \in \mathbb{R}^k} v^\top \mathbb{E}[Y_{n+1}Y_{n+1}^\top]v$  is always greater than a positive constant providing a lower bound on the smallest eigenvalue of  $C_{Y_{n+1}}$ . To achieve this goal, it is necessary to also show that  $R$  is always of full rank, so that  $R^\top v$  is never the null vector. For this we show that  $\tilde{U}_{n+1}$  is full rank.

Indeed, given the QR decomposition  $\tilde{U}_{n+1}^\top = QR$ , where  $Q$  has orthonormal columns, one has

$$\|\tilde{U}_{n+1}\|_F = \|\tilde{U}_{n+1}^\top\|_F = \|QR\|_F = \|R\|_F \tag{22}$$

and  $\text{rank}(\tilde{U}_{n+1}\tilde{U}_{n+1}^\top) \leq \text{rank}(\tilde{U}_{n+1}) = \text{rank}(QR) = \text{rank}(R)$ . Let us compute  $\tilde{U}_{n+1}\tilde{U}_{n+1}^\top$ :

$$\begin{aligned}
\tilde{U}_{n+1}\tilde{U}_{n+1}^\top &= U_n U_n^\top + U_n (C_{Y_n}^{-1} \mathbb{E}[Y_n a_n^\top] (I_{d \times d} - P_{U_n}^{\text{row}}) \Delta t_n)^\top + (C_{Y_n}^{-1} \mathbb{E}[Y_n a_n^\top] (I_{d \times d} - P_{U_n}^{\text{row}}) \Delta t_n) U_n^\top \\
&\quad + (C_{Y_n}^{-1} \mathbb{E}[Y_n a_n^\top] (I_{d \times d} - P_{U_n}^{\text{row}})) (C_{Y_n}^{-1} \mathbb{E}[Y_n a_n^\top] (I_{d \times d} - P_{U_n}^{\text{row}}))^\top (\Delta t_n)^2 \\
&= I_{k \times k} + \underbrace{(C_{Y_n}^{-1} \mathbb{E}[Y_n a_n^\top] (I_{d \times d} - P_{U_n}^{\text{row}}))}_{C} \cdot (C_{Y_n}^{-1} \mathbb{E}[Y_n a_n^\top] (I_{d \times d} - P_{U_n}^{\text{row}}))^\top (\Delta t_n)^2 \\
&= I_{k \times k} + C C^\top (\Delta t_n)^2.
\end{aligned}$$

As  $I_{k \times k}$  is symmetric positive definite with all eigenvalues equal to 1,  $(\Delta t_n)^2$  is a positive scalar, and  $C C^\top$  is symmetric positive semi-definite matrix, via Weyl's inequality [15] all the eigenvalues of  $\tilde{U}_{n+1}\tilde{U}_{n+1}^\top$  are greater than 1. This implies that  $\tilde{U}_{n+1}\tilde{U}_{n+1}^\top$  is full rank and, therefore, the same holds for  $\tilde{U}_{n+1}$  and  $R$ , which have rank equal to  $k$ . Moreover, one has that

$$R^T R = R^T Q^T Q R = \tilde{U}_{n+1}\tilde{U}_{n+1}^\top = I_{k \times k} + C C^\top (\Delta t_n)^2,$$

hence via Weyl's inequality all eigenvalues of  $R^T R$ , and also the ones of  $R R^T$ , are greater than 1.

We now provide bounds for the terms on the right-hand side of (20). For the last term in (20), since  $\mathbb{E}[\Delta W_n \Delta W_n^\top] = \Delta t_n I_{m \times m}$  we have

$$\mathbb{E}[(U_n b_n \Delta W_n)(U_n b_n \Delta W_n)^\top] = U_n \mathbb{E}[b_n \Delta W_n \Delta W_n^\top b_n^\top] U_n^\top = U_n \mathbb{E}[b_n b_n^\top] U_n^\top \Delta t_n \geq \sigma_B \cdot I_{k \times k}, \tag{23}$$

by the orthogonality of  $U_n$  and Assumption 5.

Let us analyze the term  $v^\top R\mathbb{E}[Y_n(U_n a_n \Delta t_n)^\top] R^\top v = \mathbb{E}[v^\top RY_n a_n^\top U_n^\top R^\top v] \Delta t_n$ . One has

$$\begin{aligned} |\mathbb{E}[v^\top RY_n a_n^\top U_n^\top R^\top v]| &\leq \mathbb{E}[|v^\top RY_n a_n^\top U_n^\top R^\top v|] \\ &= \mathbb{E}[|v^\top RY_n| |a_n^\top U_n^\top R^\top v|] \leq \frac{1}{2\varepsilon} \mathbb{E}[|v^\top RY_n|^2] + \frac{\varepsilon}{2} \mathbb{E}[|a_n^\top U_n^\top R^\top v|^2] \\ &= \frac{1}{2\varepsilon} v^\top R\mathbb{E}[Y_n Y_n^\top] R^\top v + \frac{\varepsilon}{2} v^\top R\mathbb{E}[U_n a_n a_n^\top U_n^\top] R^\top v. \end{aligned}$$

Putting everything together, we get

$$\begin{aligned} v^\top \mathbb{E}[Y_{n+1} Y_{n+1}^\top] v &\geq v^\top R\mathbb{E}[Y_n Y_n^\top] R^\top v - \frac{1}{\varepsilon} v^\top R\mathbb{E}[Y_n Y_n^\top] R^\top v \Delta t_n - \varepsilon v^\top R\mathbb{E}[U_n a_n a_n^\top U_n^\top] R^\top v \Delta t_n \\ &\quad + v^\top R\mathbb{E}[U_n a_n a_n^\top U_n^\top] R^\top v (\Delta t_n)^2 + v^\top R\mathbb{E}[U_n b_n b_n^\top U_n^\top] R^\top v \Delta t_n. \end{aligned} \quad (24)$$

Dividing everything by  $|R^\top v|^2$  and using (23), one finds that

$$\begin{aligned} v^\top \frac{\mathbb{E}[Y_{n+1} Y_{n+1}^\top]}{|R^\top v|^2} v &\geq \left(1 - \frac{\Delta t_n}{\varepsilon}\right) v^\top R \frac{\mathbb{E}[Y_n Y_n^\top]}{|R^\top v|^2} R^\top v + v^\top R \frac{\mathbb{E}[U_n a_n a_n^\top U_n^\top]}{|R^\top v|^2} R^\top v ((\Delta t_n)^2 - \varepsilon \Delta t_n) \\ &\quad + \sigma_B \Delta t_n. \end{aligned} \quad (25)$$

Taking  $\varepsilon = \Delta t_n$ , we have

$$v^\top \frac{\mathbb{E}[Y_{n+1} Y_{n+1}^\top]}{|R^\top v|^2} v \geq \sigma_B \Delta t_n.$$

Therefore,

$$\begin{aligned} v^\top \mathbb{E}[Y_{n+1} Y_{n+1}^\top] v &\geq \sigma_B |R^\top v|^2 \Delta t_n, \\ &\geq \sigma_B (v^\top R R^\top v) \Delta t_n, \\ &\geq \sigma_B \Delta t_n, \end{aligned} \quad (26)$$

where on the last inequality we have used that all the eigenvalues of  $R R^\top$  are greater or equal to 1 and  $v$  is unitary. Now the right-hand side is independent on  $v$  and, hence, passing to the infimum on the left-hand side we find

$$\sigma_{n+1}^k \geq \sigma_B \Delta t_n, \quad (27)$$

where  $\sigma_{n+1}^k$  is the smallest eigenvalue of  $C_{Y_{n+1}} = \mathbb{E}[Y_{n+1} Y_{n+1}^\top]$ .

As these computations are independent of  $n$ , by induction  $\sigma_n^k > 0$  and  $C_{Y_n}$  is full rank for all  $n$ .  $\square$

Given a condition on the time step dependent on the smallest singular value, the mean-squared norm of the DLR approximation is always bounded. This result shown in Lemma 4.2 will be crucial for the proofs of Proposition 4.5 and Theorem 4.7.

**Lemma 4.2** ( $L^2$ -norm bound of DLR-EM solution). *Under Assumption 2, 3, and 4, consider the discrete DLR approximation  $\{X_n = U_n^\top Y_n\}_n$  given by Algorithm 1 with an arbitrary sequence  $\{\Delta t_n\}_n$  of (non-zero) step sizes. Denote by  $\sigma_n^k$  the smallest singular value of the Gramian  $\mathbb{E}[Y_n Y_n^\top]$ . If*

$$\Delta t_n \leq \min \left\{ \frac{\sqrt{\sigma_n^k}}{\sqrt{C_{\text{lgb}}} \sqrt{(1 + \mathbb{E}[|X_0|^2]) e^{(1+7C_{\text{lgb}})t_n}}}; 1 \right\}, \quad (28)$$

then we have

$$\mathbb{E}[|X_n|^2] \leq (1 + \mathbb{E}[|X_0|^2]) e^{(1+7C_{\text{lgb}})t_n} - 1 =: K_1(t_n), \quad \forall n = 0, \dots, N. \quad (29)$$

*Proof.* Let us consider our discretized solution  $X_{n+1}$  at the step  $n+1$ :

$$\begin{aligned}
X_{n+1} &:= U_{n+1}^\top Y_{n+1} = \tilde{U}_{n+1}^\top \tilde{Y}_{n+1} \\
&= (U_n + C_{Y_n}^{-1} \mathbb{E}[Y_n a_n^\top] (I_{d \times d} - P_{U_n}^{\text{row}}) \Delta t_n)^\top (Y_n + U_n a_n \Delta t_n + U_n b_n \Delta W_n) \\
&= X_n + U_n^\top U_n a_n \Delta t_n + U_n^\top U_n b_n \Delta W_n + (I_{d \times d} - P_{U_n}^{\text{row}}) \mathbb{E}[a_n Y_n^\top] C_{Y_n}^{-1} Y_n \Delta t_n \\
&\quad + (I_{d \times d} - P_{U_n}^{\text{row}}) \mathbb{E}[a_n Y_n^\top] C_{Y_n}^{-1} [U_n a_n (\Delta t_n)^2 + U_n b_n (\Delta W_n) \Delta t_n] \\
&= X_n + (I_{d \times d} - P_{U_n}^{\text{row}}) \underbrace{\mathbb{E}[a_n Y_n^\top] C_{Y_n}^{-1} Y_n}_{=: P_{Y_n} a_n} \Delta t_n + \underbrace{U_n^\top U_n a_n \Delta t_n + U_n^\top U_n b_n \Delta W_n}_{=: P_{U_n}^{\text{row}}} \\
&\quad + (I_{d \times d} - P_{U_n}^{\text{row}}) \mathbb{E}[a_n Y_n^\top] C_{Y_n}^{-1} U_n [a_n \Delta t_n + b_n \Delta W_n] \Delta t_n.
\end{aligned}$$

Therefore, using Young's inequality, we get

$$\begin{aligned}
\mathbb{E}[|X_{n+1}|^2] &= \mathbb{E} \left[ |X_n + (I_{d \times d} - P_{U_n}^{\text{row}}) P_{Y_n} a_n \Delta t_n + P_{U_n}^{\text{row}} a_n \Delta t_n + P_{U_n}^{\text{row}} b_n \Delta W_n \right. \\
&\quad \left. + (I_{d \times d} - P_{U_n}^{\text{row}}) \mathbb{E}[a_n Y_n^\top] C_{Y_n}^{-1} U_n [a_n \Delta t_n + b_n \Delta W_n] \Delta t_n|^2 \right] \\
&= \mathbb{E}[|X_n|^2] + 2\mathbb{E}[X_n^\top a_n] \Delta t_n + \mathbb{E}[(P_{Y_n} a_n)^\top (I_{d \times d} - P_{U_n}^{\text{row}}) P_{Y_n} a_n] (\Delta t_n)^2 \\
&\quad + 2\mathbb{E}[(P_{Y_n} a_n)^\top (I_{d \times d} - P_{U_n}^{\text{row}}) \mathbb{E}[a_n Y_n^\top] C_{Y_n}^{-1} U_n a_n] (\Delta t_n)^3 \\
&\quad + \mathbb{E}[a_n^\top P_{U_n}^{\text{row}} a_n] (\Delta t_n)^2 + \mathbb{E}[(\Delta W_n)^\top b_n^\top P_{U_n}^{\text{row}} b_n \Delta W_n] \\
&\quad + \mathbb{E}[(a_n^\top \Delta t_n + \Delta W_n^\top b_n^\top) U_n^\top C_{Y_n}^{-1} \mathbb{E}[Y_n a_n^\top] (I_{d \times d} - P_{U_n}^{\text{row}}) \mathbb{E}[a_n Y_n^\top] \\
&\quad \cdot C_{Y_n}^{-1} U_n (a_n \Delta t_n + b_n \Delta W_n)] (\Delta t_n)^2 \\
&\leq \mathbb{E}[|X_n|^2] + \underbrace{(\mathbb{E}[|X_n|^2] + \mathbb{E}[|a_n|^2]) \Delta t_n}_{=: T_0} \\
&\quad + \underbrace{\mathbb{E}[|(P_{Y_n} a_n)^\top (I_{d \times d} - P_{U_n}^{\text{row}}) P_{Y_n} a_n + a_n^\top P_{U_n}^{\text{row}} a_n|]}_{=: T_1} (\Delta t_n)^2 \\
&\quad + \underbrace{2\mathbb{E}[(P_{Y_n} a_n)^\top (I_{d \times d} - P_{U_n}^{\text{row}}) \mathbb{E}[a_n Y_n^\top] C_{Y_n}^{-1} U_n a_n]}_{=: T_2} (\Delta t_n)^3 + \underbrace{|\mathbb{E}[(\Delta W_n)^\top b_n^\top P_{U_n}^{\text{row}} b_n \Delta W_n]|}_{=: T_3} \\
&\quad + \underbrace{\mathbb{E}[(a_n^\top U_n^\top C_{Y_n}^{-1} \mathbb{E}[Y_n a_n^\top] (I_{d \times d} - P_{U_n}^{\text{row}}) \mathbb{E}[a_n Y_n^\top] C_{Y_n}^{-1} U_n a_n)] (\Delta t_n)^4}_{=: T_4} \\
&\quad + \underbrace{\mathbb{E}[(\Delta W_n^\top b_n^\top) U_n^\top C_{Y_n}^{-1} \mathbb{E}[Y_n a_n^\top] (I_{d \times d} - P_{U_n}^{\text{row}}) \mathbb{E}[a_n Y_n^\top] C_{Y_n}^{-1} U_n (b_n \Delta W_n)] (\Delta t_n)^2}_{=: T_5}.
\end{aligned} \tag{30}$$

For the term  $T_1$ , we get the following upper bound

$$\begin{aligned}
T_1 &= \mathbb{E}[|(I_{d \times d} - P_{U_n}^{\text{row}}) P_{Y_n} + P_{U_n}^{\text{row}}| a_n|^2] \\
&= \mathbb{E}[|P_{X_n} a_n|^2] \\
&\leq \mathbb{E}[|a_n|^2] \leq C_{\text{lgb}}(1 + \mathbb{E}[|X_n|^2]),
\end{aligned}$$

where in the last line we exploit the fact that  $P_{X_n} : L^2(\Omega; \mathbb{R}^d) \rightarrow L^2(\Omega; \mathbb{R}^d)$  is an orthogonal projector. Similarly, for  $T_2$  we get

$$\begin{aligned}
T_2 &\leq 2\sqrt{\mathbb{E}[|P_{Y_n} a_n|^2]} \sqrt{\mathbb{E}[|\mathbb{E}[a_n Y_n^\top] C_{Y_n}^{-\frac{1}{2}} C_{Y_n}^{-\frac{1}{2}} U_n a_n|^2]} \\
&\leq 2\sqrt{\mathbb{E}[|a_n|^2]} \sqrt{\mathbb{E}[a_n Y_n^\top] C_{Y_n}^{-\frac{1}{2}} |2\mathbb{E}[|C_{Y_n}^{-\frac{1}{2}} U_n a_n|^2]|} \\
&\leq 2\sqrt{\mathbb{E}[|a_n|^2]} \sqrt{\mathbb{E}[|a_n|^2] \mathbb{E}[|C_{Y_n}^{-\frac{1}{2}} U_n a_n|^2]} \\
&\leq 2\sqrt{\mathbb{E}[|a_n|^2]} \sqrt{\mathbb{E}[|a_n|^2] \frac{1}{\sigma_n^k} \mathbb{E}[|a_n|^2]} \\
&\leq 2\sqrt{\frac{1}{\sigma_n^k} [C_{\text{lgb}}(1 + \mathbb{E}[|X_n|^2])]^{\frac{3}{2}}}
\end{aligned}$$

For the term  $T_3$  we have

$$\begin{aligned} T_3 &= \mathbb{E}[\text{Tr}(\Delta W_n)^\top b_n^\top P_{U_n}^{\text{row}} b_n \Delta W_n] \leq \mathbb{E}[\text{Tr}(b_n^\top P_{U_n}^{\text{row}} b_n \Delta W_n \Delta W_n^\top)] \\ &= \text{Tr}(\mathbb{E}[b_n^\top P_{U_n}^{\text{row}} b_n \mathbb{E}[\Delta W_n \Delta W_n^\top | \mathcal{F}_{t_n}]]) = \mathbb{E}[\text{Tr}(b_n^\top P_{U_n}^{\text{row}} b_n)] \Delta t_n \\ &= \mathbb{E}[|U_n b_n|^2] \Delta t_n \leq \mathbb{E}[|U_n|^2 \|b_n\|_{\mathbb{F}}^2] \Delta t_n \leq \mathbb{E}[\|b_n\|_{\mathbb{F}}^2] \Delta t_n \leq C_{\text{lgb}}(1 + \mathbb{E}[|X_n|^2]) \Delta t_n. \end{aligned}$$

For  $T_4$  one obtains that

$$\begin{aligned} T_4 &\leq \sqrt{\mathbb{E}[|(a_n^\top) U_n^\top C_{Y_n}^{-1} \mathbb{E}[Y_n a_n^\top]|^2]} \sqrt{\mathbb{E}[|(I_{d \times d} - P_{U_n}^{\text{row}}) \mathbb{E}[a_n Y_n^\top] C_{Y_n}^{-1} U_n a_n|^2]} \\ &\leq \mathbb{E}[|(a_n^\top) U_n^\top C_{Y_n}^{-1} \mathbb{E}[Y_n a_n^\top]|^2] = \mathbb{E}[|(a_n^\top) U_n^\top C_{Y_n}^{-\frac{1}{2}} C_{Y_n}^{-\frac{1}{2}} \mathbb{E}[Y_n a_n^\top]|^2] \\ &\leq \frac{1}{\sigma_n^k} \mathbb{E}[|a_n|^2] \mathbb{E}[|a_n|^2] \leq \frac{1}{\sigma_n^k} C_{\text{lgb}}^2 (1 + \mathbb{E}[|X_n|^2])^2. \end{aligned}$$

One can obtain a similar bound for  $T_5$

$$\begin{aligned} T_5 &\leq \mathbb{E}[|(\Delta W_n^\top b_n^\top) U_n^\top C_{Y_n}^{-1} \mathbb{E}[Y_n a_n^\top]|^2] \\ &\leq \mathbb{E}[|(\Delta W_n^\top b_n^\top) U_n^\top|^2] \sqrt{\frac{1}{\sigma_n^k} |C_{Y_n}^{-\frac{1}{2}} \mathbb{E}[Y_n a_n^\top]|^2} = \frac{1}{\sigma_n^k} \mathbb{E}[|(\Delta W_n^\top b_n^\top) U_n^\top|^2] \mathbb{E}[|a_n|^2] \\ &\leq \frac{1}{\sigma_n^k} C_{\text{lgb}}^2 (1 + \mathbb{E}[|X_n|^2])^2 \Delta t_n. \end{aligned}$$

Putting all the bounds together, we find

$$\begin{aligned} \mathbb{E}[|X_{n+1}|^2] &\leq \mathbb{E}[|X_n|^2] + \underbrace{(\mathbb{E}[|X_n|^2] + C_{\text{lgb}}(1 + \mathbb{E}[|X_n|^2])) \Delta t_n}_{T_0} + \underbrace{C_{\text{lgb}}(1 + \mathbb{E}[|X_n|^2]) (\Delta t_n)^2}_{T_1} \\ &\quad + \underbrace{2 \sqrt{\frac{1}{\sigma_n^k} [C_{\text{lgb}}(1 + \mathbb{E}[|X_n|^2])]^{\frac{3}{2}} (\Delta t_n)^3} + C_{\text{lgb}}(1 + \mathbb{E}[|X_n|^2]) \Delta t_n}_{T_2} \\ &\quad + \underbrace{\frac{1}{\sigma_n^k} C_{\text{lgb}}^2 (1 + \mathbb{E}[|X_n|^2])^2 [(\Delta t_n)^4 + (\Delta t_n)^3]}_{T_4+T_5}. \end{aligned}$$

For the sake of notation let us write  $Z_n = 1 + \mathbb{E}[|X_n|^2]$ . Trivially (29) holds for  $n = 0$ . Assume it holds for  $n$ , by the induction hypothesis, then under (28) one has

$$Z_n \leq Z_0 e^{(1+7C_{\text{lgb}}t_n)}, \quad \text{and} \quad \sqrt{Z_n} \Delta t_n \leq \frac{\sqrt{\sigma_n^k}}{\sqrt{C_{\text{lgb}}}}. \quad (31)$$

On the other hand one has

$$\begin{aligned} Z_{n+1} &\leq Z_n (1 + (1 + 2C_{\text{lgb}}) \Delta t_n + C_{\text{lgb}} (\Delta t_n)^2) \\ &\quad + 2 \sqrt{\frac{1}{\sigma_n^k} C_{\text{lgb}}^{\frac{3}{2}} (Z_n)^{\frac{3}{2}} (\Delta t_n)^3 + 2 \frac{1}{\sigma_n^k} C_{\text{lgb}}^2 (Z_n)^2 (\Delta t_n)^3} \\ &\leq Z_n (1 + (1 + 2C_{\text{lgb}}) \Delta t_n + C_{\text{lgb}} (\Delta t_n) + 4C_{\text{lgb}} \Delta t_n), \end{aligned} \quad (32)$$

which implies

$$\begin{aligned} Z_{n+1} &\leq Z_n (1 + (1 + 7C_{\text{lgb}}) \Delta t_n) \\ &\leq Z_n e^{(1+(1+7C_{\text{lgb}})\Delta t_n)} \\ &\leq (1 + \mathbb{E}[|X_0|^2]) e^{(1+7C_{\text{lgb}}t_{n+1})}, \end{aligned} \quad (33)$$

which concludes the proof.  $\square$

**Remark 4.3.** *If the diffusion coefficient is non-degenerate, then the stability bound (29) holds under a time-step condition that is independent of the smallest singular value. Indeed, under Assumption 5, Proposition 4.1 implies that condition (28) in Lemma 4.2 can be replaced by*

$$\Delta t_n \leq \min \left\{ \frac{\sigma_B}{C_{\text{lgb}}(1 + \mathbb{E}[|X_0|^2]) e^{(1+7C_{\text{lgb}})t_n}}; 1 \right\}, \quad \text{for all } n \in \{1, \dots, N\}.$$

The following lemma presents a bound on the stochastic modes  $\tilde{Y}_n$  before the QR decomposition; this result will be useful to prove convergence of the DLR Euler-Maruyama.

**Lemma 4.4** (Boundedness of the stochastic modes). *Under the assumptions of Lemma 4.2, we have that the intermediate stochastic modes  $\tilde{Y}_n$  computed by Algorithm 1 satisfy*

$$\mathbb{E}[|\tilde{Y}_n|^2] \leq K_1(T) + 3C_{\text{lgb}}(1+K_1(T))T + 12C_{\text{lgb}}(1+K_1(T))T = K_2(T), \quad \text{for all } n = \{1, \dots, N\}, \quad (34)$$

where  $K_1(T)$  is defined as in (29). Moreover, define the following piecewise continuous interpolant  $\mathcal{Y}(t)$  of the process  $\{Y_n\}_n$ :

$$\mathcal{Y}(t) := Y_n + U_n a(t_n, U_n^\top Y_n)(t - t_n) + U_n b(t_n, U_n^\top Y_n)(W_t - W_n), \quad t_n < t \leq t_{n+1}. \quad (35)$$

Then, the following bound holds

$$\mathbb{E}[\sup_{t \in [0, T]} |\mathcal{Y}(t)|^2] \leq 3(K_1(T) + C_{\text{lgb}}(T^2 + 4T)(1 + K_1(T))) := \tilde{K}(T). \quad (36)$$

*Proof.* Suppose we have just computed  $\tilde{Y}_{n+1}$  in Step 3 of Algorithm 1. To prove (34), we first note that the orthogonality of  $U_n$  implies

$$\mathbb{E}[|Y_n|^2] = \mathbb{E}[|U_n^\top Y_n|^2] = \mathbb{E}[|X_n|^2],$$

which can be bounded as in Lemma 4.2. Hence, we have

$$\begin{aligned} \mathbb{E}[|\tilde{Y}_{n+1}|^2] &= \mathbb{E}[|Y_n + U_n a(t_n, U_n^\top Y_n)\Delta t_n + U_n b(t_n, U_n^\top Y_n)\Delta W_n|^2] \\ &= \mathbb{E}[|Y_n|^2] + 2\mathbb{E}[X_n^\top a(t_n, U_n^\top Y_n)]\Delta t_n + \mathbb{E}[|U_n a(t_n, U_n^\top Y_n)|^2](\Delta t_n)^2 \\ &\quad + \mathbb{E}[|U_n b(t_n, U_n^\top Y_n)\Delta W_n|^2] \\ &\leq \mathbb{E}[|X_n|^2] + \mathbb{E}[|X_n|^2]\Delta t_n + C_{\text{lgb}}(1 + \mathbb{E}[|X_n|^2])\Delta t_n + \mathbb{E}[|a(t_n, U_n^\top Y_n)|^2](\Delta t_n)^2 + \mathbb{E}[|b_n|^2_{\text{F}}]\Delta t_n \\ &\leq \mathbb{E}[|X_n|^2] + \mathbb{E}[|X_n|^2]\Delta t_n + 2C_{\text{lgb}}(1 + \mathbb{E}[|X_n|^2])\Delta t_n + C_{\text{lgb}}(1 + \mathbb{E}[|X_n|^2])(\Delta t_n)^2 \\ &\leq K_1 + K_1 T + 2C_{\text{lgb}}(1 + K_1)T + C_{\text{lgb}}(1 + K_1)T \\ &= K_1(1 + (1 + 3C_{\text{lgb}})T) + 3C_{\text{lgb}}T. \end{aligned}$$

To show (36), let us start from  $\mathcal{Y}_t$  defined in (35). Considering its norm, passing to the sup over time, and taking the expectation, via Lemma 4.2 and the linear-growth bound one gets

$$\begin{aligned} \mathbb{E}[\sup_{t \in [0, T]} |\mathcal{Y}(t)|^2] &= \mathbb{E}[\sup_{\substack{t_n < t \leq t_{n+1} \\ n=0, \dots, N-1}} |Y_n + U_n a(t_n, U_n^\top Y_n)(t - t_n) + U_n b(t_n, U_n^\top Y_n)(W_t - W_n)|^2] \\ &\leq 3\mathbb{E}[\sup_{\substack{t_n < t \leq t_{n+1} \\ n=0, \dots, N-1}} |Y_n|^2] + 3\mathbb{E}[\sup_{\substack{t_n < t \leq t_{n+1} \\ n=0, \dots, N-1}} |U_n a(t_n, U_n^\top Y_n)|^2(t - t_n)^2] \\ &\quad + 3\mathbb{E}[\sup_{\substack{t_n < t \leq t_{n+1} \\ n=0, \dots, N-1}} |U_n b(t_n, U_n^\top Y_n)|^2|(W_t - W_n)|^2] \\ &\leq 3K_1(T) + 3C_{\text{lgb}}(1 + K_1(T))|\Delta t|^2 + 3\mathbb{E}[\sup_{\substack{t_n < t \leq t_{n+1} \\ n=0, \dots, N-1}} |U_n b(t_n, U_n^\top Y_n)|^2|(W_t - W_n)|^2]. \end{aligned}$$

In order to bound the term with the Brownian increments one can notice that thanks to their independence with respect to  $\mathcal{F}_{t_n}$  and the independence of  $U_n b(t_n, U_n^\top Y_n)$  from  $t$ , one has

$$\begin{aligned} &3\mathbb{E}[\sup_{\substack{t_n < t \leq t_{n+1} \\ n=0, \dots, N-1}} |U_n b(t_n, U_n^\top Y_n)|^2|(W_t - W_n)|^2] \\ &= 3\mathbb{E}[\sup_{\substack{t_n < t \leq t_{n+1} \\ n=0, \dots, N-1}} |U_n b(t_n, U_n^\top Y_n)|^2|(W_t - W_n)|^2 | \mathcal{F}_{t_n}] \\ &\leq 3\mathbb{E}[\sup_{n=0, \dots, N-1} |U_n b(t_n, U_n^\top Y_n)|^2 | \mathcal{F}_{t_n}] \mathbb{E}[\sup_{\substack{t_n < t \leq t_{n+1} \\ n=0, \dots, N-1}} |(W_t - W_n)|^2 | \mathcal{F}_{t_n}] \\ &\leq 3C_{\text{lgb}}(1 + K_1(T))\mathbb{E}[\sup_{\substack{t_n < t \leq t_{n+1} \\ n=0, \dots, N-1}} |W_t - W_n|^2], \end{aligned}$$

where in the second to last line and in the last one we have used the fact that  $U_n b(t_n, U_n^\top Y_n)$  is  $\mathcal{F}_{t_n}$ -measurable and Lemma 4.2, respectively. Therefore, again by Lemma 4.2 one has

$$\mathbb{E}[\sup_{t \in [0, T]} |\mathcal{Y}(t)|^2] \leq 3K_1(T) + 3C_{\text{lgb}}(1 + K_1(T))|\Delta t|^2 + 3C_{\text{lgb}}(1 + K_1(T))\mathbb{E}[\sup_{\substack{t_n < t \leq t_{n+1} \\ n=0, \dots, N-1}} |W_t - W_n|^2],$$

where  $\Delta t = \max_n \Delta t_n$ . Using Doob's martingale inequality and property of the Brownian motion, we finally get the thesis

$$\begin{aligned} \mathbb{E}[\sup_{t \in [0, T]} |\mathcal{Y}(t)|^2] &\leq 3K_1(T) + 3C_{\text{lgb}}(1 + K_1(T))\Delta t^2 + 12C_{\text{lgb}}(1 + K_1(T))\Delta t. \\ &\leq 3K_1(T) + 3C_{\text{lgb}}(1 + K_1(T))T + 12C_{\text{lgb}}(1 + K_1(T))T. \end{aligned}$$

□

The norm bound of Lemma 29 on the discretized DLR solution  $X_n$  helps us obtaining a better estimate on the lower bound of the Gramian  $C_{Y_n} = \mathbb{E}[Y_n Y_n^\top]$  than the one given in Proposition 4.1.

**Proposition 4.5.** *Suppose that Assumptions 2, 4, and 5 hold. Let us consider a DLR Euler-Maruyama discretization with a uniform time step  $\Delta t := T/N$ , with  $N \in \mathbb{N}$ . Moreover, assume that  $\Delta t$  satisfies (28) for any  $n = 0, \dots, N$ . Then, one has*

$$C_{Y_{n+1}} \geq \min\{\sigma_0, \frac{\sigma_B^2}{4C_{\text{lgb}}(1 + K_1(T))}\} + \frac{\sigma_B}{2}\Delta t \left[1 - \left(1 - \frac{1}{1 + \frac{\sigma_B}{2C_{\text{lgb}}(1 + K_1(T))\Delta t}}\right)^{n+1}\right], \quad (37)$$

where  $K_1(T)$  is defined in (29).

*Proof.* We proceed similarly to the proof of Proposition 4.1. The result follows by using relation (25), which we recall here

$$v^\top \frac{\mathbb{E}[Y_{n+1} Y_{n+1}^\top]}{|R^\top v|^2} v \geq \left(1 - \frac{\Delta t}{\varepsilon}\right) v^\top R \frac{\mathbb{E}[Y_n Y_n^\top]}{|R^\top v|^2} R^\top v + v^\top R \frac{\mathbb{E}[U_n a_n a_n^\top U_n^\top]}{|R^\top v|^2} R^\top v ((\Delta t)^2 - \varepsilon \Delta t) + \sigma_B \Delta t$$

and the norm bound obtained in Lemma 4.2. Since  $R$  is obtained by the reduced QR applied to  $\tilde{U}_{n+1}$ , we have

$$\begin{aligned} v^\top R \mathbb{E}[U_n a_n a_n^\top U_n^\top] R^\top v &\geq -|v^\top R \mathbb{E}[U_n a_n a_n^\top U_n^\top] R^\top v| \\ &\geq -|R^\top v|^2 \mathbb{E}[|U_n a_n|^2] \\ &\geq -|R^\top v|^2 \mathbb{E}[|a_n|^2] \\ &\geq -|R^\top v|^2 C_{\text{lgb}}(1 + K_1(T)). \end{aligned} \quad (38)$$

Therefore,

$$v^\top \frac{\mathbb{E}[Y_{n+1} Y_{n+1}^\top]}{|R^\top v|^2} v \geq \left(1 - \frac{\Delta t}{\varepsilon}\right) v^\top R \frac{\mathbb{E}[Y_n Y_n^\top]}{|R^\top v|^2} R^\top v - C_{\text{lgb}}(1 + K_1(T)) |(\Delta t)^2 - \varepsilon \Delta t| + \sigma_B \Delta t. \quad (39)$$

Choosing

$$\varepsilon = \Delta t + \frac{\sigma_B}{2C_{\text{lgb}}(1 + K_1(T))},$$

one obtains

$$\begin{aligned} v^\top \frac{\mathbb{E}[Y_{n+1} Y_{n+1}^\top]}{|R^\top v|^2} v &\geq \left(1 - \frac{\Delta t}{\Delta t + \frac{\sigma_B}{2C_{\text{lgb}}(1 + K_1(T))}}\right) v^\top R \frac{\mathbb{E}[Y_n Y_n^\top]}{|R^\top v|^2} R^\top v \\ &\quad - C_{\text{lgb}}(1 + K_1(T)) \left|(\Delta t)^2 - (\Delta t + \frac{\sigma_B}{2C_{\text{lgb}}(1 + K_1(T))})\Delta t\right| + \sigma_B \Delta t \\ &= \left(1 - \frac{\Delta t}{\Delta t + \frac{\sigma_B}{2C_{\text{lgb}}(1 + K_1(T))}}\right) \sigma_n^k + \frac{\sigma_B}{2} \Delta t, \end{aligned}$$

where  $\sigma_n^k$  denotes the smallest eigenvalue of  $C_{Y_n} = \mathbb{E}[Y_n Y_n^\top]$ . By taking the infimum over  $v$  on the left-hand side and setting  $A := \frac{\sigma_B}{2C_{\text{lgb}}(1+K_1(T))}$ , we obtain

$$\begin{aligned}
\sigma_{n+1}^k &\geq \left(1 - \frac{\Delta t}{\Delta t + A}\right) \sigma_n^k + \frac{\sigma_B}{2} \Delta t \\
&\geq \left(1 - \frac{1}{1 + \frac{A}{\Delta t}}\right)^{n+1} \sigma_0 + \frac{\sigma_B}{2} \Delta t \sum_{k=0}^n \left(1 - \frac{1}{1 + \frac{A}{\Delta t}}\right)^k \\
&= \left(1 - \frac{1}{1 + \frac{A}{\Delta t}}\right)^{n+1} \sigma_0 + \frac{\sigma_B}{2} \Delta t \frac{1 - \left(1 - \frac{1}{1 + \frac{A}{\Delta t}}\right)^{n+1}}{1 - \left(1 - \frac{1}{1 + \frac{A}{\Delta t}}\right)} \\
&= \left(1 - \frac{1}{1 + \frac{A}{\Delta t}}\right)^{n+1} \sigma_0 + \frac{\sigma_B}{2} (1 + \frac{A}{\Delta t}) \Delta t \left[1 - \left(1 - \frac{1}{1 + \frac{A}{\Delta t}}\right)^{n+1}\right] \\
&= \left(1 - \frac{1}{1 + \frac{A}{\Delta t}}\right)^{n+1} \sigma_0 + \frac{\sigma_B}{2} A \left[1 - \left(1 - \frac{1}{1 + \frac{A}{\Delta t}}\right)^{n+1}\right] + \frac{\sigma_B}{2} \Delta t \left[1 - \left(1 - \frac{1}{1 + \frac{A}{\Delta t}}\right)^{n+1}\right] \\
&\geq \min\{\sigma_0, \frac{\sigma_B^2}{4C_{\text{lgb}}(1+K_1(T))}\} + \frac{\sigma_B}{2} \Delta t \left[1 - \left(1 - \frac{1}{1 + \frac{A}{\Delta t}}\right)^{n+1}\right].
\end{aligned}$$

□

**Remark 4.6.** If a uniform time step  $\Delta t$  satisfies (28), then equation (37) assures that the Gramian of  $Y_n$  is lower-bounded in the matrix sense, independently of  $t$ :

$$\sigma_n^k \geq \min\{\sigma_0, \frac{\sigma_B^2}{4C_{\text{lgb}}(1+K_1(T))}\} =: \frac{1}{\gamma}, \quad (40)$$

where  $\sigma_n^k$  denotes the smallest eigenvalue of  $C_{Y_n} = \mathbb{E}[Y_n Y_n^\top]$ . This bound turns out to be identical to the one obtained in [18] for the smallest eigenvalue of the Gramian  $C_{Y(t)}$  for the continuous DLRA (6). Hence, for such  $\Delta t$ , the same upper bound

$$|C_{Y(s)}^{-1}|, |C_{Y_n}^{-1}| \leq \gamma \text{ for all } s \in [0, T] \text{ and for all } n.$$

holds for the inverse Gramians in both the continuous DLRA and DLR Euler–Maruyama scheme.

Unlike the standard Euler–Maruyama scheme, Algorithm 1 requires a non-linear operation at every time step due to the rotation of the modes  $U_n$  via QR decomposition. Despite this, we are able to establish in the next theorem that the DLR Euler–Maruyama scheme converges at the usual strong rate.

**Theorem 4.7** (Strong Convergence of DLR Euler–Maruyama to the DO solution). *Let Assumptions 1-3 hold. Consider a uniform partition  $\Delta := \{t_n = t_0 + n\Delta t, n = 0, \dots, N\}$  of  $[0, T]$  with time-step  $\Delta t$ . Define  $n_s = \max\{n = 0, 1, \dots, N : t_n \leq s\}$  and assume that (28) is satisfied. Furthermore, let us suppose that there exists a constant  $\gamma > 0$  such that  $|C_{Y(s)}^{-1}|, |C_{Y_{n_s}}^{-1}| \leq \gamma$  for all  $s \in [0, T]$ .*

Moreover, if the SDE (2) is non-autonomous, we assume that the drift  $a$  and the diffusion  $b$  satisfy the following Hölder condition in  $t$ : there exist  $\alpha > 0$  and  $C_{\text{na}} > 0$  such that

$$|a(t, x) - a(s, x)| + |b(t, x) - b(s, x)| \leq C_{\text{na}}(1 + |x|^2)|t - s|^\alpha \quad \text{for all } t, s \in [0, T], \text{ for all } x \in \mathbb{R}^d. \quad (41)$$

Then, the DLR Euler–Maruyama method with constant time step  $\Delta t$  has strong order of convergence equal to  $\min\{1/2, \alpha\}$ , i.e. there exists a constant  $C := C(\gamma, k, T)$  independent of  $\Delta t$  such that for all  $0 \leq t \leq T$ :

$$\sqrt{\mathbb{E}[\sup_{0 \leq s \leq t} |X_{n_s} - X(s)|^2]} \leq C(\Delta t)^{\min\{1/2, \alpha\}}. \quad (42)$$

*Proof.* Fix  $n$ . Suppose that we have just completed Step 6 of Algorithm 1; then we know

$$X_{n+1} = U_{n+1}^\top Y_{n+1} = \tilde{U}_{n+1}^\top \tilde{Y}_{n+1},$$

where  $\tilde{U}_{n+1}, \tilde{Y}_{n+1}$  are the update of the deterministic and stochastic modes before the QR decomposition in Step 6 of Algorithm 1, respectively. They satisfy (10) in  $[t_n, t_{n+1}]$ , and  $\tilde{U}_{n+1}$  is not necessarily orthogonal.

We notice that the error  $|X(s) - X_{n_s}|^2$  for  $s \in [t_n, t_{n+1}]$  can be bounded by the error on the deterministic and stochastic modes:

$$\begin{aligned} |X(s) - X_{n_s}|^2 &= |U(s)^\top Y(s) - U_{n_s}^\top Y_{n_s}|^2 = |U(s)^\top Y(s) - \tilde{U}_{n_s}^\top \tilde{Y}_{n_s}|^2 \\ &= |U(s)^\top (Y(s) - \tilde{Y}_{n_s}) - (U(s)^\top - \tilde{U}_{n_s}^\top) \tilde{Y}_{n_s}|^2 \\ &\leq 2|U(s)^\top|^2 |Y(s) - \tilde{Y}_{n_s}|^2 + 2|U(s)^\top - \tilde{U}_{n_s}^\top|^2 |\tilde{Y}_{n_s}|^2 \\ &\leq 2|Y(s) - \tilde{Y}_{n_s}|^2 + 2\|U(s)^\top - \tilde{U}_{n_s}^\top\|_F^2 |\tilde{Y}_{n_s}|^2. \end{aligned}$$

Taking the supremum over  $[0, t]$  leads to

$$\sup_{0 \leq s \leq t} |X(s) - X_{n_s}|^2 \leq 2 \sup_{0 \leq s \leq t} |Y(s) - \tilde{Y}_{n_s}|^2 + 2 \sup_{0 \leq s \leq t} \|U(s)^\top - \tilde{U}_{n_s}^\top\|_F^2 \sup_{0 \leq s \leq t} |\tilde{Y}_{n_s}|^2,$$

and hence

$$\begin{aligned} \mathbb{E}[\sup_{0 \leq s \leq t} |X(s) - X_{n_s}|^2] &\leq 2\mathbb{E}[\sup_{0 \leq s \leq t} |Y(s) - \tilde{Y}_{n_s}|^2] + 2 \sup_{0 \leq s \leq t} \|U(s)^\top - \tilde{U}_{n_s}^\top\|_F^2 \mathbb{E}[\sup_{0 \leq s \leq t} |\tilde{Y}_{n_s}|^2], \\ &\leq 2\mathbb{E}[\sup_{0 \leq s \leq t} |Y(s) - \tilde{Y}_{n_s}|^2] + 2 \sup_{0 \leq s \leq t} \|U(s)^\top - \tilde{U}_{n_s}^\top\|_F^2 \mathbb{E}[\sup_{0 \leq s \leq t} |\mathcal{Y}_s|^2] \\ &\leq 2\mathbb{E}[\sup_{0 \leq s \leq t} |Y(s) - \tilde{Y}_{n_s}|^2] + 2\tilde{K} \sup_{0 \leq s \leq t} \|U(s)^\top - \tilde{U}_{n_s}^\top\|_F^2, \end{aligned}$$

where in the last line we use (36) in Lemma 4.4.

Letting  $C_1 := \sqrt{\max\{2, 2\tilde{K}\}}$  one has that

$$\sqrt{\mathbb{E}[\sup_{0 \leq s \leq t} |X(s) - X_{n_s}|^2]} \leq \sqrt{C_1^2 \mathbb{E}[\sup_{0 \leq s \leq t} |Y(s) - \tilde{Y}_{n_s}|^2] + C_1^2 \sup_{0 \leq s \leq t} \|U(s)^\top - \tilde{U}_{n_s}^\top\|_F^2}, \quad (43)$$

Therefore we just need to show the convergence for the deterministic and stochastic components  $\tilde{U}_n$  and  $\tilde{Y}_n$  to prove convergence of  $X_{n_s}$  to  $X(s)$ . To this end, we introduce the following piecewise continuous processes by interpolating  $U_n$  and  $Y_n$ :

$$\begin{aligned} \mathcal{Y}(t) &:= Y_n + U_n a(t_n, U_n^\top Y_n)(t - t_n) + U_n b(t_n, U_n^\top Y_n)(W_t - W_n), \quad t_n < t \leq t_{n+1}, \\ \mathcal{U}(t) &:= U_n + C_{Y_n}^{-1} \mathbb{E} [Y_n a(t_n, U_n^\top Y_n)^\top] (I_{d \times d} - P_{U_n}^{\text{row}}) (t - t_n), \quad t_n < t \leq t_{n+1}. \end{aligned}$$

Let us first consider the error of the stochastic component for all  $0 \leq t \leq T$ :

$$\begin{aligned} \mathbb{E}[\sup_{0 \leq s \leq t} |\tilde{Y}_{n_s} - Y(s)|^2] &= \mathbb{E}[\sup_{0 \leq s \leq t} |\mathcal{Y}(t_{n_s}) - Y(s)|^2] \\ &\leq 4 \left( \underbrace{\mathbb{E}[\sup_{0 \leq s \leq t} \left| \int_0^{t_{n_s}} U_{n_r} a(t_{n_r}, U_{n_r}^\top Y_{n_r}) - U(r) a(r, U(r)^\top Y(r)) dr \right|^2]}_{T_1} \right. \\ &\quad \left. + \mathbb{E}[\sup_{0 \leq s \leq t} \left| \int_0^{t_{n_s}} U_{n_r} b(t_{n_r}, U_{n_r}^\top Y_{n_r}) - U(r) b(r, U(r)^\top Y(r)) dW_r \right|^2] \right. \\ &\quad \left. + \mathbb{E}[\sup_{0 \leq s \leq t} \left| \int_{t_{n_s}}^s U(r) a(r, U(r)^\top Y(r)) dr \right|^2] \right. \\ &\quad \left. + \mathbb{E}[\sup_{0 \leq s \leq t} \left| \int_{t_{n_s}}^s U(r) b(r, U(r)^\top Y(r)) dW_r \right|^2] \right). \end{aligned} \quad (44)$$

Concerning  $T_1$ , through the orthogonality hypothesis on  $U$ , Assumption 1 and (41), Lemma 4.4, and (29), we obtain:

$$\begin{aligned}
T_1 &= \mathbb{E} \left[ \sup_{0 \leq s \leq t} \left| \int_0^{t_{n_s}} U_{n_r} a(t_{n_r}, U_{n_r}^\top Y_{n_r}) - U(r) a(r, U(r)^\top Y(r)) dr \right|^2 \right] \\
&\leq T \mathbb{E} \left[ \sup_{0 \leq s \leq t} \int_0^{t_{n_s}} |U_{n_r} a(t_{n_r}, U_{n_r}^\top Y_{n_r}) - U(r) a(r, U(r)^\top Y(r))|^2 dr \right] \\
&= T \mathbb{E} \left[ \sup_{0 \leq s \leq t} \sum_{n=0}^{n_s-1} \int_{t_n}^{t_{n+1}} |U_{n_r} a(t_{n_r}, U_{n_r}^\top Y_{n_r}) - U(r) a(r, U(r)^\top Y(r))|^2 dr \right] \\
&\leq T \mathbb{E} \left[ \sum_{n=0}^{n_t-1} \int_{t_n}^{t_{n+1}} |U_{n_r} a(t_{n_r}, U_{n_r}^\top Y_{n_r}) - U(r) a(t_{n_r}, U_{n_r}^\top Y_{n_r}) + U(r) a(t_{n_r}, U_{n_r}^\top Y_{n_r}) - U(r) a(r, U_{n_r}^\top Y_{n_r}) \right. \\
&\quad \left. + U(r) a(r, U_{n_r}^\top Y_{n_r}) - U(r) a(r, U(r)^\top Y_{n_r}) + U(r) a(r, U(r)^\top Y_{n_r}) - U(r) a(r, U(r)^\top Y(r))|^2 dr \right] \\
&\leq 4T \left[ \sum_{n=0}^{n_t-1} \int_{t_n}^{t_{n+1}} C_{\text{lgb}} (1 + K_1(T)) \|U_{n_r} - U(r)\|_{\text{F}}^2 + C_{\text{na}} (1 + K_1(T)) |t_{n_r} - r|^{2\alpha} \right. \\
&\quad \left. + C_{\text{Lip}} K_1(T) \|U_{n_r} - U(r)\|_{\text{F}}^2 + C_{\text{Lip}} \mathbb{E}[|Y_{n_r} - Y(r)|^2] dr \right] \\
&\leq 4T \left[ \sum_{n=0}^{n_t-1} \int_{t_n}^{t_{n+1}} (C_{\text{lgb}} + C_{\text{Lip}}) (1 + K_1(T)) \|U_{n_r} - U(r)\|_{\text{F}}^2 + C_{\text{na}} (1 + K_1(T)) |t_{n_r} - r|^{2\alpha} \right. \\
&\quad \left. + C_{\text{Lip}} \mathbb{E}[|Y_{n_r} - Y(r)|^2] dr \right] \\
&\leq 4T \left[ \sum_{n=0}^{n_t-1} \int_{t_n}^{t_{n+1}} (C_{\text{lgb}} + C_{\text{Lip}}) (1 + K_1(T)) \sup_{0 \leq p \leq r} \|U_{n_p} - U(p)\|_{\text{F}}^2 + C_{\text{na}} (1 + K_1(T)) (\Delta t)^{2\alpha} \right. \\
&\quad \left. + C_{\text{Lip}} \mathbb{E}[ \sup_{0 \leq p \leq r} |Y_{n_p} - Y(p)|^2] dr \right] \\
&\leq 4T (C_{\text{lgb}} + C_{\text{Lip}}) (1 + K_1(T)) \int_0^{t_{n_t}} \sup_{0 \leq p \leq r} \|\mathcal{U}(t_{n_p}) - U(p)\|_{\text{F}}^2 dr + 4T^2 C_{\text{na}} (1 + K_1(T)) (\Delta t)^{2\alpha} \\
&\quad + 4TC_{\text{Lip}} \int_0^{t_{n_t}} \mathbb{E}[ \sup_{0 \leq p \leq r} |\mathcal{Y}(t_{n_p}) - Y(p)|^2] dr.
\end{aligned}$$

We have similar estimates on  $T_2$ , using the Doob's maximal inequality, Itô's isometry and  $\Delta t \leq 1$ :

$$\begin{aligned}
T_2 &= \mathbb{E} \left[ \sup_{0 \leq s \leq t} \left| \int_0^{t_{n_s}} U_{n_r} b(t_{n_r}, U_{n_r}^\top Y_{n_r}) - U(r) b(r, U(r)^\top Y(r)) dW_r \right|^2 \right] \\
&\leq 4 \mathbb{E} \left[ \int_0^{t_{n_t}} |U_{n_r} b(t_{n_r}, U_{n_r}^\top Y_{n_r}) - U(r) b(r, U(r)^\top Y(r))|^2 dr \right] \\
&\leq 4 \mathbb{E} \left[ \int_0^{t_{n_t}} \sup_{0 \leq p \leq r} |U_{n_p} b(t_{n_p}, U_{n_p}^\top Y_{n_p}) - U(p) b(p, U(p)^\top Y(p))|^2 dr \right] \\
&\leq 4(C_{\text{lgb}} + C_{\text{Lip}}) (1 + K_1(T)) \int_0^{t_{n_t}} \sup_{0 \leq p \leq r} \|\mathcal{U}(t_{n_p}) - U(p)\|_{\text{F}}^2 dr + 4C_{\text{na}} (1 + K_1(T)) (\Delta t)^{2\alpha} \\
&\quad + 4C_{\text{Lip}} \int_0^{t_{n_t}} \mathbb{E}[ \sup_{0 \leq p \leq r} |\mathcal{Y}(t_{n_p}) - Y(p)|^2] dr.
\end{aligned}$$

[18, Lemma 3.5] tells us that there exists a constant  $K_3(T) > 0$  such that  $\sup_{0 \leq t \leq T} \mathbb{E}[|Y_t|^2] < K_3(T)$ . Then, via using again Doob's maximal inequality and Itô's isometry, by exploiting the orthogonality hypothesis on  $U$ , as well as the bounds given in Lemma 4.4 and Lemma 4.2,

we deduce from (44) that

$$\begin{aligned}
\mathbb{E}[\sup_{0 \leq s \leq t} |\tilde{Y}_{n_s} - Y(s)|^2] &= \mathbb{E}[\sup_{0 \leq s \leq t} |\mathcal{Y}(t_{n_s}) - Y(s)|^2] \\
&\leq 4(C_{\text{lgb}} + C_{\text{Lip}})(1 + K_1(T))(1 + T) \int_0^{t_{n_t}} \sup_{0 \leq p \leq r} \|U_{n_p} - U(p)\|_{\text{F}}^2 dr \\
&\quad + 4TC_{\text{na}}(1 + K_1(T))(1 + T)(\Delta t)^{2\alpha} \\
&\quad + 4C_{\text{Lip}}(1 + T) \int_0^{t_{n_t}} \mathbb{E}[\sup_{0 \leq p \leq r} |Y_{n_p} - Y(p)|^2] dr \\
&\quad + 4\mathbb{E}[\sup_{0 \leq s \leq t} \left| \int_{t_{n_s}}^s U(r) a(r, U(r)^\top Y(r)) dr \right|^2] \\
&\quad + 4\mathbb{E}[\sup_{0 \leq s \leq t} \left| \int_0^s U(r) b(r, U(r)^\top Y(r)) \mathbb{1}_{r \geq t_{n_s}}(r) dW_r \right|^2] \\
&\leq 4(C_{\text{lgb}} + C_{\text{Lip}})(1 + K_1(T))(1 + T) \int_0^t \sup_{0 \leq p \leq r} \|U_{n_p} - U(p)\|_{\text{F}}^2 dr \\
&\quad + 4C_{\text{na}}(1 + K_1(T))(1 + T)(\Delta t)^{2\alpha} \\
&\quad + 4C_{\text{Lip}}(1 + T) \int_0^t \mathbb{E}[\sup_{0 \leq p \leq r} |Y_{n_p} - Y(p)|^2] dr + 4((\Delta t)^2 + \Delta t) C_{\text{lgb}}(1 + K_3(T)) \\
&\leq A_y \int_0^t \sup_{0 \leq p \leq r} \|\mathcal{U}(t_{n_p}) - U(p)\|_{\text{F}}^2 dr + B_y \int_0^t \mathbb{E}[\sup_{0 \leq p \leq r} |\mathcal{Y}(t_{n_p}) - Y(p)|^2] dr \\
&\quad + C_y(\Delta t)^{2\alpha} + D_y \Delta t,
\end{aligned}$$

where from the first to the second line we also use Doob's inequality, while in the last one we use condition (28).  $A_y = 4(C_{\text{lgb}} + C_{\text{Lip}})(1 + K_1(T))(1 + T)$ ,  $B_y = 4C_{\text{Lip}}(1 + T)$ ,  $D_y = 8C_{\text{lgb}}(1 + K_3(T))$  are positive constants, and  $C_y = 4TC_{\text{na}}(1 + K_1(T))(1 + T)$  is a non-negative constant, equal to zero if  $a$  and  $b$  are autonomous.

We now turn to the error on the deterministic modes. The extra difficulty with respect to the stochastic case is the presence of the inverse Gramians  $C_{Y(s)}^{-1}$ ,  $C_{Y_{n_s}}^{-1}$  in the equation for the deterministic modes. We will use [16, Lemma 3.5] which says that, if  $|C_{Y(s)}^{-1}|, |C_{Y_{n_s}}^{-1}| \leq \gamma$  holds, then there exists a constant  $K_\gamma > 0$  such that  $\|C_{Y_{n_s}}^{-1} - C_{Y(s)}^{-1}\|_{\text{F}}^2 \leq K_\gamma \mathbb{E}[|Y_{n_s} - Y(s)|^2]$  for all  $s \in [0, T]$ .

Therefore, we have

$$\begin{aligned}
\sup_{0 \leq s \leq t} \|\tilde{U}_{n_s} - U(s)\|_{\text{F}}^2 &= \sup_{0 \leq s \leq t} \|\mathcal{U}_{t_{n_s}} - U(s)\|_{\text{F}}^2 \\
&= \sup_{0 \leq s \leq t} \left\| \int_0^{t_{n_s}} C_{Y_{n_r}}^{-1} \mathbb{E}[Y_{n_r} a(t_{n_r}, U_{n_r}^\top Y_{n_r})^\top] [I_{d \times d} - U_{n_r}^\top U_{n_r}] \right. \\
&\quad \left. - C_{Y(r)}^{-1} \mathbb{E}[Y(r) a(r, U(r)^\top Y(r))^\top] [I_{d \times d} - U(r)^\top U(r)] dr \right. \\
&\quad \left. - \int_{t_{n_s}}^s C_{Y(r)}^{-1} \mathbb{E}[Y(r) a(r, U(r)^\top Y(r))^\top] [I_{d \times d} - U(r)^\top U(r)] dr \right\|_{\text{F}}^2 \\
&\leq 3 \sup_{0 \leq s \leq t} T \underbrace{\int_0^{t_{n_s}} \|C_{Y_{n_r}}^{-1} \mathbb{E}[Y_{n_r} a(t_{n_r}, U_{n_r}^\top Y_{n_r})^\top] - C_{Y(r)}^{-1} \mathbb{E}[Y(r) a(r, U(r)^\top Y(r))^\top]\|_{\text{F}}^2 dr}_{\text{T}_3} \\
&\quad + 3 \sup_{0 \leq s \leq t} T \underbrace{\int_0^{t_{n_s}} \|C_{Y_{n_r}}^{-1} \mathbb{E}[Y_{n_r} a(t_{n_r}, U_{n_r}^\top Y_{n_r})^\top] U_{n_r}^\top U_{n_r} - C_{Y(r)}^{-1} \mathbb{E}[Y(r) a(r, U(r)^\top Y(r))^\top] U(r)^\top U(r)\|_{\text{F}}^2 dr}_{\text{T}_4} \\
&\quad + 3 \sup_{0 \leq s \leq t} (s - t_{n_s}) \int_{t_{n_s}}^s \gamma C_{\text{lgb}}(1 + K_1(T)) dr,
\end{aligned}$$

where in the last term we first employ Jensen's inequality, then Cauchy-Schwarz inequality.

ity, and the orthogonality of the projector. Concerning  $T_3$ , it holds that

$$\begin{aligned}
T_3 &\leq \int_0^{t_{n_s}} \|C_{Y_{n_r}}^{-1} \mathbb{E}[Y_{n_r} a(t_{n_r}, U_{n_r}^\top Y_{n_r})^\top] - C_{Y(r)}^{-1} \mathbb{E}[Y_{n_r} a(t_{n_r}, U_{n_r}^\top Y_{n_r})^\top] + C_{Y(r)}^{-1} \mathbb{E}[Y_{n_r} a(t_{n_r}, U_{n_r}^\top Y_{n_r})^\top] \\
&\quad - C_{Y(r)}^{-1} \mathbb{E}[Y(r) a(t_{n_r}, U_{n_r}^\top Y_{n_r})^\top] + C_{Y(r)}^{-1} \mathbb{E}[Y(r) a(t_{n_r}, U_{n_r}^\top Y_{n_r})^\top] - C_{Y(r)}^{-1} \mathbb{E}[Y(r) a(r, U_{n_r}^\top Y_{n_r})^\top] \\
&\quad + C_{Y(r)}^{-1} \mathbb{E}[Y(r) a(r, U_{n_r}^\top Y_{n_r})^\top] - C_{Y(r)}^{-1} \mathbb{E}[Y(r) a(r, U(r)^\top Y_{n_r})^\top] \\
&\quad + C_{Y(r)}^{-1} \mathbb{E}[Y(r) a(r, U(r)^\top Y_{n_r})^\top] - C_{Y(r)}^{-1} \mathbb{E}[Y(r) a(r, U(r)^\top Y(r))^\top]\|_F^2 dr \\
&\leq \int_0^{t_{n_s}} 5K_\gamma K_1(T) C_{\text{lgb}}(1 + K_1(T)) \mathbb{E}[|Y_{n_r} - Y(r)|^2] + 5\gamma C_{\text{lgb}}(1 + K_1(T)) \mathbb{E}[|Y_{n_r} - Y(r)|^2] \\
&\quad + 5\gamma K_1(T) C_{\text{na}}(1 + K_1(T)) (\Delta t)^{2\alpha} + 5\gamma K_3(T) K_1(T) C_{\text{Lip}} \|U_{n_r} - U(r)\|_F^2 \\
&\quad + 5\gamma K_1(T) C_{\text{Lip}} \mathbb{E}[|Y_{n_r} - Y(r)|^2] dr \\
&\leq \int_0^{t_{n_s}} [(5K_\gamma K_1(T) + 5\gamma K_3(T)) C_{\text{lgb}}(1 + K_1(T)) + 5\gamma K_1(T) C_{\text{Lip}}] \mathbb{E}[\sup_{0 \leq p \leq r} |\mathcal{Y}(t_{n_p}) - Y(p)|^2] dr \\
&\quad + 5\gamma K_3(T) T C_{\text{na}}(1 + K_1(T)) (\Delta t)^{2\alpha} + \int_0^{t_{n_s}} 5\gamma K_3(T) K_1(T) C_{\text{Lip}} \sup_{0 \leq p \leq r} \|\mathcal{U}(t_{n_p}) - U(p)\|_F^2 dr.
\end{aligned}$$

For  $T_4$ , we have similarly

$$\begin{aligned}
T_4 &= \int_0^{t_{n_s}} \|C_{Y(r)}^{-1} \mathbb{E}[Y(r) a(r, U(r)^\top Y(r))^\top] U(r)^\top U(r) - C_{Y(r)}^{-1} \mathbb{E}[Y(r) a(r, U(r)^\top Y(r))^\top] U(r)^\top U_{n_r} \\
&\quad + C_{Y(r)}^{-1} \mathbb{E}[Y(r) a(r, U(r)^\top Y(r))^\top] U(r)^\top U_{n_r} \\
&\quad - C_{Y(r)}^{-1} \mathbb{E}[Y(r) a(r, U(r)^\top Y(r))^\top] U_{n_r}^\top U_{n_r} + C_{Y(r)}^{-1} \mathbb{E}[Y(r) a(r, U(r)^\top Y(r))^\top] U_{n_r}^\top U_{n_r} \\
&\quad - C_{Y_{n_r}}^{-1} \mathbb{E}[Y_{n_r} a(t_{n_r}, U_{n_r}^\top Y_{n_r})^\top] U_{n_r}^\top U_{n_r}\|_F^2 dr \\
&\leq \int_0^{t_{n_s}} 6\gamma K_3(T) C_{\text{lgb}}(1 + K_3(T)) \|U_{n_r} - U(r)\|_F^2 dr \\
&\quad + 15 \int_0^{t_{n_s}} [(K_\gamma K_1(T) + \gamma K_3(T)) C_{\text{lgb}}(1 + K_1(T)) + \gamma K_1(T) C_{\text{Lip}}] \cdot \mathbb{E}[\sup_{0 \leq p \leq r} |\mathcal{Y}(t_{n_p}) - Y(p)|^2] dr \\
&\quad + 15\gamma K_3(T) T C_{\text{na}}(1 + K_1(T)) (\Delta t)^{2\alpha} + 15 \int_0^{t_{n_s}} \gamma K_3(T) K_1(T) C_{\text{Lip}} \sup_{0 \leq p \leq r} \|\mathcal{U}(t_{n_p}) - U(p)\|_F^2 dr.
\end{aligned}$$

This leads us to:

$$\begin{aligned}
\sup_{0 \leq s \leq t} \|\tilde{U}_{n_s} - U(s)\|_F^2 &= \sup_{0 \leq s \leq t} \|\mathcal{U}(t_{n_s}) - U(s)\|_F^2 \\
&\leq 3T \sup_{0 \leq s \leq t} [6\gamma K_3(T) C_{\text{lgb}}(1 + K_3(T)) + 20\gamma K_3(T) K_1(T) C_{\text{Lip}}] \int_0^{t_{n_s}} \|U_{n_r} - U(r)\|_F^2 dr \\
&\quad + 3T \sup_{0 \leq s \leq t} 20[(K_\gamma K_1(T) + \gamma K_3(T)) C_{\text{lgb}}(1 + K_1(T)) + \gamma K_1(T) C_{\text{Lip}}] \\
&\quad \cdot \int_0^{t_{n_s}} \mathbb{E}[|Y_{n_r} - Y(r)|^2] dr \\
&\quad + 60\gamma K_3(T) T^2 C_{\text{na}}(1 + K_1(T)) (\Delta t)^{2\alpha} + 3 \sup_{0 \leq s \leq t} (s - t_{n_s}) \int_{t_{n_s}}^s \gamma C_{\text{lgb}}(1 + K_3(T)) dr \\
&\leq A_u \int_0^t \sup_{0 \leq p \leq r} \|U(t_{n_p}) - U(p)\|_F^2 dr + B_u \int_0^t \mathbb{E}[\sup_{0 \leq p \leq r} |\mathcal{Y}(t_{n_p}) - Y(p)|^2] dr \\
&\quad + C_u (\Delta t)^{2\alpha} + D_u (\Delta t)^2,
\end{aligned} \tag{45}$$

where  $A_u = 3T[6\gamma K_3(T) C_{\text{lgb}}(1 + K_3(T)) + 20\gamma K_3(T) K_1(T) C_{\text{Lip}}]$ ,  $B_u = 60T[(K_\gamma K_1(T) + \gamma K_3(T)) C_{\text{lgb}}(1 + K_1(T)) + \gamma K_1(T) C_{\text{Lip}}]$ ,  $D_u = 3C_{\text{lgb}}(1 + K_1(T))$  are positive constants and  $C_u = 60\gamma K_1(T) T^2 C_{\text{na}}(1 + K_1(T))$  is non-negative and equal to zero if the drift  $a$  and the diffusion  $b$  are autonomous.

Finally, using Gronwall's lemma and  $\Delta t \leq 1$  we find:

$$\begin{aligned}
& \mathbb{E} \left[ \sup_{0 \leq s \leq t} |\tilde{Y}_{n_s} - Y(s)|^2 \right] + \sup_{0 \leq s \leq t} \|\tilde{U}_{n_s} - U(s)\|_{\mathbb{F}}^2 = \sup_{0 \leq s \leq t} \|\mathcal{U}(t_{n_s}) - U(s)\|_{\mathbb{F}}^2 + \mathbb{E} \left[ \sup_{0 \leq s \leq t} |\mathcal{Y}(t_{n_s}) - Y(s)|^2 \right] \\
& \leq A \int_0^t \sup_{0 \leq p \leq r} \|\mathcal{U}(t_{n_p}) - U(p)\|_{\mathbb{F}}^2 dr \\
& \quad + B \int_0^t \mathbb{E} \left[ \sup_{0 \leq p \leq r} |\mathcal{Y}(t_{n_p}) - Y(p)|^2 \right] dr + C(\Delta t)^{2\alpha} + D(\Delta t) \\
& \leq \max\{A, B\} \int_0^t \sup_{0 \leq p \leq r} \|U_{n_r} - U(r)\|_{\mathbb{F}}^2 + \mathbb{E} \left[ \sup_{0 \leq p \leq r} |\mathcal{Y}(t_{n_p}) - Y(p)|^2 \right] dr \\
& \quad + C(\Delta t)^{2\alpha} + D(\Delta t) \\
& \leq \exp^{\max(A, B)T} \cdot 2(C + D)((\Delta t)^{\min\{1, 2\alpha\}}), \tag{46}
\end{aligned}$$

where  $A = A_u + A_y$ ,  $B = B_u + B_y$ ,  $D = D_u + D_y$  are positive constants and  $C = C_u + C_y$  is non-negative and equal to zero if  $a$  and  $b$  are autonomous. The thesis therefore is obtained from (43) and (46):

$$\sqrt{\mathbb{E} \left[ \sup_{0 \leq s \leq t} |X_{n_s} - X(s)|^2 \right]} \leq C_1 \sqrt{(C + D)} \exp^{\max(A, B) \frac{T}{2}} \cdot ((\Delta t)^{\min\{\frac{1}{2}, \alpha\}}).$$

□

**Remark 4.8.** *To obtain the accuracy result of Theorem 4.7 we need to assume the lower-boundedness by a positive constant in a matrix-sense of the Gramian. This is the reason why this type of bounds are given in Propositions 4.1 and 4.5 under suitable assumptions.*

**Remark 4.9.** *A closer inspection on the constant  $C := C(\gamma, k, T)$  in (42) shows that it depends exponentially on  $\gamma$  (see inequality (45) in the proof of Theorem 4.7), i.e. it blows up exponentially fast when the smallest singular values of the DLR solution and its DLR Euler-Maruyama approximation goes to zero. This shows that the Euler-Maruyama discretization is not robust with respect to the smallest singular value. We verify this statement numerically in Section 7.*

As a final result of this subsection, we study the error between the exact solution  $X^{\text{true}}$  of the SDE and its DLR Euler-Maruyama approximation.

**Theorem 4.10** (Error estimate of DLR-EM). *Denote by  $X(t)$  and  $X_{n_t}$  the DLR solution of chosen rank  $k$  and the DLR approximation via DLR Euler-Maruyama method, respectively, where we use the notation  $n_s = \max\{n = 0, 1, \dots, N : t_n \leq s\}$ . Under the same assumptions of Theorem 4.7, let  $\varepsilon := \varepsilon(k) \geq 0$  be defined as*

$$\varepsilon^2 := \sup_{\substack{t \in [0, T] \\ Z \in L^2(\Omega, \mathbb{R}^d) \text{ of rank } k \\ \text{with } \mathbb{E}[|Z|^2] \leq \tilde{K}}} \max\{\mathbb{E}[|a(t, Z) - P_Z a(t, Z)|^2], \mathbb{E}[\|b(t, Z) - \mathcal{P}_{\mathcal{U}(Z)} b(t, Z)\|_{\mathbb{F}}^2]\}, \tag{47}$$

where  $\tilde{K} := \min\{K > 0 \text{ such that } \max\{\mathbb{E}[\sup_{0 \leq t \leq T} |X_t|^2], \mathbb{E}[\max_{0 \leq n \leq N} |X_n|^2]\} \leq K\}$ ,  $P_Z[\cdot] := (I_{d \times d} - \mathcal{P}_{\mathcal{U}(Z)})[\cdot] \mathcal{P}_{\mathcal{Y}(Z)} + \mathcal{P}_{\mathcal{U}(Z)}[\cdot]$  is an orthogonal projector, whereas  $P_{\mathcal{U}(Z)}$  and  $\mathcal{P}_{\mathcal{Y}(Z)}$  denote the projection onto range and corange of  $Z$ , respectively. Then, for all  $n = 1, \dots, N$

$$\begin{aligned}
& \sqrt{\mathbb{E} \left[ \sup_{0 \leq s \leq t} |X^{\text{true}}(s) - X_{n_s}|^2 \right]} \leq c_1(T) \sqrt{\mathbb{E}[|X_0^{\text{true}} - X_0|^2]} + c_2(T) \varepsilon \\
& \quad + c_3(\gamma, k, T) (\Delta t)^{\min\{\frac{1}{2}, \alpha\}}, \tag{48}
\end{aligned}$$

where  $c_1 := c_1(T)$ ,  $c_2 := c_2(k, T)$  are positive constants dependent on the final time  $T$  and the rank  $k$ , and  $c_3 := c_3(\gamma, k, T)$  is the positive constant  $C$  appearing in Theorem 4.7, which depends on the final time  $T$ , the rank  $k$ , and  $\gamma$ .

*Proof.* For the solution  $X^{\text{true}}(t)$  of (2) over the interval  $[0, T]$ , there exists a constant  $K(T)$ , depending on the final time  $T$ , such that  $\mathbb{E}[\|X^{\text{true}}(t)\|^2] \leq K(T)$  for all  $t \in [0, T]$  [23, Theorem 4.5.4]. For each path  $\omega$ , the following relation holds

$$\sup_{0 \leq s \leq t} |X^{\text{true}}(s) - X_{n_s}|^2 \leq 2 \sup_{0 \leq s \leq t} |X^{\text{true}}(s) - X(s)|^2 + 2 \sup_{0 \leq s \leq t} |X(s) - X_{n_s}|^2 \quad (49)$$

and, hence, via monotonicity of the mean and of the square root

$$\begin{aligned} \sqrt{\mathbb{E}[\sup_{0 \leq s \leq t} |X^{\text{true}}(s) - X_{n_s}|^2]} &\leq \sqrt{2\mathbb{E}[\sup_{0 \leq s \leq t} |X^{\text{true}}(s) - X(s)|^2] + 2\mathbb{E}[\sup_{0 \leq s \leq t} |X(s) - X_{n_s}|^2]}, \\ &\leq \sqrt{2\mathbb{E}[\sup_{0 \leq s \leq t} |X^{\text{true}}(s) - X(s)|^2]} + \sqrt{2\mathbb{E}[\sup_{0 \leq s \leq t} |X(s) - X_{n_s}|^2]}. \end{aligned}$$

In order to bound the right-hand side in (49), we need a convenient expression of the DLR solution. So recall that from the Itô's formula one has

$$dX(t) = (dU(t)^\top)Y(t) + U(t)^\top dY(t) + \underbrace{\sum_{i=1}^k d\langle U^i(t), Y^i(t) \rangle}_{=0},$$

which is equivalent to

$$\begin{aligned} X(t) &= X_0 + \int_0^t \left( I_{d \times d} - P_{U(s)}^{\text{row}} \right) \mathbb{E} [a(s, X(s))Y(s)^\top] C_{Y(s)}^{-1} Y(s) ds \\ &\quad + \int_0^t U(s)^\top U(s) a(s, X(s)) ds + \int_0^t U(s)^\top U(s) b(s, X(s)) dW_s. \end{aligned}$$

Let us analyze the difference  $X^{\text{true}}(s) - X(s)$ : we have

$$\begin{aligned} &\mathbb{E}[\sup_{0 \leq s \leq t} |X^{\text{true}}(s) - X(s)|^2] \\ &\leq 3\mathbb{E}[|X_0^{\text{true}} - X_0|^2] + 3 \underbrace{\mathbb{E}[\sup_{0 \leq s \leq t} \left| \int_0^s b(r, X^{\text{true}}(r)) - U(r)^\top U(r) b(r, X(r)) dW_r \right|^2]}_{:= T_2} \\ &\quad + 3 \underbrace{\mathbb{E}[\sup_{0 \leq s \leq t} \left| \int_0^s a(r, X^{\text{true}}(r)) - \left( I_{d \times d} - P_{U(r)}^{\text{row}} \right) \mathbb{E} [a(r, X(r))Y(r)^\top] C_{Y(r)}^{-1} Y(r) - U(r)^\top U(r) a(r, X(r)) dr \right|^2]}_{:= T_1}. \end{aligned}$$

We want to find a specific bound for the terms  $T_1$  and  $T_2$ . Regarding  $T_1$ , we exploit condition (47)

$$\begin{aligned} T_1 &\leq \mathbb{E}[t \int_0^t |a(r, X^{\text{true}}(r)) - \left( I_{d \times d} - P_{U(r)}^{\text{row}} \right) \mathbb{E} [a(r, X(r))Y(r)^\top] C_{Y(r)}^{-1} Y(r) - U(r)^\top U(r) a(r, X(r))|^2 dr] \\ &\leq t \int_0^t \mathbb{E}[|a(r, X^{\text{true}}(r)) - a(r, X(r)) + a(r, X(r)) - \mathcal{P}_{X(r)} a(r, X(r))|^2] dr \\ &\leq 2T \int_0^t \mathbb{E}[\sup_{0 \leq s \leq t} |a(r, X^{\text{true}}(r)) - a(r, X(r))|^2] dr + 2T \int_0^t \mathbb{E}[|a(r, X(r)) - \mathcal{P}_{X(r)} a(r, X(r))|^2] dr. \\ &\leq 2TC_{\text{Lip}} \int_0^t \mathbb{E}[\sup_{0 \leq s \leq t} |X^{\text{true}}(r) - X(r)|^2] dr + 2T \int_0^t \mathbb{E}[|a(r, X(r)) - \mathcal{P}_{X(r)} a(r, X(r))|^2] dr. \end{aligned}$$

Whereas for  $T_2$ , we have

$$\begin{aligned} T_2 &= \mathbb{E}[\sup_{0 \leq s \leq t} \left| \int_0^s b(r, X^{\text{true}}(r)) - b(r, X(r)) + b(r, X(r)) - U(r)^\top U(r) b(r, X(r)) dW_r \right|^2] \\ &\leq 4\mathbb{E}[\int_0^t |b(r, X^{\text{true}}(r)) - b(r, X(r)) + b(r, X(r)) - U(r)^\top U(r) b(r, X(r))|^2 dr] \\ &\leq 8\mathbb{E}[\int_0^t C_{\text{Lip}} |X^{\text{true}}(r) - X(r)|^2 dr] + 8\mathbb{E}[\int_0^t |b(r, X(r)) - U(r)^\top U(r) b(r, X(r))|^2 dr], \end{aligned}$$

where in the second line we employ the Itô's isometry and the Doob's inequality. Putting all together we find by Gronwall's lemma and (47)

$$\begin{aligned} \mathbb{E}[\sup_{0 \leq s \leq t} |X^{\text{true}}(s) - X(s)|^2] &\leq 3\mathbb{E}[|X_0^{\text{true}} - X_0|^2] + 6(T+4)T\varepsilon^2 \\ &\quad + 6C_{\text{Lip}}(T+4)T \left( \int_0^t \mathbb{E}[\sup_{0 \leq s \leq t} |X^{\text{true}}(s) - X(s)|^2] ds \right) \\ &\leq [3\mathbb{E}[|X_0^{\text{true}} - X_0|^2] + 6C_{\text{Lip}}(T+4)T\varepsilon^2] e^{6C_{\text{Lip}}(T+4)T}. \end{aligned}$$

Finally, using Theorem 4.7 yields the thesis:

$$\begin{aligned} \sqrt{\mathbb{E}[\sup_{0 \leq s \leq t} |X^{\text{true}}(s) - X_{n_s}|^2]} &\leq \sqrt{2\mathbb{E}[\sup_{0 \leq s \leq t} |X^{\text{true}}(s) - X(s)|^2]} + \sqrt{2\mathbb{E}[\sup_{0 \leq s \leq t} |X(s) - X_{n_s}|^2]} \\ &\leq \sqrt{6}e^{6C_{\text{Lip}}(T+4)\frac{T}{2}} \sqrt{\mathbb{E}[|X_0^{\text{true}} - X_0|^2]} + \sqrt{6}Te^{6C_{\text{Lip}}(T+4)\frac{T}{2}}\varepsilon \\ &\quad + \sqrt{2}C(\gamma, k, T)(\Delta t)^{\min\{\frac{1}{2}, \alpha\}}. \end{aligned}$$

□

Notice that Theorems 4.7 and 4.10 require an upper bound on  $\sup_{t \in [0, T]} \|C_{Y(t)}^{-1}\|_2$  and  $\sup_{n \in \{1, \dots, N\}} |C_{Y_n}^{-1}|$  in order to obtain convergence. This requirement practically excludes the case of ill-conditioned Gram matrices. However, if the diffusion coefficient  $b$  is non-degenerate as in Assumption 5, then this condition is satisfied thanks to Propositions 4.1, 4.5 and [18, Proposition 4.5].

**Remark 4.11** (On the modelling error (47)). *The quantity in (47) defines the maximal projection error of the drift and diffusion terms, when evaluated on a rank- $k$  function onto the tangent space to the manifold of rank- $k$  processes. Roughly speaking, this condition estimates the low-rankness of our SDE full system (2) through time: indeed, the smaller the  $\varepsilon$ , the better the DLRA of rank- $k$  surrogate approximate (2) over time. This is similar to standard assumptions in the DLRA literature (see e.g. [24, 21]). In light of this, it is reasonable to expect that the rank has an effect on  $\varepsilon$ : the larger the rank  $k$ , the smaller  $\varepsilon$ .*

**Remark 4.12** (Comments on the constants of Theorem 4.10). *We observe that the constant  $c_1$  on the right-hand side of (48) does not depend on the rank  $k$ . This is expected, as the only source of rank dependence in the error associated with the rank- $k$  approximation of the initial datum. On the other hand, although the constant  $c_2$  in the second term does not explicitly depend on the rank  $k$ , this term still implicitly depends on  $k$  through  $\varepsilon$ , which is given in (47).*

**Remark 4.13** (Rank error in the initial condition  $X_0^{\text{true}}$ ). *One can also go deeper in analyzing the error of  $T_1$  in the proof of Theorem 4.10. For instance consider the covariance  $\mathbb{E}[X_0^{\text{true}}(X_0^{\text{true}})^\top] \in \mathbb{R}^{d \times d}$ , which is a symmetric and semi-positive definite matrix, and, hence, admits the following decomposition*

$$\mathbb{E}[X_0^{\text{true}}(X_0^{\text{true}})^\top] = Q \text{diag}(\lambda_1, \dots, \lambda_d) Q^\top,$$

where  $Q = [q_i]_i \in \mathbb{R}^{d \times d}$  is an orthogonal matrix with  $q_i$  the  $i$ -th orthonormal column and  $\lambda_i$  is the non-negative eigenvalue associated to  $q_i$ , with  $(\lambda_i)_i$  ordered decreasingly. Moreover, there exists an orthonormal system  $(\zeta_i)_{i=1, \dots, d}$ , with  $\zeta_i \in L^2(\Omega, \mathbb{R})$ , such that one has

$$X_0^{\text{true}} = \sum_{i=1}^d \sqrt{\lambda_i} q_i \zeta_i;$$

for details see e.g. [18, Section 2]. Then, if one chooses  $X_0 = \sum_{i=1}^k \sqrt{\lambda_i} q_i \zeta_i$ , then the error is

$$\mathbb{E}[\|X_0^{\text{true}} - X_0\|_{\text{F}}^2] = \sum_{i=k+1}^d \lambda_i.$$

## 5 Analysis of the DLR Projector Splitting for EM

We now study the discretization scheme defined by Algorithm 2. As we saw in Section 3.2, Algorithm 2 can be viewed as a projector-splitting scheme. Importantly, the projector-splitting scheme converges independently of the smallest singular value of the Gram matrix. This is in stark contrast to the DLR Euler–Maruyama method, for which convergence—at least under our proof strategy—may blow up exponentially fast with respect to the inverse of the smallest singular value and requires a time-step condition that imposes a lower bound on the same singular value. To establish such singular-value-independent results, we first present the following lemma on an  $L^2$ -norm bound. Notably, we do not impose any condition on  $\Delta t_n$ , in contrast to the analogous result in Lemma 4.2 for the DLR-EM scheme.

**Lemma 5.1** ( $L^2$ -norm bound of DLR Projector Splitting for EM). *Let  $X_n = U_n^\top Y_n$ ,  $n = 0, \dots, N$  be the solution produced by Algorithm 2 with an arbitrary step-size  $\Delta t_n$  such that  $\sum_{n=1}^N \Delta t_n = T$ . Under Assumptions 2–3, the following bound on the mean square norm of  $X_n$  holds*

$$\mathbb{E}[|X_n|^2] \leq (\mathbb{E}[|X_0|^2] + 1) e^{(1+C_{\text{lgb}}(2+T))t_n} - 1 := K_4(t_n). \quad (50)$$

*Proof.* The proof follows a similar structure to that of Lemma 4.2. Thanks to Lemma 3.2 we have that

$$\mathbb{E}[|X_{n+1}|^2] \leq \mathbb{E}[|X_n|^2] + 2\mathbb{E}[X_n^\top a_n] \Delta t_n + \mathbb{E}[|a_n|^2] (\Delta t_n)^2 + \mathbb{E}[|b_n|^2] \Delta t$$

Then, via Assumption 2, Young inequality, Cauchy–Schwarz inequality, properties of orthogonal projectors, and properties of the Brownian increments, one gets

$$\begin{aligned} \mathbb{E}[|X_{n+1}|^2] &\leq \mathbb{E}[|X_n|^2] + \mathbb{E}[|X_n|^2] \Delta t_n + C_{\text{lgb}}(1 + \mathbb{E}[|X_n|^2]) \Delta t_n + C_{\text{lgb}}(1 + \mathbb{E}[|X_n|^2]) \Delta t_n^2 \\ &\quad + C_{\text{lgb}}(1 + \mathbb{E}[|X_n|^2]) \Delta t_n \\ &= \mathbb{E}[|X_n|^2] + \mathbb{E}[|X_n|^2] \Delta t_n + 2C_{\text{lgb}}(1 + \mathbb{E}[|X_n|^2]) \Delta t_n + C_{\text{lgb}}(1 + \mathbb{E}[|X_n|^2]) \Delta t_n^2 \\ &\leq \mathbb{E}[|X_n|^2] + \mathbb{E}[|X_n|^2] \Delta t_n + C_{\text{lgb}}(2 + T)(1 + \mathbb{E}[|X_n|^2]) \Delta t_n, \end{aligned} \quad (51)$$

where in the last line we used the trivial fact that  $\Delta t_n \leq T$ .

For the ease of notation, define  $Z_n = 1 + \mathbb{E}[|X_n|^2]$ . The result follows by induction, as done in the proof of Lemma 4.2; we claim that

$$Z_n \leq Z_0 e^{(1+C_{\text{lgb}}(2+T))t_n}, \quad \forall n. \quad (52)$$

By construction, the induction hypothesis holds for  $n = 0$ . On the other hand, from (51) by adding 1 on the left-hand side and  $1 + \Delta t_n$  on the right-hand side one has that

$$Z_{n+1} \leq Z_n + (1 + C_{\text{lgb}}(2 + T))Z_n \Delta t_n.$$

Then, using (52) one gets

$$\begin{aligned} Z_{n+1} &\leq Z_n (1 + (1 + C_{\text{lgb}}(2 + T)) \Delta t_n) \\ &\leq Z_0 e^{(1+C_{\text{lgb}}(2+T))t_n} (1 + (1 + C_{\text{lgb}}(2 + T)) \Delta t_n) \\ &\leq Z_0 e^{(1+C_{\text{lgb}}(2+T))t_n} e^{(1+C_{\text{lgb}}(2+T))\Delta t_n} \\ &= Z_0 e^{(1+C_{\text{lgb}}(2+T))t_{n+1}}, \end{aligned}$$

which concludes the proof.  $\square$

In Lemma 4.2, we derived a mean-squared bound of the DLR Euler–Maruyama solution, subject to a time-step condition dependent on the smallest singular value of the Gramian of  $Y_n$ . This result is subsequently applied in Proposition 5.1 to derive a lower bound on the smallest singular value of the Gramian under assumption of uniformly elliptic noise.

In contrast, for the DLR Projector Splitting for EM method, Lemma 4.2 imposes no restrictions on  $\Delta t_n$ . Consequently, the following Proposition, analogous to Propositions 4.1 and 4.5, derives a lower-bound on the smallest singular value of the Gramian under no time step-restrictions if the noise is uniformly elliptic.

**Proposition 5.2.** Suppose Assumption 5 is satisfied. Then for any sequence of step-sizes  $\{\Delta t_n\}_n$  we have:

$$C_{Y_{n+1}} \succ \sigma_B \Delta t_n \cdot I_{k \times k}. \quad (53)$$

If, moreover, Assumption 4 holds as well, then for a uniform step-size  $\Delta t$  one has

$$C_{Y_{n+1}} \succeq \min\{\sigma_0, \frac{\sigma_B^2}{4C_{\text{lgb}}(1+K_4(T))}\} + \frac{\sigma_B}{2} \Delta t \left[ 1 - \left( 1 - \frac{1}{1 + \frac{\sigma_B}{2C_{\text{lgb}}(1+K_4(T))\Delta t}} \right)^{n+1} \right]. \quad (54)$$

*Proof.* The proof closely follows those of Propositions 4.1 and 4.5.  $\square$

The following result establishes the accuracy of the DLR solution and its numerical approximation given by Algorithm 2.

**Proposition 5.3** (Numerical Convergence of Algorithm 2 to the continuous DLRA). Consider a uniform partition  $\Delta := \{t_n = t_0 + n\Delta t, n = 0, \dots, N\}$  of  $[0, T]$  with time-step  $\Delta t$  and define  $n_s = \max\{n = 0, 1, \dots, N : t_n \leq s\}$ . Let us denote by  $X_n^{\text{EM}}$  the numerical approximation of (2) obtained by a standard Euler-Maruyama method and by  $\mathcal{X}^{\text{EM}}(t)$  its continuous interpolation computed at time  $t$  starting at  $X_0^{\text{true}}$ , namely:

$$\mathcal{X}^{\text{EM}}(t) = X_n^{\text{EM}} + \int_{t_n}^t a(t_n, X_n^{\text{EM}}) ds + b(t_n, X_n^{\text{EM}}) dW_s, \quad t_n \leq t < t_{n+1}.$$

Let us denote by  $X_n$  the numerical DLR solution obtained with the Algorithm 2. Assume (41) and (47) to be valid. Then

$$\sqrt{\mathbb{E} \left[ \sup_{0 \leq s \leq t} |X_{n_s} - \mathcal{X}^{\text{EM}}(t_{n_s})|^2 \right]} \leq C \left( \sqrt{\mathbb{E}[|X_0 - X_0^{\text{true}}|^2]} + (\Delta t)^{\frac{1}{2}} + \varepsilon + \frac{\varepsilon}{\sqrt{\Delta t}} \right),$$

holds for some positive constant  $C$  independent of the smallest singular value of the covariance matrices  $\mathbb{E}[Y(t)Y^\top(t)]$  for all  $t \in [0, T]$  and  $\mathbb{E}[Y_n Y_n^\top]$  for all  $n \in \{0, 1, \dots, N\}$ .

*Proof.* Recall  $n_s = \max\{n = 0, 1, \dots, N : t_n \leq s\}$ . We define the following continuous approximation for all  $0 \leq n \leq N-1$ :

$$\mathcal{X}(t) := X_n + P_{U_n^\top \tilde{Y}_{n+1}} [a(t_n, U_n^\top Y_n)(t - t_n) + b_n(W_t - W_n)], \quad t_n < t \leq t_{n+1}.$$

where  $Y_n$  and  $U_n$  are obtained at the end of time  $t_n$  in Algorithm 2.

In the interval  $t_n \leq t < t_{n+1}$ , we define the following projector

$$\mathcal{P}_{\mathcal{X}(t)}[B] := (I - \mathcal{P}_{\mathcal{U}(t)}) \mathcal{P}_{\mathcal{Y}(t)}[B] + \mathcal{P}_{\mathcal{U}(t)}[B], \quad \text{for all } B \in L^2(\Omega, \mathbb{R}^d),$$

where  $\mathcal{P}_{\mathcal{U}(t)}$  is the projector onto the range of  $X(t)$ , where  $\mathcal{P}_{\mathcal{Y}(t)}$  is the projector onto the corange of  $X(t)$ . Then, one has

$$\mathcal{X}(t) = X_n + P_{U_n^\top \tilde{Y}_{n+1}} \left[ \int_{t_n}^t a_n ds + \int_{t_n}^t b_n dW_s \right].$$

Therefore, we can write:

$$\begin{aligned}
\mathbb{E} \left[ \sup_{0 \leq s \leq t} |X_{n_s} - \mathcal{X}^{\text{EM}}(t_{n_s})|^2 \right] &= \mathbb{E} \left[ \sup_{0 \leq s \leq t} |\mathcal{X}(t_{n_s}) - \mathcal{X}^{\text{EM}}(t_{n_s})|^2 \right] \\
&\leq \left( \mathbb{E} \left[ \sup_{0 \leq s \leq t} \left| X_0 - X_0^{\text{true}} + \sum_{n=0}^{n_s-1} P_{U_n^{\top} \tilde{Y}_{n+1}} \left[ \int_{t_n}^{t_{n+1}} a_n \, dr + b_n \, dW_r \right] \right. \right. \right. \\
&\quad \left. \left. \left. - \left( \int_0^{t_{n_s}} a(t_{n_r}, X_{n_r}^{\text{EM}}) \, dr + b(t_{n_r}, X_{n_r}^{\text{EM}}) \, dW_r \right) \right|^2 \right] \right) \\
&\leq 3 \left( \mathbb{E} [|X_0 - X_0^{\text{true}}|^2] \right. \\
&\quad \left. + \mathbb{E} \left[ \sup_{0 \leq s \leq t} \left| \sum_{n=0}^{n_s-1} \left( \int_{t_n}^{t_{n+1}} P_{U_n^{\top} \tilde{Y}_{n+1}} a_n \, dr - \int_{t_n}^{t_{n+1}} a(t_n, X_n^{\text{EM}}) \, dr \right) \right|^2 \right] \right. \\
&\quad \left. + \mathbb{E} \left[ \sup_{0 \leq s \leq t} \left| \left( \sum_{n=0}^{n_s-1} P_{U_n^{\top} \tilde{Y}_{n+1}} \left[ \int_{t_n}^{t_{n+1}} b_n \, dW_r \right] - \int_{t_n}^{t_{n+1}} b(t_n, X_n^{\text{EM}}) \, dW_r \right) \right|^2 \right] \right) \\
&\leq 3\mathbb{E} [|X_0 - X_0^{\text{true}}|^2] + 3\mathbb{E} \left[ \sup_{0 \leq s \leq t} \left| \left( \int_0^{t_{n_s}} P_{U_{n_r}^{\top} \tilde{Y}_{n_r+1}} a_{n_r} - a(t_{n_r}, X_{n_r}^{\text{EM}}) \, dr \right) \right|^2 \right] \\
&\quad + 3\mathbb{E} \left[ \sup_{0 \leq s \leq t} \left| \left( \sum_{n=0}^{n_s-1} P_{U_n^{\top} \tilde{Y}_{n+1}} \left[ \int_{t_n}^{t_{n+1}} b_n \, dW_r \right] - \int_{t_n}^{t_{n+1}} b(t_n, X_n^{\text{EM}}) \, dW_r \right) \right|^2 \right] \\
&\leq 3\mathbb{E} [|X_0 - X_0^{\text{true}}|^2] + 3T \underbrace{\left( \int_0^t \mathbb{E} \left[ \left| P_{U_{n_r}^{\top} \tilde{Y}_{n_r+1}} a_{n_r} - a(t_{n_r}, X_{n_r}^{\text{EM}}) \right|^2 \right] \, dr \right)}_{:= T_1} \\
&\quad + 3 \underbrace{\mathbb{E} \left[ \sup_{0 \leq s \leq t} \left| \left( \sum_{n=0}^{n_s-1} P_{U_n^{\top} \tilde{Y}_{n+1}} [b_n \Delta W_n] - b(t_n, X_n^{\text{EM}}) \Delta W_n \right) \right|^2 \right]}_{:= T_2}.
\end{aligned}$$

Concerning  $T_1$  we have by (41), (47), (50) and Assumptions 1 and 2 that

$$\begin{aligned}
\mathbb{E} [|P_{U_n^{\top} \tilde{Y}_{n+1}} a_n - a(t_n, X_n^{\text{EM}})|^2] &= \mathbb{E} [| - P_{U_n^{\top} \tilde{Y}_{n+1}}^{\perp} a_n + P_{U_n^{\top} \tilde{Y}_{n+1}}^{\perp} a_n + P_{U_n^{\top} \tilde{Y}_{n+1}} a_n - a(t_n, X_n^{\text{EM}})|^2] \\
&= \mathbb{E} [| - P_{U_n^{\top} \tilde{Y}_{n+1}}^{\perp} a_n + a_n - a(t_n, X_n^{\text{EM}})|^2] \\
&= \mathbb{E} [|P_{U_n^{\top} \tilde{Y}_{n+1}}^{\perp} [-a_n - a(t_n, U_n^{\top} \tilde{Y}_{n+1}) + a(t_n, U_n^{\top} \tilde{Y}_{n+1})] + a_n - a(t_n, X_n^{\text{EM}})|^2] \\
&\leq 3\mathbb{E} [|P_{U_n^{\top} \tilde{Y}_{n+1}}^{\perp} [a_n - a(t_n, U_n^{\top} \tilde{Y}_{n+1})]|^2] \\
&\quad + 3\mathbb{E} [|P_{U_n^{\top} \tilde{Y}_{n+1}}^{\perp} a(t_n, U_n^{\top} \tilde{Y}_{n+1})|^2] + 3\mathbb{E} [|a_n - a(t_n, X_n^{\text{EM}})|^2] \\
&\leq 3\mathbb{E} [|P_{U_n^{\top} \tilde{Y}_{n+1}}^{\perp} [a(t_n, U_n^{\top} Y_n) - a(t_n, U_n^{\top} \tilde{Y}_{n+1})]|^2] + 3\varepsilon^2 + 3C_{\text{Lip}}\mathbb{E} [|X_n - X^{\text{EM}}(t_n)|^2] \\
&\leq 3C_{\text{Lip}}\mathbb{E} [|Y_n - \tilde{Y}_{n+1}|^2] + 3\varepsilon^2 + 3C_{\text{Lip}}\mathbb{E} [|X_n - X^{\text{EM}}(t_n)|^2] \\
&\leq 3C_{\text{Lip}}\mathbb{E} [|U_n a_n \Delta t + U_n b_n \Delta W_n|^2] + 3\varepsilon^2 + 3C_{\text{Lip}}\mathbb{E} [|X_n - X^{\text{EM}}(t_n)|^2] \\
&\leq 6C_{\text{Lip}}C_{\text{lgb}}(1 + K_4(T)) ((\Delta t)^2 + \Delta t) + 3\varepsilon^2 + 3C_{\text{Lip}}\mathbb{E} \left[ \sup_{0 \leq s \leq t} |X_{n_s} - X^{\text{EM}}(t_{n_s})|^2 \right].
\end{aligned}$$

On the other hand, for  $T_2$  from

$$\begin{aligned}
P_{U_n^{\top} \tilde{Y}_{n+1}} [b_n \Delta W_n] - b(t_n, X_n^{\text{EM}}) \Delta W_n &= (I_{d \times d} - P_{U_n}^{\text{row}}) \mathbb{E} \left[ (b_n \Delta W_n) \tilde{Y}_{n+1}^{\top} \right] C_{\tilde{Y}_{n+1}}^{-1} \tilde{Y}_{n+1} + P_{U_n}^{\text{row}} b_n \Delta W_n \\
&\quad + (P_{U_n}^{\text{row}})^{\perp} [b_n \Delta W_n] - (P_{U_n}^{\text{row}})^{\perp} [b_n \Delta W_n] - b(t_n, X_n^{\text{EM}}) \Delta W_n \\
&= \mathbb{E} \left[ (I_{d \times d} - P_{U_n}^{\text{row}}) (b_n \Delta W_n) \tilde{Y}_{n+1}^{\top} \right] C_{\tilde{Y}_{n+1}}^{-1} \tilde{Y}_{n+1} \\
&\quad - (P_{U_n}^{\text{row}})^{\perp} [b_n \Delta W_n] + (b_n - b(t_n, X_n^{\text{EM}})) \Delta W_n.
\end{aligned}$$

and usual inequalities one has

$$\begin{aligned} T_2 &\leq 3\mathbb{E}\left[\sup_{0 \leq s \leq t} \left| \left( \sum_{n=0}^{n_s-1} \mathbb{E}\left[\left(I_{d \times d} - P_{U_n}^{\text{row}}\right) (b_n \Delta W_n) \tilde{Y}_{n+1}^{\top}\right] C_{\tilde{Y}_{n+1}}^{-1} \tilde{Y}_{n+1} \right) \right|^2\right] \\ &\quad + 3\mathbb{E}\left[\sup_{0 \leq s \leq t} \left| \sum_{n=0}^{n_s-1} \int_{t_n}^{t_{n+1}} (P_{U_n}^{\text{row}})^{\perp} [b_n] dW_s \right|^2\right] + 3\mathbb{E}\left[\sup_{0 \leq s \leq t} \left| \int_0^{t_{n_s}} (b_{n_r} - b(t_{n_r}, X_{n_r}^{\text{EM}})) dW_r \right|^2\right]. \end{aligned}$$

Using Cauchy-Schwarz inequality and (47), one obtains that

$$\begin{aligned} &\mathbb{E}\left[\sup_{0 \leq s \leq t} \left| \left( \sum_{n=0}^{n_s-1} \mathbb{E}\left[\left(I_{d \times d} - P_{U_n}^{\text{row}}\right) (b_n \Delta W_n) \tilde{Y}_{n+1}^{\top}\right] C_{\tilde{Y}_{n+1}}^{-1} \tilde{Y}_{n+1} \right) \right|^2\right] \\ &= \mathbb{E}\left[\sup_{0 \leq s \leq t} \left| \left( \sum_{n=0}^{n_s-1} \mathbb{E}\left[\left(I_{d \times d} - P_{U_n}^{\text{row}}\right) (b_n \Delta W_n) \tilde{Y}_{n+1}^{\top} C_{\tilde{Y}_{n+1}}^{-\frac{1}{2}}\right] C_{\tilde{Y}_{n+1}}^{-\frac{1}{2}} \tilde{Y}_{n+1} \right) \right|^2\right] \\ &\leq \mathbb{E}\left[\sup_{0 \leq s \leq t} \left| \left( \sum_{n=0}^{n_s-1} \left| \left( \mathbb{E}\left[\left(I_{d \times d} - P_{U_n}^{\text{row}}\right) b_n\right]^2 \right)^{\frac{1}{2}} \left( \mathbb{E}\left[\left|\Delta W_n \tilde{Y}_{n+1}^{\top} C_{\tilde{Y}_{n+1}}^{-\frac{1}{2}}\right|^2\right] \right)^{\frac{1}{2}} C_{\tilde{Y}_{n+1}}^{-\frac{1}{2}} \tilde{Y}_{n+1} \right) \right|^2\right] \\ &\leq \mathbb{E}\left[\sup_{0 \leq s \leq t} \left| \left( \sum_{n=0}^{n_s-1} (\varepsilon^2)^{\frac{1}{2}} (\mathbb{E}\left[\left|\Delta W_n\right|^2\right])^{\frac{1}{2}} \left| C_{\tilde{Y}_{n+1}}^{-\frac{1}{2}} \tilde{Y}_{n+1} \right| \right) \right|^2\right] \\ &\leq \varepsilon^2 \mathbb{E}\left[\left| \sum_{n=0}^{n_t-1} (\Delta t)^{\frac{1}{2}} \left| C_{\tilde{Y}_{n+1}}^{-\frac{1}{2}} \tilde{Y}_{n+1} \right| \right|^2\right] \\ &\leq \varepsilon^2 \Delta t n_t \mathbb{E}\left[\sum_{n=0}^{n_t-1} \left| C_{\tilde{Y}_{n+1}}^{-\frac{1}{2}} \tilde{Y}_{n+1} \right|^2\right] \leq \frac{\varepsilon^2}{\Delta t} T^2 \end{aligned}$$

where in the last line we used the properties of the orthogonal projector in  $L^2$ . Then one has

$$\begin{aligned} T_2 &\leq 3\frac{\varepsilon^2}{\Delta t} T^2 + 12\mathbb{E}\left[\sum_{n=0}^{n_t-1} \int_{t_n}^{t_{n+1}} \left| (P_{U_n}^{\text{row}})^{\perp} b_n \right|^2 ds\right] + 12 \int_0^{t_{n_t}} \mathbb{E}[|b_{n_r} - b(t_{n_r}, X_{n_r}^{\text{EM}})|^2] dr \\ &\leq 3\frac{\varepsilon^2}{\Delta t} T^2 + 12 \int_0^{t_{n_t}} \varepsilon^2 dr + 12 \int_0^{t_{n_t}} \mathbb{E}[|b_{n_r} - b(t_{n_r}, X_{n_r}^{\text{EM}})|^2] dr \\ &\leq 3\frac{\varepsilon^2}{\Delta t} T^2 + 12T\varepsilon^2 + 12 \int_0^{t_{n_t}} C_{\text{Lip}} \mathbb{E}[|X_{n_r} - X_{n_r}^{\text{EM}}|^2] dr, \\ &\leq 3\frac{\varepsilon^2}{\Delta t} T^2 + 12T\varepsilon^2 + 12 \int_0^{t_{n_t}} C_{\text{Lip}} \mathbb{E}\left[\sup_{0 \leq s \leq r} |X_{n_s} - X^{\text{EM}}(t_{n_s})|^2\right] dr, \end{aligned}$$

where in the second inequality on the right-hand side we use the Doob's maximal inequality and from the second to the third inequality one employs (47).

Finally, by Gronwall's lemma we have

$$\begin{aligned} \mathbb{E}\left[\sup_{0 \leq s \leq t} |X_{n_s} - X^{\text{EM}}(t_{n_s})|^2\right] &\leq 3\mathbb{E}[|X_0 - X_0^{\text{EM}}|^2] + 3\frac{\varepsilon^2}{\Delta t} T^2 + 12T\varepsilon^2 \\ &\quad + T \int_0^{t_{n_t}} (18C_{\text{Lip}} C_{\text{lgb}} (1 + K_4(T)) ((\Delta t)^2 + \Delta t) + 9\varepsilon^2 \\ &\quad + 21C_{\text{Lip}} \mathbb{E}\left[\sup_{0 \leq s \leq r} |X_{n_s} - X^{\text{EM}}(t_{n_s})|^2\right]) dr \\ &\leq \left[ 3\mathbb{E}[|X_0^{\text{true}} - X_0|^2] + ((\Delta t)^2 + \Delta t) \right. \\ &\quad \left. \cdot [18C_{\text{Lip}} C_{\text{lgb}} (1 + K_4(T)) T^2] + 3T(4 + 3T)\varepsilon^2 + 3\frac{\varepsilon^2}{\Delta t} T^2 \right] e^{21C_{\text{Lip}} T}. \end{aligned}$$

These computations yield the result.  $\square$

**Remark 5.4** (Comments on convergence in Proposition 2). *The presence of the full diffusion term in the expectation given by the  $L^2$ -projection onto the stochastic basis makes the*

numerical solution be non-adapted at the filtration, which adds more difficulties in proving the convergence of the DLR Projector Splitting for EM. In case the  $\varepsilon$  quantity described by (47) were null, i.e.  $X^{\text{true}}$  is equal to  $X^{\text{DLRA}}$ , one would recover a time convergence of  $o(\sqrt{\Delta t})$  to the standard Euler-Maruyama. In addition, given the discretization provided by Algorithm 2, if one knows that for  $p > \frac{1}{2}$  one has

$$P_{U_n^\top \tilde{Y}_{n+1}}^\perp [a_n \Delta t + b_n \Delta W_n] \sim o(\Delta t^p),$$

then Proposition 2 gives us  $o(\Delta t^{\min\{\frac{1}{2}, p - \frac{1}{2}\}})$  as order of convergence in time between the numerical DLRA and the standard Euler-Maruyama approximation.

We conclude the section by the following result between a general SDE and the numerical solution of its DLR approximation given by the DLR Projector Splitting for EM.

**Theorem 5.5** (Numerical Convergence of the DLR Projector Splitting for EM). *Denote by  $X^{\text{true}}(t)$  the strong solution of (2) and by  $X_n$  the numerical solution obtained by the Algorithm 2. Suppose Assumptions (1)-(2) hold as well as (41) and (47). Then, there exists a constant  $C > 0$  independent of the smallest singular value of the covariance matrices  $\mathbb{E}[Y(t)Y^\top(t)]$  for all  $t \in [0, T]$  and  $\mathbb{E}[Y_n Y_n^\top]$  for all  $n \in \{0, 1, \dots, N\}$  such that*

$$\sqrt{\mathbb{E}[\sup_{0 \leq s \leq t} |X_{n_s} - X^{\text{true}}(s)|^2]} \leq C \left( \sqrt{\mathbb{E}[|X_0 - X_0^{\text{true}}|^2]} + (\Delta t)^{\min\{1/2, \alpha\}} + \varepsilon + \frac{\varepsilon}{\sqrt{\Delta t}} \right),$$

with  $n_s := \max\{n = 0, 1, \dots, N : t_n \leq s\}$ .

*Proof.* Let us denote by  $X_n^{\text{EM}}$  Euler-Maruyama numerical solution of (2) and by  $\mathcal{X}^{\text{EM}}(t)$  its continuous interpolation computed at time  $t$  starting from  $X_0^{\text{true}}$ . It holds

$$\mathbb{E}[\sup_{0 \leq s \leq t} |X_{n_s} - X^{\text{true}}(s)|^2] \leq 2\mathbb{E}[\sup_{0 \leq s \leq t} |X_{n_s} - \mathcal{X}_{n_s}^{\text{EM}}|^2] + 2\mathbb{E}[\sup_{0 \leq s \leq t} |\mathcal{X}_{n_s}^{\text{EM}} - X^{\text{true}}(s)|^2].$$

Considering the convergence of Euler-Maruyama method [23, Theorem 10.22], one has

$$\sqrt{\mathbb{E}[\sup_{0 \leq s \leq t} |X_{n_s}^{\text{EM}} - X^{\text{true}}(s)|^2]} \leq C(\Delta t)^{\min\{1/2, \alpha\}}.$$

Using Theorem 5.3, the thesis follows.  $\square$

## 5.1 Mean Square Stability of the DLR Projector Splitting for EM

In this section, we study the mean-square stability of the proposed DLR Projector Splitting for EM. Its projected nature turns out to be extremely beneficial in terms of stability, also because it allows us to retrieve an easy-to-verify sufficient condition for mean-square stability. Assuming that

$$a(t, 0) \equiv 0, \quad b(t, 0) \equiv 0, \quad t \in [0, T],$$

we will consider the following definition of  $p$ -stability [20, 29] throughout this work.

**Definition 5.6** ( $p$ -stability and asymptotically  $p$ -stability). *Let us denote with  $X^{s,x}$  the solution of (2) with initial condition  $X^{\text{true}}(s) = x \in \mathbb{R}^d$ , with  $s > 0$ . A solution  $X^{\text{true}}(t, \omega) \equiv 0$  of (2) is said to be  $p$ -stable for  $t \geq 0$  if*

$$\lim_{\delta \rightarrow 0} \sup_{\{|x| \leq \delta, t \geq s\}} \mathbb{E}[|X^{s,x}|^p] = 0.$$

Moreover, if there exists  $\delta := \delta(s) > 0$  such that

$$\lim_{t \rightarrow +\infty} \mathbb{E}[|X^{s,x}|^p] = 0$$

also holds for all  $s > 0$  and  $|x| < \delta$ , then  $X(t, \omega) \equiv 0$  is said to be asymptotically  $p$ -stable.

We will focus, in particular, to the case  $p = 2$ , which is the so-called *mean-square stability*. A mean-square stable system is also mean stable ( $p = 1$ ). For the sake of completeness, we recall that for autonomous linear equations (asymptotical)  $p$ -stability implies (asymptotical) stability in probability [2, 20], namely for all  $s \geq 0$ , and for all  $\varepsilon > 0$   $\lim_{x \rightarrow 0} \mathbb{P}\{\sup_{t \geq s} |X^{s,x}(t)| > \varepsilon\} = 0$ , and the asymptotically  $p$ -stability implies the asymptotically stability in probability, i.e.  $\lim_{x \rightarrow 0} \mathbb{P}\{\lim_{t \rightarrow \infty} |X^{s,x}(t)| > \varepsilon\} = 0$ .

To study the stability of the DLR Projector splitting scheme for EM, we restrict to the case of a linear SDE [36, 14, 35], as it is common in the literature. More precisely, given time-dependent deterministic matrices  $A(t), B_k(t) \in \mathbb{R}^{d \times d}$ , for  $k = 1, \dots, m$ , we consider the SDE:

$$dX^{\text{true}}(t) = A(t)X^{\text{true}}(t)dt + \sum_{k=1}^m B_k(t)X^{\text{true}}(t)dW_t^k, \quad \text{for all } t \in [0, +\infty), X_0 = c \in \mathbb{R}^d, \quad (55)$$

where the initial datum  $X_0$  can be deterministic or random, as it does not have any influence on the stability analysis [29]. Via an Itô's formula argument we find the following inequality

$$d\mathbb{E}[(X^{\text{true}}(t))^{\top} X^{\text{true}}(t)] \leq \left( \lambda_{\max}(A(t) + A^{\top}(t)) + \sum_{k=1}^m |B_k(t)|^2 \right) \mathbb{E}[|X^{\text{true}}(t)|^2]dt, \quad (56)$$

which implies that (55) is asymptotically mean-square (AMS) stable if

$$\lambda_{\max}(A(t) + A^{\top}(t)) < - \sum_{k=1}^m |B_k(t)|^2. \quad (57)$$

As the next proposition shows, a sufficient condition for AMS stability of the DLR approximation of (55) is still (57), that is, under (57), both the SDE and its continuous DLRA are AMS stable.

**Proposition 5.7** (Mean-square stability of the continuous DLRA). *Under condition (57), the DLR approximation of (55) is AMS stable.*

*Proof.* The DO equations for (55) read as follows

$$\begin{aligned} \dot{U}(t) &= U(t)A^{\top}(t) \left( I_{d \times d} - P_{U(t)}^{\text{row}} \right), \\ dY(t) &= U(t)A(t)U(t)^{\top}Y(t)dt + U(t) \sum_{k=1}^m B_k(t)U(t)^{\top}Y(t)dW_t^k, \end{aligned}$$

and, hence, our DLR approximation is expressed via

$$dX(t) = A(t)U(t)^{\top}Y(t)dt + U^{\top}(t)U(t) \sum_{k=1}^m B_k(t)U(t)^{\top}Y(t)dW_t^k. \quad (58)$$

We compute an upper bound of the second moment of the solution  $X(t)$  via Itô's formula:

$$d\mathbb{E}[X(t)^{\top} X(t)] \leq \lambda_{\max}(A(t) + A^{\top}(t))\mathbb{E}[|X(t)|^2]dt + \mathbb{E}[|X(t)|^2] \sum_{k=1}^m |U(t)B_k(t)|^2dt.$$

Therefore, one finally gets

$$\frac{d\mathbb{E}[|X(t)|^2]}{dt} \leq \left( \lambda_{\max}(A(t) + A^{\top}(t)) + \sum_{k=1}^m |B_k(t)|^2 \right) \mathbb{E}[|X(t)|^2], \quad (59)$$

and, hence,

$$\lim_{t \rightarrow \infty} \mathbb{E}[|X(t)|^2] = 0,$$

under (57).  $\square$

One can notice that no dependence on the smallest singular value is present in (59), as the deterministic modes evolve independently of the stochastic ones for this simple linear model.

Let us now turn to the numerical discretization. The usual Euler-Maruyama method for equation (55) reads as follows:

$$X_{n+1} = X_n + A(t_n)X_n\Delta t_n + \sum_{k=i}^m B_k(t_n)X_n\Delta W_n^k,$$

and, its mean-square norm can be bounded as

$$\begin{aligned} \mathbb{E}[|X_{n+1}|^2] &= \mathbb{E}[|X_n|^2] + \mathbb{E}[X_n^\top A(t_n)X_n]\Delta t_n + \mathbb{E}[X_n^\top A^\top(t_n)X_n]\Delta t_n + \mathbb{E}[X_n^\top A^\top(t_n)A(t_n)X_n](\Delta t_n)^2 \\ &\quad + \mathbb{E}[X_n^\top \sum_{k=1}^m B_k^\top(t_n)B_k(t_n)X_n](\Delta t_n) \\ &\leq \mathbb{E}[|X_n|^2] \left( 1 + \lambda_{\max}(A(t_n) + A^\top(t_n))\Delta t_n + \sigma_{\max}(A(t_n))^2(\Delta t_n)^2 + \sum_{k=1}^m |B_k(t_n)|^2(\Delta t_n) \right). \end{aligned}$$

Therefore, a sufficient condition for AMS stability for the Euler-Maruyama scheme is

$$\left| 1 + \lambda_{\max}(A(t_n) + A^\top(t_n))\Delta t_n + \sigma_{\max}(A(t_n))^2(\Delta t_n)^2 + \sum_{k=1}^m |B_k(t_n)|^2\Delta t_n \right| < 1. \quad (60)$$

The next proposition shows that the DLR Projector Splitting for EM (Algorithm 2) is AMS stable under the same condition (60) as the standard Euler-Maruyama scheme.

**Proposition 5.8** (Mean-square stability of the DLR Projector Splitting for EM). *Under condition (60), the DLR Projector Splitting for EM applied to (55) is AMS stable.*

*Proof.* The DLR Projector Splitting for EM applied to equation (58) reads as follows:

$$X_{n+1} = X_n + \underbrace{\left( (I_{d \times d} - P_{U_n}^{\text{row}}) P_{\tilde{Y}_{n+1}} + P_{U_n}^{\text{row}} \right)}_{P_{U_n^\perp \tilde{Y}_{n+1}}} [A(t_n)X_n\Delta t_n + \left( \sum_{k=1}^m B_k(t_n)X_n\Delta W_n^k \right)].$$

It follows that

$$\mathbb{E}[X_n^\top (X_{n+1} - X_n)] = \mathbb{E}[X_n^\top A(t_n)X_n]\Delta t_n,$$

and, via using Lemma 3.2, that

$$\begin{aligned} \mathbb{E}[(X_{n+1} - X_n)^\top (X_{n+1} - X_n)] &\leq \mathbb{E}[|A(t_n)X_n|^2](\Delta t_n)^2 + \sum_{k=1}^m \mathbb{E}[|B_k(t_n)X_n|^2](\Delta t_n) \\ &\leq \left( \sigma_{\max}(A(t_n))^2(\Delta t_n)^2 + \sum_{k=1}^m |B_k(t_n)|^2(\Delta t_n) \right) \mathbb{E}[|X_n|^2]. \end{aligned}$$

Exploiting the relation

$$\mathbb{E}[X_n^\top (X_{n+1} - X_n)] + \mathbb{E}[(X_{n+1} - X_n)^\top X_n] = \mathbb{E}[|X_{n+1}|^2] - \mathbb{E}[|X_n|^2] - \mathbb{E}[(X_{n+1} - X_n)^\top (X_{n+1} - X_n)], \quad (61)$$

we obtain

$$\begin{aligned} \mathbb{E}[|X_{n+1}|^2] &\leq \mathbb{E}[|X_n|^2] + \mathbb{E}[X_n^\top (A(t_n) + A^\top(t_n))X_n]\Delta t_n + \left( \sigma_{\max}(A(t_n))^2(\Delta t_n)^2 \right. \\ &\quad \left. + \sum_{k=1}^m |B_k(t_n)|^2(\Delta t_n) \right) \mathbb{E}[|X_n|^2] \\ &\leq \mathbb{E}[|X_n|^2] \left( 1 + \lambda_{\max}(A(t_n) + A^\top(t_n))\Delta t_n + \sigma_{\max}(A(t_n))^2(\Delta t_n)^2 + \sum_{k=1}^m |B_k(t_n)|^2(\Delta t_n) \right), \end{aligned} \quad (62)$$

hence the scheme is AMS stable under (60).  $\square$

The previous proposition shows that the DLR projector splitting scheme for EM is AMS stable under a condition that does not depend on the smallest singular value of the numerical DLR solution.

## 6 Analysis of the DLR Projector Splitting for SDEs

In this section, convergence and mean-square stability analyses of Algorithm 3 are briefly shown. By being a projected scheme as Algorithm 2, one can retrieve computational results akin to the ones of Section 5 via similar proofs, and constants independent of the smallest singular value of the numerical DLR solution.

**Lemma 6.1** ( $L^2$ -norm bound of DLR Projector Splitting for SDEs). *Let  $X_n = U_n^\top Y_n$ ,  $n = 0, \dots, N$  be the solution produced by Algorithm 3 with an arbitrary step-size  $\Delta t_n$  such that  $\sum_{n=1}^N \Delta t_n = T$ . Under Assumptions 2-3, the following bound on the mean square norm of  $X_n$  holds:*

$$\mathbb{E}[|X_n|^2] \leq (\mathbb{E}[|X_0|^2] + 1) e^{(1+C_{\text{lgb}}(2+T))t_n} - 1 = K_4(T). \quad (63)$$

**Proposition 6.2** (Lower bound of the Gramian of the stochastic modes). *Suppose Assumption 5 is satisfied. Then for any sequence of step-size  $\{\Delta t_n\}_n$  with  $\Delta t_n = t_{n+1} - t_n$  we have:*

$$C_{Y_{n+1}} \succ \sigma_B \Delta t_n \cdot I_{k \times k}. \quad (64)$$

If Assumption 4 holds as well, then for a uniform step-size  $\Delta t$  one has

$$C_{Y_{n+1}} \succeq \min\{\sigma_0, \frac{\sigma_B^2}{4C_{\text{lgb}}(1+K_4(T))}\} + \frac{\sigma_B}{2} \Delta t \left[ 1 - \left( 1 - \frac{1}{1 + \frac{\sigma_B}{2C_{\text{lgb}}(1+K_4(T))\Delta t}} \right)^{n+1} \right]. \quad (65)$$

Unlike the DLR Projector Splitting for EM, Algorithm 3 does not present the full noise term inside the expectation. This structure provides a numerical algorithm that is adapted and an easier analysis of convergence, that results in a simpler dependence on the projection bound (47) than Algorithm 2.

**Theorem 6.3** (Numerical Convergence of the DLR Projector Splitting for SDEs). *Denote by  $X^{\text{true}}(t)$  the strong solution of (2) and by  $X_n$  the numerical solution obtained by Algorithm 3. Suppose Assumptions (1)-(2) hold as well as (41) and (47). Then, there exists a constant  $C > 0$  independent of the smallest singular value of the covariance matrices  $\mathbb{E}[Y(t)Y^\top(t)]$  for all  $t \in [0, T]$  and  $\mathbb{E}[Y_n Y_n^\top]$  for all  $n \in \{0, 1, \dots, N\}$  such that*

$$\sqrt{\mathbb{E}[\sup_{0 \leq s \leq t} |X^{\text{true}}(s) - X_{n_s}|^2]} \leq C \left( \sqrt{\mathbb{E}[|X_0^{\text{true}} - X_0|^2]} + (\Delta t)^{\min\{1/2, \alpha\}} + \varepsilon \right).$$

with  $n_s := \max\{n = 0, 1, \dots, N : t_n \leq s\}$ .

In Part II of this work, we will compare all the numerical algorithms to the continuous DLRA solution. For the number of samples that goes to infinity, we only managed to prove the convergence of stochastic discretization of this algorithm to the latter DLRA. Therefore, in order to use the DLR Projector Splitting for SDEs algorithm as a fully discretized procedure to well approximate the continuous DLRA (6), one needs to show convergence in time, too. Then, we conclude this section with a related basic result.

**Theorem 6.4** (Strong Convergence of DLR Projector Splitting for SDEs with respect to the DO solution). *Assume that  $a, b$  satisfy (1) and (2). Moreover, suppose that (41) holds. Consider a uniform partition  $\Delta := \{t_n : 0 = t_0 < t_1 < \dots < t_{N-1} < t_N = T\}$  of  $[0, T]$  and the time step  $\Delta t = t_{n+1} - t_n$  for all  $n$ . Define  $n_s = \max\{n = 0, 1, \dots, N : t_n \leq s\}$ . Furthermore, let us suppose that there exists a constant  $\gamma > 0$  such that  $|C_{Y(s)}^{-1}|, |C_{Y_{n_s}}^{-1}| \leq \gamma$  for all  $s \in [0, T]$ .*

*Then, the DLR Projector Splitting for SDEs method with constant time step  $\Delta t$  has strong order of convergence equal to  $\min\{\frac{1}{2}, \alpha\}$ , i.e. there exists a constant  $C := C(\gamma, k, T)$  independent of  $\Delta t$  such that for all  $0 \leq t \leq T$ :*

$$\sqrt{\mathbb{E}[\sup_{0 \leq s \leq t} |X_{n_s} - X(s)|^2]} \leq C(\Delta t)^{\min\{1/2, \alpha\}} + o((\Delta t)^{\min\{1/2, \alpha\}}).$$

*Proof.* The proof follows very closely to the one of Theorem 4.7, hence we will present only the key steps here. Fix  $n$ . Suppose that we have just completed Step 6 of Algorithm 3; then we know

$$X_{n+1} = U_{n+1}^\top Y_{n+1} = \tilde{U}_{n+1}^\top \tilde{Y}_{n+1},$$

where  $\tilde{U}_{n+1}, \tilde{Y}_{n+1}$  are the update of the deterministic and stochastic modes before the QR decomposition in Step 6 of Algorithm 3, respectively. We define the following continuous approximation for all  $0 \leq n \leq N-1$ :

$$\begin{aligned} \mathcal{X}(t) &:= X_n + U_n^\top U_n a_n(t - t_n) + U_n^\top U_n b_n(W_t - W_n) \quad t_n \leq t < t_{n+1} \\ &\quad + (I_{d \times d} - P_{U_n}^{\text{row}}) \underbrace{\mathbb{E} \left[ (a_n(t - t_n)) \tilde{Y}_{n+1}^\top \right] C_{\tilde{Y}_{n+1}}^{-1} \tilde{Y}_{n+1}}_{:= P_{\tilde{Y}_{n+1}}(dA(t, X_n))}, \\ &= X_n + \underbrace{\left( P_{U_n}^{\text{row}} + (I_{d \times d} - P_{U_n}^{\text{row}}) P_{\tilde{Y}_{n+1}} \right)}_{:= P_{U_n^\top \tilde{Y}_{n+1}}} [a(t_n, U_n^\top Y_n)(t - t_n)] + P_{U_n}^{\text{row}} b_n(W_t - W_n), \quad t_n \leq t < t_{n+1}. \end{aligned}$$

where  $Y_n$  and  $U_n$  are obtained at the end of time  $t_n$  in Algorithm 3. In the interval  $t_n \leq t < t_{n+1}$ , one has

$$\begin{aligned} \mathcal{X}(t) &= X_n + P_{U_n^\top \tilde{Y}_{n+1}} \left[ \int_{t_n}^t a_n ds \right] + P_{U_n}^{\text{row}} \left[ \int_{t_n}^t b_n dW_s \right] \\ &= X_n + \int_{t_n}^t P_{U_n^\top \tilde{Y}_{n+1}} [a_n] ds + \int_{t_n}^t P_{U_n}^{\text{row}} [b_n] dW_s. \end{aligned}$$

We want to estimate the error

$$\begin{aligned} \mathbb{E} \left[ \sup_{0 \leq s \leq t} |X(s) - X_{n_s}|^2 \right] &\leq 3\mathbb{E} \left[ \sup_{0 \leq s \leq t} \left| \int_0^{t_{n_s}} P_{X(r)} [a(r, X(r))] - P_{U_n^\top \tilde{Y}_{n+1}} [a_n] dr \right|^2 \right] \\ &\quad + 3\mathbb{E} \left[ \sup_{0 \leq s \leq t} \left| \int_0^{t_{n_s}} P_{U_r}^{\text{row}} [b(r, X(r))] - P_{U_n}^{\text{row}} [b_n] dW_r \right|^2 \right] \\ &\quad + 3\mathbb{E} \left[ \sup_{0 \leq s \leq t} \left| \int_{t_{n_s}}^s P_{X(r)} [a(r, X(r))] dr + P_{U_r}^{\text{row}} b(r, X(r)) dW_r \right|^2 \right] \\ &\leq 3T \int_0^{t_{n_t}} \mathbb{E} \left[ |P_{X(r)} [a(r, X(r))] - P_{U_n^\top \tilde{Y}_{n+1}} [a_n]|^2 \right] dr \\ &\quad + 12\mathbb{E} \left[ \left| \int_0^{t_{n_t}} P_{U_r}^{\text{row}} [b(r, X(r))] - P_{U_n}^{\text{row}} [b_n] dW_r \right|^2 \right] \\ &\quad + 3\mathbb{E} \left[ \sup_{0 \leq s \leq t} \left| \int_{t_{n_s}}^s P_{X(r)} [a(r, X(r))] dr + P_{U_r}^{\text{row}} b(r, X(r)) dW_r \right|^2 \right] \\ &= 3T \sum_{n=0}^{n_t-1} \int_{t_n}^{t_{n+1}} \mathbb{E} \left[ |P_{X(r)} [a(r, X(r))] - P_{U_n^\top \tilde{Y}_{n+1}} [a_n]|^2 \right] dr \\ &\quad + 12 \sum_{n=0}^{n_t-1} \int_{t_n}^{t_{n+1}} \mathbb{E} \left[ |P_{U_r}^{\text{row}} [b(r, X(r))] - P_{U_n}^{\text{row}} [b_n]|^2 \right] dr \\ &\quad + 3C_{\text{lgb}}(1 + K_1(T)) ((\Delta t)^2 + 4(\Delta t)) \\ &\leq 3T \sum_{n=0}^{n_t-1} \int_{t_n}^{t_{n+1}} \mathbb{E} \left[ |P_{X(r)} [a(r, X(r))] - P_{U_n^\top \tilde{Y}_{n+1}} [a_n]|^2 \right] dr \\ &\quad + 12 \sum_{n=0}^{n_t-1} \int_{t_n}^{t_{n+1}} \mathbb{E} \left[ |P_{U_r}^{\text{row}} [b(r, X(r))] - P_{U_n}^{\text{row}} [b_n]|^2 \right] dr \\ &\quad + 3C_{\text{lgb}}(1 + K_1(T)) ((\Delta t)^2 + 4(\Delta t)), \end{aligned}$$

where in the second line we use the Jensen's inequality and the Doob's inequality, in the third line we use the Itô's isometry, whereas for the last term in the right-hand side we use

the linear-growth bound, Lemma 63, Jensen's and Doob's inequalities, and Itô's isometry. For the first term on the right-hand side, using relations (3), (4), (41) [18, Proposition A.3], and Lemma 6.1, one can easily get that

$$\begin{aligned}
& \mathbb{E} \left[ |P_{X(r)}[a(r, X(r))] - P_{U_n^\top \tilde{Y}_{n+1}}[a_n]|^2 \right] \\
&= \mathbb{E} \left[ |P_{X(r)}[a(r, X(r))] - P_{X(r)}[a(t_n, X(r))] + P_{X(r)}[a(t_n, X(r))] - P_{X(r)}[a_n] \right. \\
&\quad \left. + P_{X(r)}[a_n] - P_{U_n^\top \tilde{Y}_{n+1}}[a_n]|^2 \right] \\
&\leq 3C_{\text{na}}(1 + K_1(T))(\Delta t)^\alpha + 3\mathbb{E} [|P_{X(r)}[a(t_n, X(r)) - a_n]|^2] + 3\mathbb{E} [|(\mathbb{P}_{X(r)} - P_{U_n^\top \tilde{Y}_{n+1}})[a_n]|^2] \\
&\leq 3C_{\text{na}}(1 + K_1(T))(\Delta t)^\alpha + 3C_{\text{Lip}}\mathbb{E} [|X(r) - X_n|^2] + 6C_{\text{lgb}}(1 + K_1(T))\gamma\mathbb{E} [|X(r) - U_n^\top \tilde{Y}_{n+1}|^2] \\
&\leq 3C_{\text{na}}(1 + K_1(T))(\Delta t)^\alpha + 3C_{\text{Lip}}\mathbb{E} [|X(r) - X_n|^2] \\
&\quad + 6C_{\text{lgb}}(1 + K_1(T))\gamma\mathbb{E} [|X(r) - X_n - U_n^\top U_n a_n \Delta t - U_n^\top U_n b_n \Delta W_n|^2] \\
&\leq 3C_{\text{na}}(1 + K_1(T))(\Delta t)^\alpha + 3C_{\text{Lip}}\mathbb{E} [|X(r) - X_n|^2] \\
&\quad + 18C_{\text{lgb}}(1 + K_1(T))\gamma\mathbb{E} [|X(r) - X_n|^2] + 18C_{\text{lgb}}^2(1 + K_1(T))^2 ((\Delta t)^2 + 4\Delta t).
\end{aligned}$$

Similarly, one can get that

$$\begin{aligned}
& \mathbb{E} [|P_{U_r}^{\text{row}}[b(r, X(r))] - P_{U_n}^{\text{row}}[b_n]|^2] \\
&\leq 3C_{\text{na}}(1 + K_1(T))(\Delta t)^\alpha + 3C_{\text{Lip}}\mathbb{E} [|X(r) - X_n|^2] + 6C_{\text{lgb}}(1 + K_1(T))\gamma\mathbb{E} [|X(r) - X_n|^2]
\end{aligned}$$

These computations lead us to

$$\begin{aligned}
\mathbb{E} \left[ \sup_{0 \leq s \leq t} |X(s) - X_{n_s}|^2 \right] &\leq 3T \int_0^T 3C_{\text{na}}(1 + K_1(T))(\Delta t)^\alpha + 3C_{\text{Lip}}\mathbb{E} [|X(r) - X_n|^2] \, dr \\
&\quad + 3T \int_0^T 18C_{\text{lgb}}(1 + K_1(T))\gamma\mathbb{E} [|X(r) - X_n|^2] \, dr \\
&\quad + 3T \int_0^T 18C_{\text{lgb}}^2(1 + K_1(T))^2 ((\Delta t)^2 + 4(\Delta t)) \, dr \\
&\quad + 12 \int_0^T 3C_{\text{na}}(1 + K_1(T))(\Delta t)^\alpha + 3C_{\text{Lip}}\mathbb{E} [|X(r) - X_n|^2] \, dr \\
&\quad + 12 \int_0^T 6C_{\text{lgb}}(1 + K_1(T))\gamma\mathbb{E} [|X(r) - X_n|^2] \, dr \\
&\quad + 3C_{\text{lgb}}(1 + K_1(T)) ((\Delta t)^2 + 4\Delta t).
\end{aligned}$$

Using the property of the sup on the right-hand side and Gronwall's lemma, we finally get the thesis.  $\square$

## 6.1 Mean Square Stability of the DLR Projector Splitting for SDEs

Finally, let us analyze the AMS stability of the DLR Projector Splitting for SDEs applied to the linear SDE (55). Having the same projected nature of the DLR Projector Splitting for EM turns out to be favorable in term of stability.

**Proposition 6.5** (Mean-square stability of the DLR Projector Splitting for SDEs). *Under condition (60), the DLR Projector Splitting for SDEs applied to (55) is AMS stable.*

*Proof.* The DLR Projector Splitting for SDEs applied to (55) reads as

$$X_{n+1} = X_n + P_{U_n^\top \tilde{Y}_{n+1}}[A(t_n)X_n]\Delta t_n + P_{U_n}^{\text{row}} \left[ \left( \sum_{k=1}^m B_k(t_n)X_n \Delta W_n^k \right) \right].$$

Then, similarly to what done in the proof of Proposition 5.8 we observe that

$$\mathbb{E}[X_n^\top (X_{n+1} - X_n)] = \mathbb{E}[X_n^\top A(t_n)X_n]\Delta t_n$$

and

$$\begin{aligned}
\mathbb{E}[(X_{n+1} - X_n)^\top (X_{n+1} - X_n)] &= \mathbb{E}[|P_{U_n^\top \tilde{Y}_{n+1}}[A(t_n)X_n]|^2](\Delta t_n)^2 + \sum_{k=1}^m \mathbb{E}[|P_{U_n}^{\text{row}}[B_k(t_n)X_n]|^2]\Delta t \\
&\leq \mathbb{E}[|A(t_n)X_n|^2](\Delta t_n)^2 + \sum_{k=1}^m \mathbb{E}[|B_k(t_n)X_n|^2]\Delta t \\
&\leq \left( \sigma_{\max}(A(t_n))^2(\Delta t_n)^2 + \sum_{k=1}^m |B_k(t_n)|^2(\Delta t_n) \right) \mathbb{E}[|X_n|^2].
\end{aligned}$$

This implies that (60) is a sufficient condition for the AMS stability of Algorithm 3, too.  $\square$

## 7 Numerical Experiments

In this section, we validate the results of Sections 4, 5, and 6 via computational experiments. All the averages in the computations in Algorithms 1, 2, and 3 as well as those needed in computing the  $L^2(\Omega)$ -errors, are calculated using a Monte-Carlo method (sample averages) using independent Brownian motions. The orthonormalization procedure done in the three aforementioned algorithms is always performed using a QR decomposition.

In all the simulations, we plot two types of errors for the three algorithms presented in Section 3. The first is the strong error which is measured against the continuous DLRA. Since a closed-form of the continuous DLRA solution is not available, we approximate it using a DLR Projector Splitting for SDEs on a finer time mesh, with the same number of particles as the numerical surrogate being tested. The choice of computing the reference DLRA via the DLR Projector Splitting for SDEs has been made due to the fact that we only manage to prove the convergence of this algorithm to the continuous DLRA with respect to both time discretization (see Theorem 6.4) and stochastic discretization via Monte Carlo method (see [19] for more details). For the sake of notation, in the caption of the figures of this section sometimes we will denote the continuous DLRA as  $DLR$ , whereas  $DLR_n$  will denote any of its numerical discretizations. The second type of error is also a strong error, but measured against the true solution  $X^{\text{true}}$  of the SDE under study. In all the simulations, we compute it using a standard Euler-Maruyama method [23] with the same number of time steps and paths used to compute the reference ‘‘continuous’’ DLR. We will refer to  $L^2 - \sup_{t \in [0, T]}$  as the following error between the two processes  $X, X^{\text{true}}$

$$\sqrt{\mathbb{E}[\sup_{t \in [0, T]} |X(t) - X^{\text{true}}(t)|^2]} \approx \sqrt{\mathbb{E}[\sup_{n \in [0, N]} |X_n - X^{\text{true}}(t_n)|^2]} \quad (66)$$

whereas the relative (rel.)  $L^2 - \sup_{t \in [0, T]}$  error will indicate

$$\sqrt{\frac{\mathbb{E}[\sup_{t \in [0, T]} |X(t) - X^{\text{true}}(t)|^2]}{\mathbb{E}[\sup_{t \in [0, T]} |X^{\text{true}}(t)|^2]}} \approx \sqrt{\frac{\mathbb{E}[\sup_{n \in [0, N]} |X_n - X^{\text{true}}(t_n)|^2]}{\mathbb{E}[\sup_{t \in [0, T]} |X^{\text{true}}(t)|^2]}}. \quad (67)$$

One can notice that fixed the true solution  $X^{\text{true}}$  that we want to approximate, the discrete error (67) is proportional to (66). Therefore, one expects to retrieve the same order of convergence obtained in Sections 4, 5, and 6. In the illustrated figures of this section, we will always consider (67), as it also gives us a direct ratio on how well the DLRA algorithms approximate the true solution pathwise.

Throughout this section,  $\sigma_i(C)$  denotes the  $i$ -th largest singular value of a matrix  $C \in \mathbb{R}^{n \times p}$ . Moreover, for the sake of notation, in the legends of the presented figures Algorithms 1, 2, and 3 will be denoted by DLR EM, DLR PS EM, and DLR PS SDE, respectively.

### 7.1 Basic SDE examples

First, we aim to corroborate the results of Propositions 4.1, 4.5, 5.2, and 6.2, as well as to numerically demonstrate convergence results. We simulate the following low-dimensional

stochastic process

$$\begin{pmatrix} dX_1^{\text{true}}(t) \\ dX_2^{\text{true}}(t) \\ dX_3^{\text{true}}(t) \end{pmatrix} = \begin{pmatrix} -0.1 \cdot X_1^{\text{true}}(t) & 0.1 \cdot X_2^{\text{true}}(t) & 0.001 \cdot X_3^{\text{true}}(t) \\ -0.1 \cdot X_1^{\text{true}}(t) & 0.1 \cdot X_2^{\text{true}}(t) & 0.001 \cdot X_3^{\text{true}}(t) \\ -4 \cdot X_1^{\text{true}}(t) & -4 \cdot X_2^{\text{true}}(t) & -4 \cdot X_3^{\text{true}}(t) \end{pmatrix} dt \\ + \sqrt{\sigma_B} \begin{bmatrix} 1 + 6(|X_1^{\text{true}}(t)| + |X_2^{\text{true}}(t)|) & 0 & 0 \\ 0 & 1 + 6(|X_1^{\text{true}}(t)| + |X_2^{\text{true}}(t)|) & 0 \\ 0 & 0 & 1 \end{bmatrix} \cdot \begin{pmatrix} dW_1(t) \\ dW_2(t) \\ dW_3(t) \end{pmatrix} \quad (68)$$

with  $t \in [0, 10]$ . The initial datum is given by the random vector of component  $X_i^{\text{true}}(0) = 0.1 - \text{Un}_i$ , for  $i = 1, 2$ , where each  $\text{Un}_i$  is an independent uniform random variable taking values in the interval  $[-0.0001, 0.0001]$ . Therefore the initial condition  $X^{\text{true}}$  has rank equal to 2. Moreover, we choose  $\sigma_B = 10^{-8}$ . For this numerical experiment we compute  $M = 10000$  paths and choose a rank  $k = 2$ .

To initialize all the DLRA algorithms, we employ a low-rank approximation of the “discretized” initial datum. Specifically, the initial condition of Algorithms 1, 2, and 3, is the rank- $k$  best approximation with respect to the Frobenius norm of  $[X_1^{\text{true}}(0), \dots, X_M^{\text{true}}(0)] \in \mathbb{R}^{d \times M}$ , namely the rank- $k$  truncated SVD of the matrix whose columns are the  $M$  realizations of  $X_0^{\text{true}}$ . In relation (68), we remark that the drift and the diffusion coefficients for the first two components are the same, up to different Brownian motions. Moreover, the diffusion coefficient is constructed so that  $\sigma_B$  is actually the lower-bound quantity described in Assumption 5. Then, we expect that for all the DLRA algorithms of rank  $k = 2$  we obtain a good approximation of the full-order solution of (68) over time discretization and that the covariance of the stochastic basis is always strictly positive definite, according to results in Sections 4, 5, and 6.

Figure 1 presents the smallest singular value  $\sigma_k$  over time for all three algorithms, across varying time step-sizes. These plots also include the corresponding two quantities (19) and (37). We observe that in all cases, the smallest singular value  $\sigma_k$  of the discretized DLR solutions is lower bounded by (19) and (37); this behavior supports Propositions 4.1, 4.5, 5.2, and 6.2.

On the left panel of Figure 2, the singular values of the true solution  $X^{\text{true}}$  are shown, while its right panel illustrates the  $L^2$  strong errors between each discretization method of Sections 3 and the exact solution of  $X^{\text{true}}$  or its continuous DLRA. The reference  $X^{\text{true}}$  and the continuous DLR solutions have been computed with  $\Delta t = 1 \cdot 10^{-2}$ . We notice that  $\sigma_3(\mathbb{E}[X^{\text{true}}(t)(X^{\text{true}})^\top(t)])$  approaches  $10^{-9}$  almost immediately and continued to be constant over time, where  $\sigma_2(\mathbb{E}[X^{\text{true}}(t)(X^{\text{true}})^\top(t)])$  slowly increases over time. Consequently, the decision to employ DLRA algorithms with rank  $k = 2$  is motivated by numerical evidences, too. In Figure 2 we notice that the rank-2 DLRA discretization still manages to retrieve the pathwise convergence over  $\Delta t$  for all the algorithms, with the Projector Splitting methods that seem to converge over time with a smaller constant than the DLR Euler-Maruyama. This empirical observation is consistent with Theorems 4.7, 5.3, and 6.3.

It is worth noticing that Equation (68) has a linear deterministic drift. In this case, the deterministic modes of the DLR Euler-Maruyama evolve independently of the Gramian  $C_{Y_n}$  (see (11)). Therefore, in this setting the DLR Euler-Maruyama is not affected by the smallest singular value, too. To provide numerical evidence of this property let us consider a slight modification of the problem, given by

$$\begin{pmatrix} dX_1^{\text{true}}(t) \\ dX_2^{\text{true}}(t) \\ dX_3^{\text{true}}(t) \end{pmatrix} = \begin{pmatrix} -0.1 \cdot X_1^{\text{true}}(t) & 0.1 \cdot X_2^{\text{true}}(t) & 0.001 \cdot X_3^{\text{true}}(t) \\ -0.1 \cdot X_1^{\text{true}}(t) & 0.1 \cdot X_2^{\text{true}}(t) & 0.001 \cdot X_3^{\text{true}}(t) \\ -4 \cdot X_1^{\text{true}}(t) & -4 \cdot X_2^{\text{true}}(t) & -4 \cdot X_3^{\text{true}}(t) \end{pmatrix} dt \\ + \sqrt{\sigma_B} \begin{bmatrix} 1 & 0 & 0 \\ 0 & 1 & 0 \\ 0 & 0 & 0 \end{bmatrix} \cdot \begin{pmatrix} dW_1(t) \\ dW_2(t) \\ dW_3(t) \end{pmatrix} \quad (69)$$

with  $t \in [0, 10]$ . The initial datum is given by the random vector of component  $X_i^{\text{true}}(0) = 0.1 - \text{Un}_i$ , for  $i = 1, 2$ , where  $\text{Un}_1$  is a uniform random variable taking values in the interval  $[-0.0001, 0.0001]$ , whereas  $\text{Un}_2$  is a uniform random variable, independent of  $\text{Un}_1$ , taking values in the interval  $[-10^{-9}, 10^{-9}]$ . Therefore, the initial condition  $X^{\text{true}}$  has rank equal

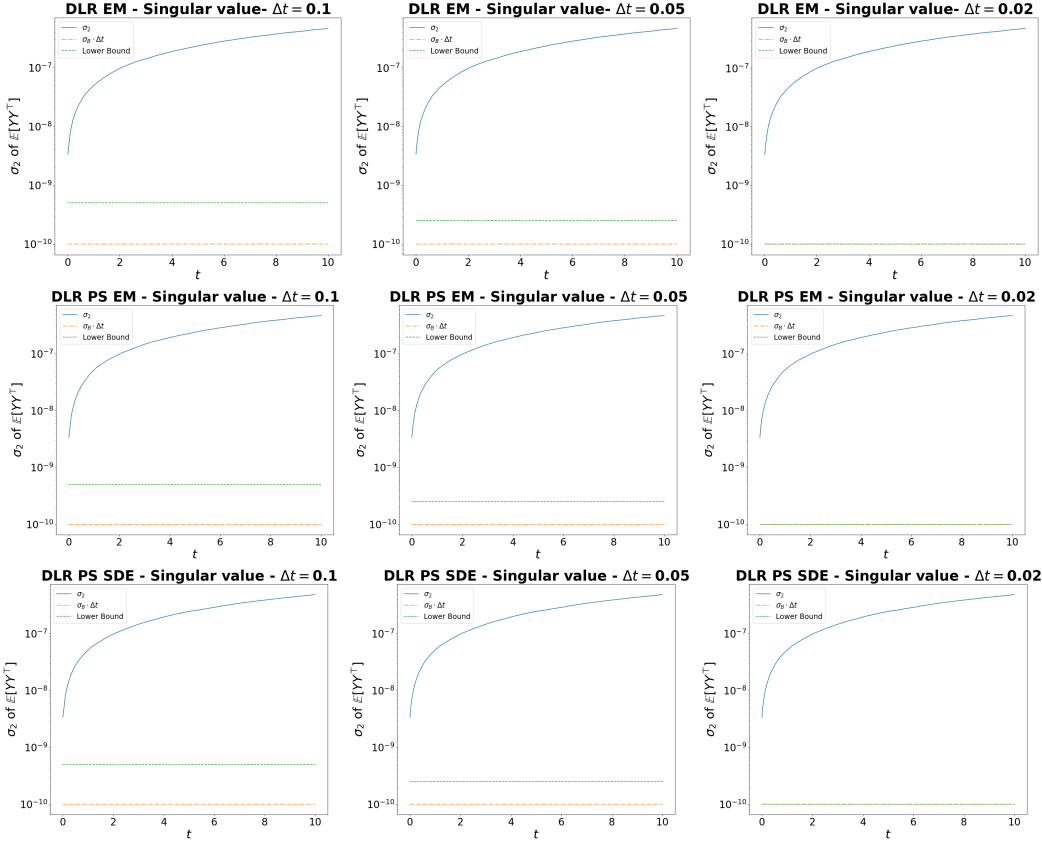


Figure 1: For  $\Delta t = 0.1, 0.05, 0.02$ ,  $k = 2$ ,  $M = 10000$ ,  $\sigma_B = 10^{-8}$  for (68). (Top) Smallest singular values of  $\mathbb{E}[Y_n Y_n^\top]$  for the DLR Euler-Maruyama, (Center) for the DLR Projector Splitting for EM, (Bottom) for the DLR Projector Splitting for SDEs. Lower bounds of  $\sigma_k$  refer to (37), (54), and (65) for all the three algorithms, respectively.

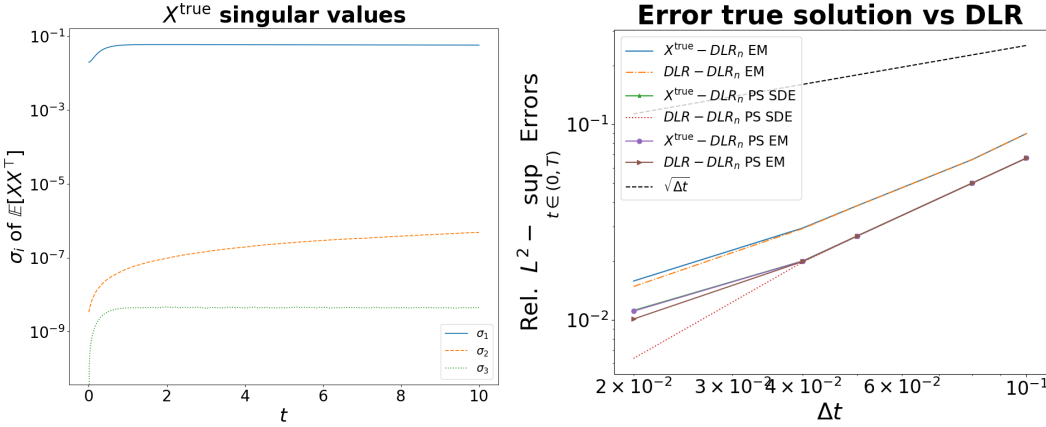


Figure 2: (Left) Singular values for the process  $X^{\text{true}}(t)$ , solution of equation (68). (Right) Relative errors for the DLR Euler-Maruyama, DLR Projector Splitting for EM, and the DLR Projector Splitting for SDEs, with respect to the true solution  $X^{\text{true}}$  and the continuous DLRA of rank  $k = 2$ .  $M = 10000$  paths are used in all methods to approximate expectations.

to 2, but close to be rank deficient. Furthermore, we choose  $\sigma_B = 10^{-19}$ , which implies the addition of noise close to the zero machine in absolute value. With these properties, (69) is assumed to be similar to a rank-1 dynamics. Indeed, in Figure 3 we illustrate the smallest singular value  $\sigma_2$  over time for all three algorithms, across varying time step-sizes, and we notice that their value is close to the zero machine.

However, one can see from the error plots (Figure 4) that this behavior of the smallest

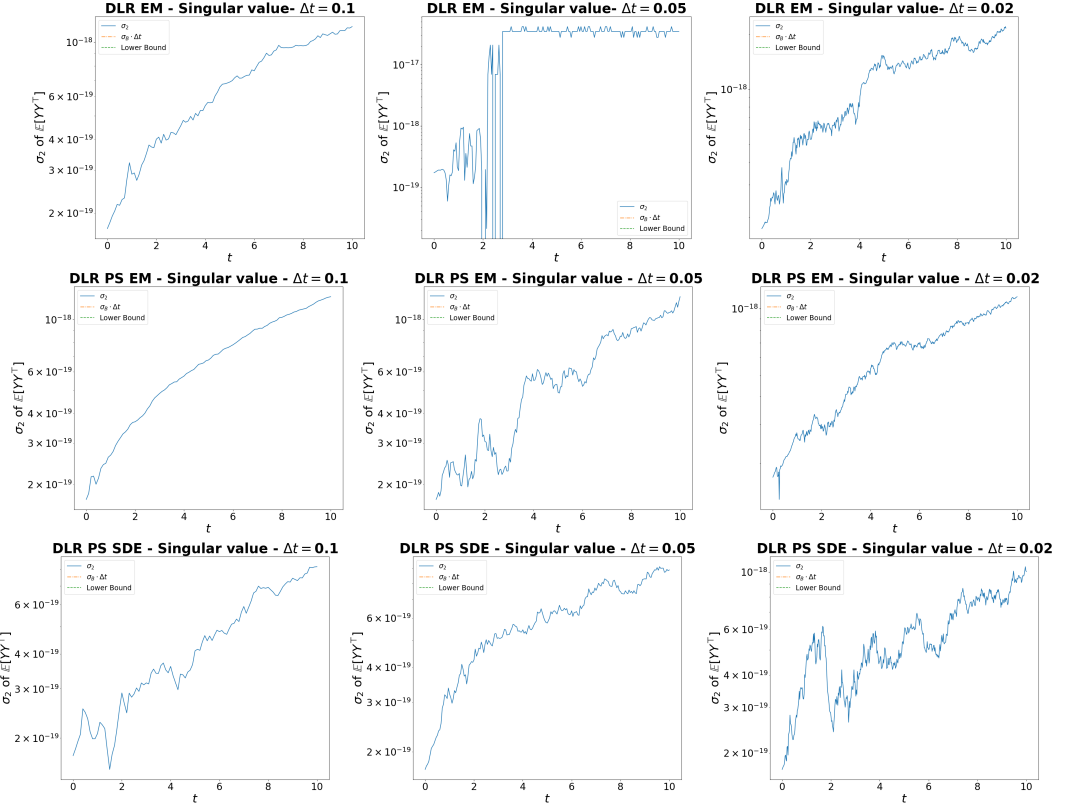


Figure 3: For  $\Delta t = 0.1, 0.05, 0.02$ ,  $k = 2$ ,  $M = 10000$ ,  $\sigma_B = 10^{-19}$ . (Top) Smallest singular values of  $\mathbb{E}[Y_n Y_n^\top]$  for the DLR Euler-Maruyama, (Center) for the DLR Projector Splitting for EM, (Bottom) for the DLR Projector Splitting for SDEs for Problem (69).

singular values of the stochastic basis does not affect the convergence of any of the algorithms. Moreover, one can notice a convergence in time of order  $o(\Delta t)$ ; this numerical trend is in compliance with usual accuracy of the standard Euler-Maruyama method for additive noise [30].

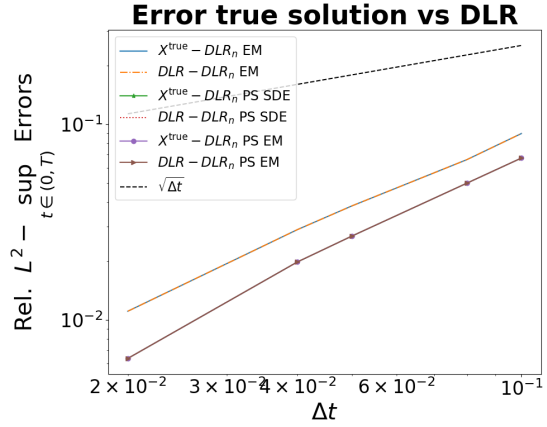


Figure 4: Relative errors for the DLR Euler-Maruyama, DLR Projector Splitting for EM, and the DLR Projector Splitting for SDEs, with respect to the true solution  $X^{\text{true}}$  and the continuous DLRA of rank  $k = 2$  for Problem (69).  $M = 10000$  paths are used in all methods to approximate expectations.

In the last example of this section, we consider a slight modification of the drift in (69) by introducing some nonlinearity. In this case, the deterministic basis  $U$  of the DLR Euler-Maruyama cannot evolve independently of the stochastic basis  $Y$ , leading to possible

instabilities in case of nearly singular Gramian  $C_{Y_n}$ . We consider the following system

$$\begin{aligned} \begin{pmatrix} dX_1^{\text{true}}(t) \\ dX_2^{\text{true}}(t) \\ dX_3^{\text{true}}(t) \end{pmatrix} &= \begin{pmatrix} -3 \cdot \sin(X_1^{\text{true}}(t)) & 0.1 \cdot X_2^{\text{true}}(t) & 0.001 \cdot X_3^{\text{true}}(t) \\ -3 \cdot \sin(X_1^{\text{true}}(t)) & 0.1 \cdot X_2^{\text{true}}(t) & 0.001 \cdot X_3^{\text{true}}(t) \\ -4 \cdot \sin(X_1^{\text{true}}(t)) & -4 \cdot X_2^{\text{true}}(t) & -4 \cdot X_3^{\text{true}}(t) \end{pmatrix} dt \\ &+ \sqrt{\sigma_B} \begin{bmatrix} 1 & 0 & 0 \\ 0 & 1 & 0 \\ 0 & 0 & 0 \end{bmatrix} \cdot \begin{pmatrix} dW_1(t) \\ dW_2(t) \\ dW_3(t) \end{pmatrix} \end{aligned} \quad (70)$$

for the exact same setting data as in (69). In Figure 5 we observe that the smallest singular value  $\sigma_2$  remains close to the zero machine for all the three algorithms, for various values of the time step-sizes. For this setting, we expect the convergence of the Euler-Maruyama to be badly affected by the inverse of  $\sigma_2$  (see Theorem 4.7), unlike the two Projector Splitting algorithms (see Theorems 5.3 and 6.4).

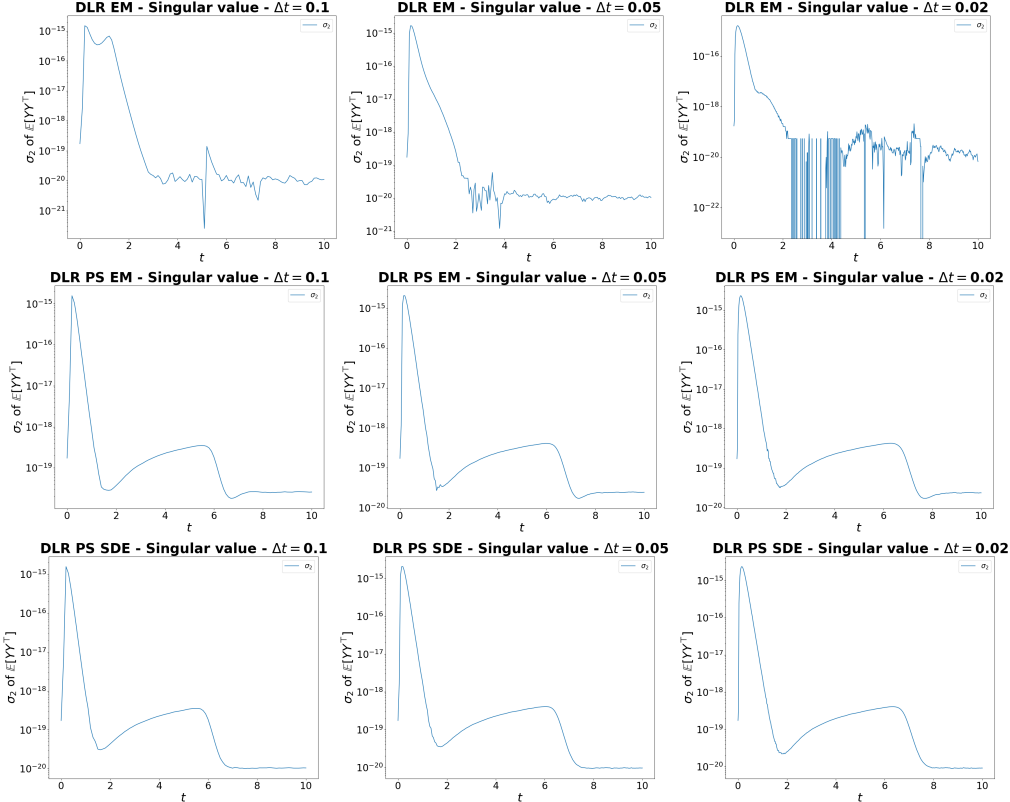


Figure 5: For  $\Delta t = 0.1, 0.05, 0.02$ ,  $k = 2$ ,  $M = 10000$ ,  $\sigma_B = 10^{-19}$ . For Problem (70) (Top) smallest singular values of  $\mathbb{E}[Y_n Y_n^\top]$  for the DLR Euler-Maruyama, (Center) for the DLR Projector Splitting for EM, (Bottom) for the DLR Projector Splitting for SDEs

Figure 6 provides numerical evidence for this behavior. Indeed, the accuracy of the DLR Euler-Maruyama is not acceptable, as it is not showing convergence over time. On the other hand, the DLR Projector Splitting for EM and SDEs present error precision unaffected by the trend of the smallest singular value  $\sigma_2$ .

## 7.2 Mean-square stability

In this section, we verify that conditions found in Sections 5.1 and 6.1 are sufficient for the mean-square stability of the studied system. We consider a process SDE  $X^{\text{true}}(t, \omega) \in \mathbb{R}^d$  for all  $\omega \in \Omega$  and  $t \in [0, +\infty)$ , whose  $i$ -th component  $X_i^{\text{true}}(t)$  satisfies the SDE

$$dX_i^{\text{true}}(t) = a_{ii} X_i^{\text{true}}(t) dt + B_i X_i^{\text{true}}(t) dW_t^i, \quad (71)$$

where  $A = (a_{ij})_{ij} \in \mathbb{R}^{d \times d}$ , with  $a_{ii} = -22$  if  $i = 1, 2, 3$ , else  $a_{ii} = -22 + 1 \sin(3\pi t)$ , and  $a_{ij} = 0$  for  $i \neq j$ , whereas  $B_i = (b_{ij})_{ij}$  with  $b_{ii} = 0.1$ , otherwise  $b_{ij} = 0$ . The initial datum

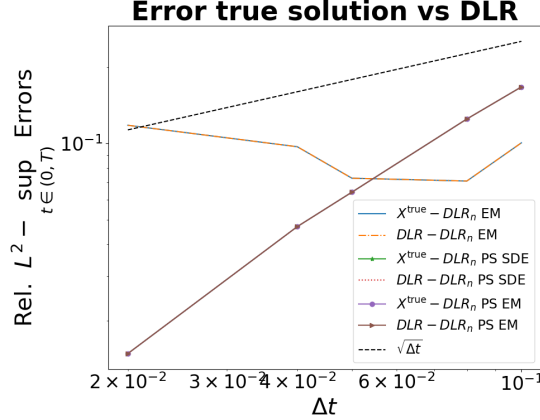


Figure 6: Relative errors for the DLR Euler-Maruyama, DLR Projector Splitting for EM, and the DLR Projector Splitting for SDEs, with respect to the true solution  $X$  and the continuous DLRA of rank  $k = 2$  for equation (70).  $M = 10000$  paths are used in all methods to approximate expectations.

is  $X_i^{\text{true}}(0) = 1 + 0.005 \sin(\pi \frac{i}{10}) \mathcal{N}_1(0, 1) + 0.005 \sin(2\pi \frac{i}{10}) \mathcal{N}_2(0, 1) + 0.005 \sin(3\pi \frac{i}{10}) \mathcal{N}_3(0, 1)$ , where  $\mathcal{N}_1(0, 1)$ ,  $\mathcal{N}_2(0, 1)$ ,  $\mathcal{N}_3(0, 1)$  are independent standard normal random variables. Moreover,  $\{W_t^i\}_i$  are independent Brownian motions, also independent of the initial condition  $X^{\text{true}}(0)$ . Then, the stability condition on  $\Delta t$  for the (standard) Euler-Maruyama for SDE, the DLR Projector Splitting for EM and the DLR Projector Splitting for SDEs applied to (71) is

$$\Delta t \leq \frac{-\lambda_{\max}(A(t_n) + A^\top(t_n)) - \sum_{k=1}^m |B_k(t_n)|^2}{\sigma_{\max}(A(t_n))} \approx 0.0907 \quad (72)$$

We initialize all the DLR algorithms as described in Section 7.1. Figures 7, 8, and 9 show the trend of the second moment through time for  $\Delta t = 0.0907$ ,  $\Delta t = 0.0909$ ,  $\Delta t = 0.0911$ , respectively. Figure 7 shows that the tendency of the second moment seems to be numerically stable as expected, as the chosen  $\Delta t$  satisfies (72). Instead, Figure 8 illustrates that the DLR EM Algorithm is not stable when the (72) is violated, unlike the other two projection-method procedures. This behavior highlights the superior stability of the Projector Splitting methods. However, Figure 9 tells us that (72) is pretty sharp, as for  $\Delta t = 0.0911$ , whose value is higher than (72), all algorithms do not converge to the null solution.

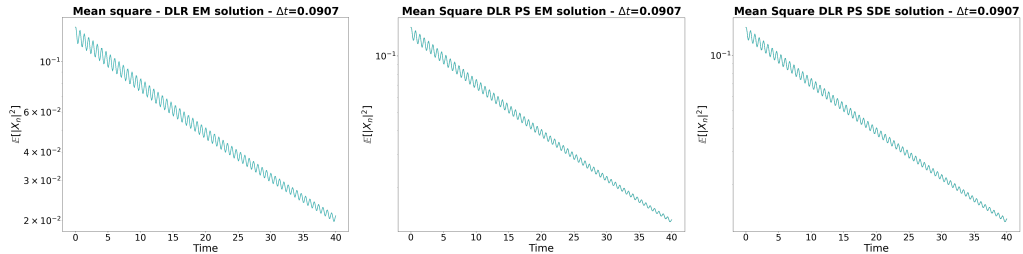


Figure 7: For  $\Delta t = 0.0907$ , for equation (71) (Left) Mean-square norm of the numerical solution  $X_n$ , i.e.  $\mathbb{E}[|X_n|^2]$ , for the DLR Euler-Maruyama, (Center) for the DLR Projector Splitting for EM, (Right) for the DLR Projector Splitting for SDEs,  $M = 2000$  paths.

### 7.3 Additive Noise: Stochastic Advection-Diffusion-Reaction PDE in 1D

In this section, we provide a numerical example consisting of a one-dimensional advection-diffusion-reaction system under low-rank additive diffusion suitably discretized in space, and we want to test the numerical convergence of the three algorithms and conditions on the

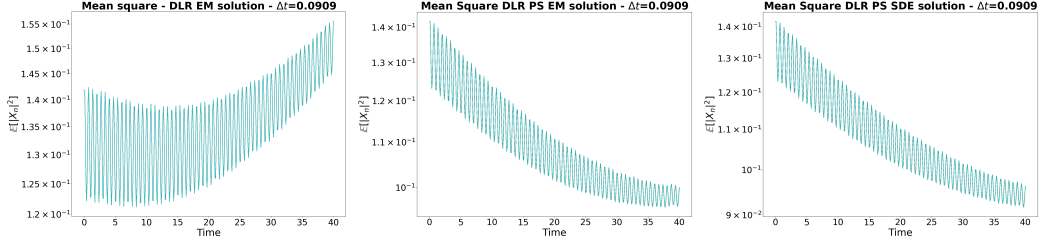


Figure 8: For  $\Delta t = 0.0909$ , for equation (71) (Left) Mean-square norm of the numerical solution  $X_n$ , i.e.  $\mathbb{E}[|X_n|^2]$ , for the DLR Euler-Maruyama, (Center) for the DLR Projector Splitting for EM, (Right) for the DLR Projector Splitting for SDEs,  $M = 2000$  paths.

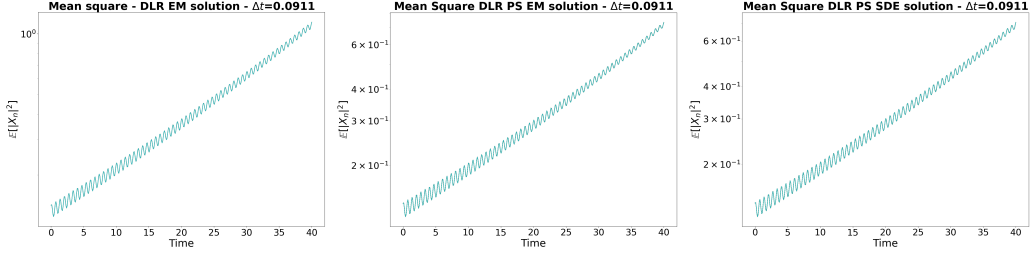


Figure 9: For  $\Delta t = 0.0911$ , for equation (71) (Left) Mean-square norm of the numerical solution  $X_n$ , i.e.  $\mathbb{E}[|X_n|^2]$ , for the DLR Euler-Maruyama, (Center) for the DLR Projector Splitting for EM, (Right) for the DLR Projector Splitting for SDEs,  $M = 2000$  paths.

time step based on the smallest singular values of the Gramian of the stochastic basis  $Y_n$ . The spatial domain is  $[0, L]$  with  $L = 1$ , where we consider Neumann boundary conditions, while the temporal domain is  $[0, T]$ , with  $T = 10$ . The studied equation is the following

$$\begin{cases} \partial_t u(x, t, \omega) = Lu(x, t, \omega) + \sum_{i=1}^m \phi_i(x) \dot{W}^i(\omega), & (x, t, \omega) \in [0, L] \times [0, T] \times \Omega, \\ u_0(x, \omega) = \sum_{i=1}^m \frac{1}{(2\pi i)^2} \sin\left(\frac{\pi(i+1)x}{L}\right) (0.5 - \text{Un}_i(-10^{-4}, 10^{-4})), & (x, \omega) \in [0, L] \times \Omega \\ \partial_x u(0, t, \omega) = \partial_x u(1, t, \omega) = 0, & (t, \omega) \in [0, T] \times \Omega, \end{cases} \quad (73)$$

where in (73) the linear operator  $L$  is given by  $Lu(x, t, \omega) = a\partial_x^2 u(x, t, \omega) - v\partial_x u(x, t, \omega) + r \sin(u(x, t, \omega))$ ,  $\{\text{Un}_i(-10^{-4}, 10^{-4})\}_{i=1, \dots, m}$  are i.i.d. uniform random variables in  $[0, 1]$  independent of the one-dimensional Brownian motions  $(W^i)_{i=1, \dots, m}$ ,  $a = 0.005$ ,  $v = 0.3$ , and  $r = 0.1$ . Concerning the diffusion term, we set  $\phi_i(x) = 0.5 \sin(\frac{i\pi x}{L})$  for all  $i = 1, \dots, m$ . We discretize in space (73) by second order centered finite differences, with a first order upwinding treatment of the advection term, using a uniform grid with mesh size  $dx = 0.04$ . Therefore, the physical dimension is  $d = 25$ . The time discretization for the reference true solution  $u$  of (73) is made with forward Euler-Maruyama with mesh size  $\Delta t = 2 \cdot 10^{-3}$ . The number of paths simulated is  $M = 2000$ . We choose  $m = 5$  and, as the initial condition and the noise increments are i.i.d., we employ a DLR approximation of rank  $k = 18$ . Moreover, we initiate all the DLRA algorithms as described in Section 7.1. Notice that with this choice of the rank we would overapproximate the number of stochastic components, given by the initial condition and by the noise term, that affect the system. Moreover, the reaction term is not linear and, hence, the DLR Euler-Maruyama algorithm will follow (7) as evolution equation for its deterministic basis, and not (11). With this construction, we expect that this algorithm would not be numerically stable and its error accuracy would be worse than the other two staggered methods.

Indeed, we recall that the convergence of the DLR Euler-Maruyama may deteriorate if  $\Delta t$  is not sufficiently small relatively to the smallest singular value of  $\mathbb{E}[Y_n Y_n^\top]$ ; see Theorem 4.7, which requires the condition (28) on  $\Delta t$  for convergence in time. In contrast, the DLR Projector Splitting methods do not require such a condition to ensure convergence; see Theorems 5.3, and 6.3. We aim to illustrate this numerically. To this end, in Figures 14,

15, and 16 we plot the following quantity related to (28)

$$\widehat{\Delta t_n} := \frac{\sqrt{\sigma_n^k}}{\sqrt{C_{\text{lgb}}} \sqrt{(1 + \sup_{n \in \{1, \dots, N\}} \mathbb{E}[|X_n|^2])}}, \quad (74)$$

where we recall that  $\sigma_n^k$  is the  $k$ -th singular value (the smallest) of the Gramian  $C_{Y_n}$ . Notice that the constraint (74) is less restrictive than (28) which uses, instead an a priori upper bound on  $\sup_{n \in \{1, \dots, N\}} \mathbb{E}[|X_n|^2]$ .

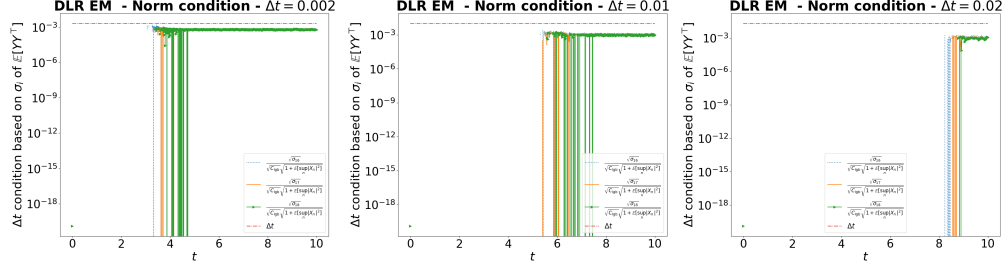


Figure 10: Condition (74) related to the square root of the singular values  $\sigma_i$  of the Gramian  $\mathbb{E}[X_n X_n^\top]$  for DLR Euler-Maruyama with  $\Delta t = 0.002, 0.01, 0.02$  for equation (73).

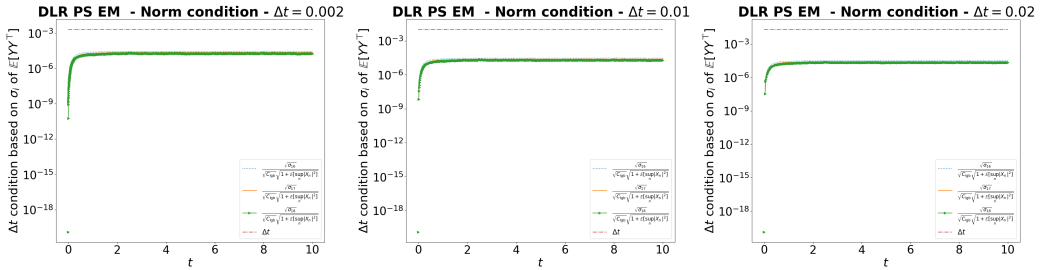


Figure 11: Condition (74) related to the square root of the singular values  $\sigma_i$  of the Gramian  $\mathbb{E}[X_n X_n^\top]$  for DLR Projector Splitting for EM with  $\Delta t = 0.002, 0.01, 0.02$  for equation (73).

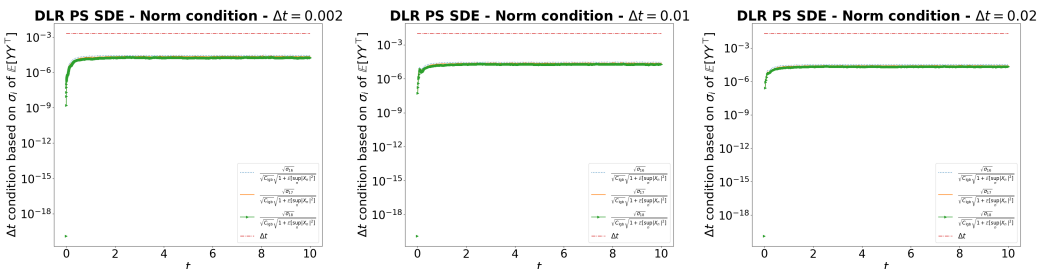


Figure 12: Condition (74) related to the square root of the singular values  $\sigma_i$  of the Gramian  $\mathbb{E}[X_n X_n^\top]$  for DLR Projector Splitting for SDEs with  $\Delta t = 0.002, 0.01, 0.02$  for equation (73).

Figures 10, 11 and 12 show how the quantity in (74), related to the square root of the  $i$ -th largest singular value  $\sigma_i$  of the Gramian  $\mathbb{E}[Y_n Y_n^\top]$ , evolves over time, with  $\Delta t$  held fixed in each case, but varying across the plots. Figure 10 corresponds to the DLR Euler-Maruyama method, Figure 11 to the DLR Projector Splitting for EM, and Figure 12 to the DLR Projector Splitting for SDEs. In all cases, we see that the time-step does not always satisfy (74) in  $[0, T]$ , which we interpret as a violation of the condition (28). Therefore, we expect that the DLR Euler-Maruyama method presents a not-sharp accuracy, unlike the two other staggered methods, which are theoretically unaffected by condition (28).

In Figure 13, we show the relative errors between the DLR algorithms and the continuous DLRA or the true solution for different values of  $\Delta t$ . Projection-based methods, Algorithms

2 and 3, appear to be more accurate than the DLR Euler-Maruyama scheme. This trend supports Theorems 4.7, 5.3, and 6.3. Moreover, we notice that Algorithm 2 has smaller error with respect to the true solution unlike the DLR Projector Splitting for SDEs. This trend may motivate further investigation of the theoretical convergence of Algorithm 2.

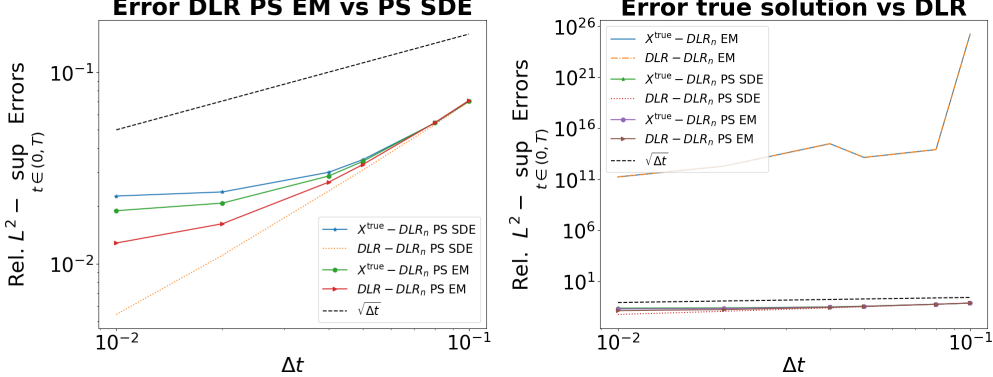


Figure 13: Rel. errors in  $L^2 - \sup_{t \in [0, T]}$  norm for equation (73),  $k = 18$ ,  $M = 2000$  paths, (Blue (—)) error between the true solution and the DLRA algorithms and between the continuous DLR and the DLRA algorithms

## 7.4 Multiplicative noise: Stochastic Laplacian in 1D

In this numerical example we consider a stochastic Laplacian problem in 1D with Dirichlet boundary conditions under multiplicative colored noise. Like the previous section, we want to test the numerical convergence of the three algorithms and their dependence on the smallest singular values of the Gramian of the stochastic basis. We will see that the numerical results validate once again the theoretical statements (Theorems 4.7, 5.3, and 6.3) in the case of multiplicative noise, too. The spatial domain is  $[0, 1]$ , while the temporal domain is  $[0, T]$ , with  $T = 10$ . More precisely, we aim to find the numerical solution of the following system:

$$\begin{cases} \partial_t u(x, t, \omega) = 0.001 \cdot \Delta u(x, t, \omega) + F(x, t) + G(u, x) \dot{W}(\omega), & (x, t, \omega) \in [0, 1] \times [0, 10] \times \Omega, \\ u_0(x, \omega) = \sum_{\ell=1}^{13} \sin(\pi \ell x) \cdot \mathcal{N}_\ell(0, 1)(\omega) + 8 \cdot 10^{-7} \sin(8\pi x) \cdot \mathcal{N}_{14}(0, 1)(\omega), & (x, \omega) \in [0, 1] \times \Omega \\ u(0, t, \omega) = u(1, t, \omega) = 0, & (t, \omega) \in [0, 4] \times \Omega. \end{cases} \quad (75)$$

In (75),  $\{\mathcal{N}_\ell(0, 1)\}_{\ell=1, \dots, 14}$ , are i.i.d. normal random variables, while  $GdW$  represents a colored noise in space, which is rough in time, defined as

$$G(u, x) dW(\omega) = \sum_{\ell=1}^N \gamma_\ell \langle u(x, t, \omega), \cos(2\pi \ell x) + \sin(2\pi \ell x) \rangle_{L^2(0, 1)} dW_t^\ell(\omega),$$

where  $W_t^\ell$ , for  $\ell \in \{1, \dots, N\}$ , are independent Brownian motions, also independent of the initial condition  $u_0$ , with  $\gamma_\ell = \frac{1}{2\pi\ell} \exp^{-2\pi\ell}$  and  $N = 26$ . The deterministic force term  $F(t)$  is an even periodic function defined as

$$F(x, t) = \begin{cases} 3, & x \in ]vt, l + vt[, \quad \text{if } t \leq \frac{1-l}{v}, \\ 0, & x \notin ]vt, l + vt[, \quad \text{if } t \leq \frac{1-l}{v}, \end{cases} \quad (76)$$

with  $l = 0.12$ ,  $v = 0.4$ , and with period  $\bar{T} = 2(\frac{1-l}{v}) = 2.2$ . To approximate  $u$ , we consider a DLR solution  $X$  of rank  $k = 14$ , simulating  $M = 2200$  paths. This choice of the rank has been made considering the rank of the initial condition. We highlight that in  $u_0$  the term  $8 \cdot 10^{-7} \sin(8\pi x) \cdot \mathcal{N}_{14}(0, 1)(\omega)$  is nearly negligible and it may cause problems of overapproximation. Moreover, notice that (75) is well posed in the sense of mild solutions [7, Theorem 6.7].

We discretize the laplacian operator  $\Delta$  using centered finite differences for each fixed path  $\omega$  on a uniform mesh  $\{(ih); i \in \{0, \dots, N\} : Nh = 1\}$  with mesh size  $h = 0.04$

$$\Delta u(ih, \omega) \approx \frac{u((i-1)h, \omega) - 2 \cdot u(ih, \omega) + u((i+1)h, \omega)}{h^2}.$$

This leads to a SDE of dimension  $d = 26$ , as we count the boundary points, too, to which we apply the different DLRA algorithms. We initiate all the DLRA procedures as described in Section 7.1. The time discretization for the reference true solution  $u$  of (75) and the continuous DLR are made with forward Euler-Maruyama and DLR Projector Splitting for SDEs, respectively, with mesh size  $\Delta t = 2.5 \cdot 10^{-3}$ .

Also in this example, we show in Figures 14, 15, and 16 the quantity (74) related to the  $i$ -th largest singular values  $\sigma_i$  of the Gramian  $\mathbb{E}[Y_n Y_n^\top]$  for all the three algorithms over time. We consider these plots to understand if the condition on  $\Delta t$  for the numerical boundedness of the solution is satisfied and if the error accuracy remains unaffected by the smallest singular values.

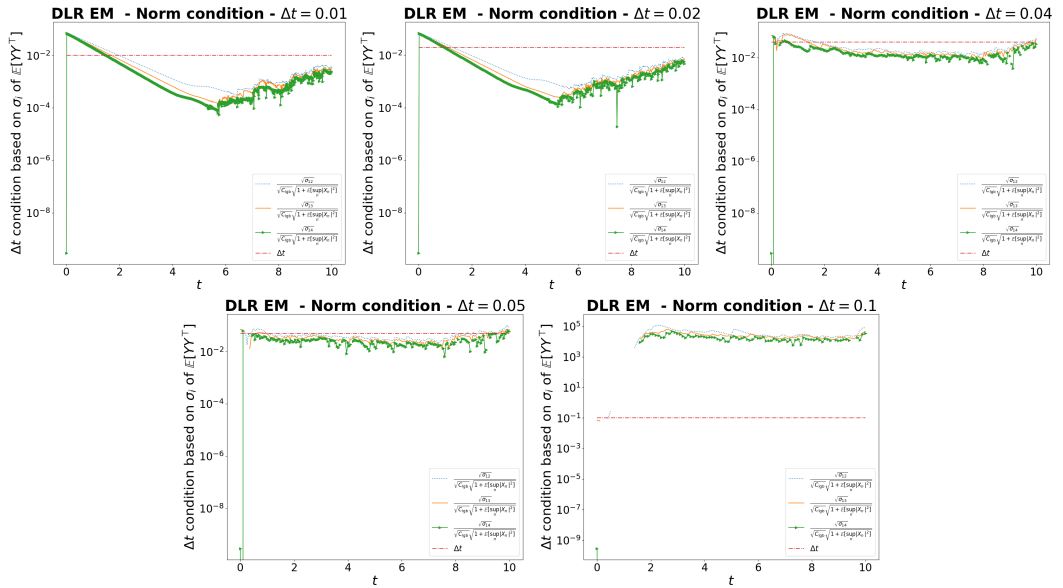


Figure 14: Condition (74) related to the square root of the singular values  $\sigma_i$  of the Gramian  $\mathbb{E}[X_n X_n^\top]$  for DLR Euler-Maruyama with  $\Delta t = 0.01, 0.02, 0.04, 0.05, 0.1$  for Problem (75).

Figures 14, 15, and 16 illustrate that the time step does not always satisfy (74) in  $[0, T]$ . Again, we judge this behavior as a violation of the condition (28) and we expect that the DLR Euler-Maruyama would not present sharp error decay over time, unlike the two Projector Splitting methods.

Figure 17 presents relative errors between the DLRA algorithms and the continuous DLRA and the true solution for different values of  $\Delta t$ . We observe that the projector-based methods, Algorithms 2 and 3, are unaffected by condition (28) and their convergence to the true solution  $X^{\text{true}}$  is not influenced by the smallest singular value of the Gramian matrix of the stochastic basis, as stated in Theorems 5.3 and 6.3. On the other hand, the DLR Euler-Maruyama presents a huge constant multiplying the convergence rate in time. This numerical behavior supports Theorem 4.7.

## 8 Conclusion

In the first part of this work, we proposed three numerical schemes to discretize DLRA for SDEs. The first scheme was built by discretizing both the deterministic and stochastic modes forward in time, followed by an orthonormalization procedure applied to the deterministic modes. Despite this final nonlinear operation, it turned out that this algorithm is convergent. However, its convergence depends on a time step condition involving the smallest singular value of the Gramian matrix of the stochastic modes. If this condition is not met, the DLRA

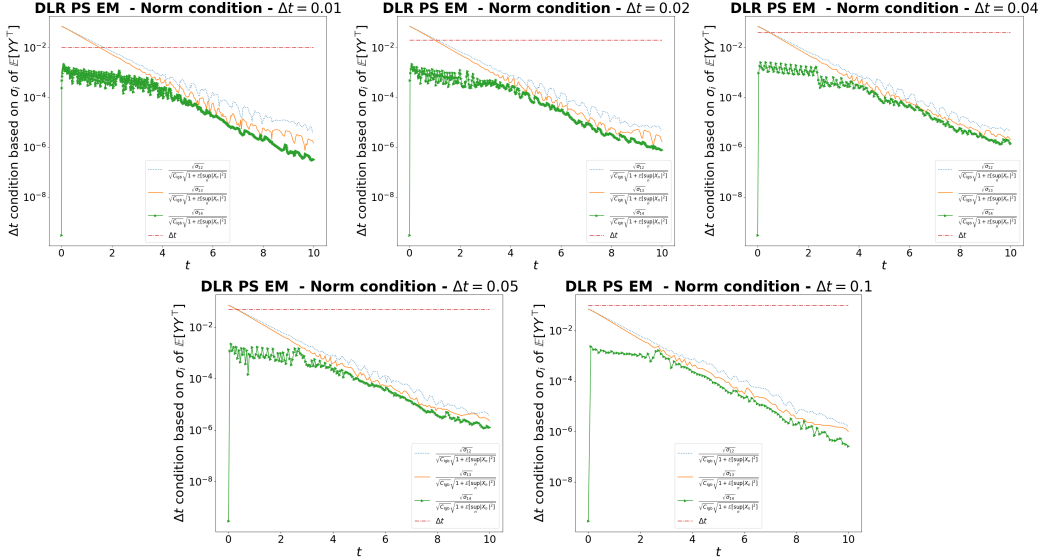


Figure 15: Condition (74) related to the square root of the singular values  $\sigma_i$  of the Gramian  $\mathbb{E}[X_n X_n^\top]$  for DLR Projector Splitting for EM with  $\Delta t = 0.01, 0.02, 0.04, 0.05, 0.1$  for the Problem (75).

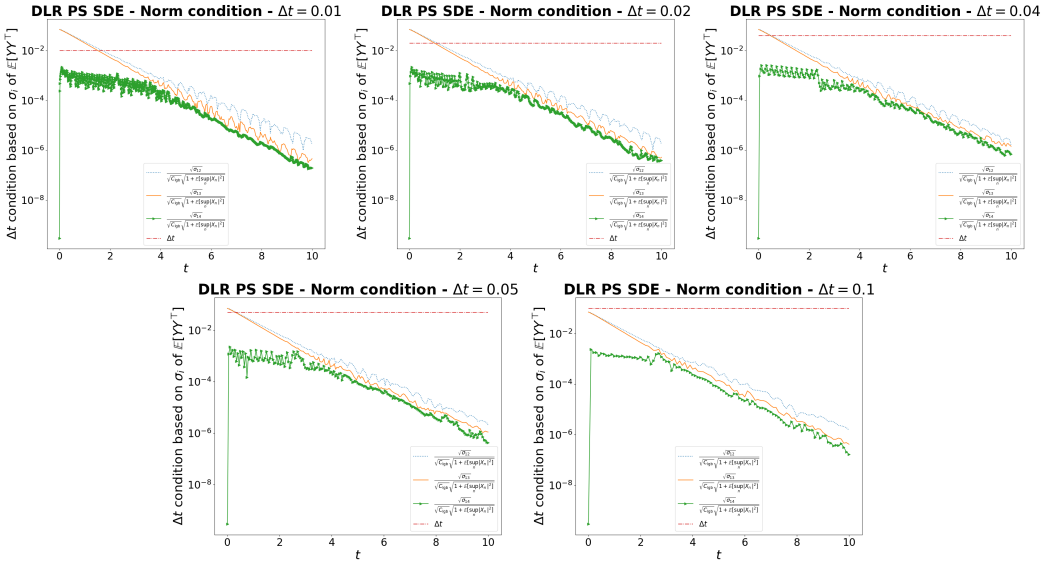


Figure 16: Condition (74) related to the square root of the singular values  $\sigma_i$  of the Gramian  $\mathbb{E}[X_n X_n^\top]$  for DLR Projector Splitting for SDEs with  $\Delta t = 0.01, 0.02, 0.04, 0.05, 0.1$  for the Problem (75).

may not be accurate, as also our numerical experiments show. Under the same condition, in a bounded interval of time, we proved that the Gramian of the stochastic modes is always lower-bounded in a matrix sense by a strictly positive constant if the noisy diffusion is strictly positive in the same sense. This result is consistent with the theory of DLRA for SDEs, as in the continuous case the Gramian satisfies this lower bound under the same condition on the diffusion [18].

The second and the third discretization procedures consist in evolving the stochastic modes forward in time via a standard Euler-Maruyama method (as in the previous scheme), whereas the deterministic modes are computed using the just-evaluated stochastic components before the orthonormalization. These algorithms differ in the arguments inside the expectation present in the equation of the modes: the former involved both drift and diffusion increments, the latter only the drift. Even without the aforementioned time-step condition, both methods converge to the true solution with a similar accuracy to the former

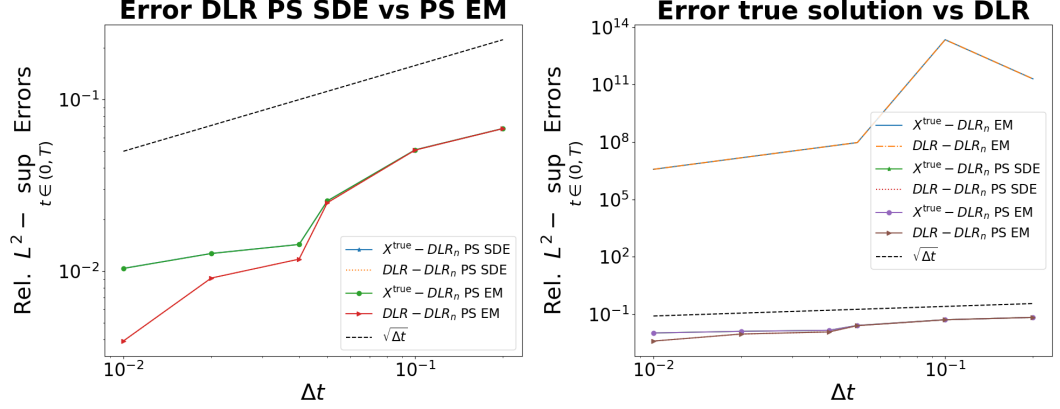


Figure 17: Rel. errors in  $L^2 - \sup_{t \in [0, T]} \text{Errors}$  for the Problem (75),  $k = 14$ ,  $M = 2200$  paths, (Blue (—)) error between the true solution and the DLRA algorithms and between the continuous DLRA and the DLRA algorithms

and continue to satisfy the previously stated lower-boundedness property of the Gramian. Their similar convergence behavior in time is further supported by numerical simulations.

Among possible directions of research, an in-depth theoretical analysis of the mean-square stability of the DLR Euler-Maruyama for Equation (55) can be of interest. Indeed, in this case the method takes the form

$$\begin{aligned}
 X_{n+1} = & X_n + A(t_n)X_n\Delta t_n + U_n^\top U_n \sum_{k=1}^m B_k(t_n)X_n\Delta W_n^k, \\
 & + (I_{d \times d} - U_n^\top U_n) A(t_n)U_n^\top U_n A(t)X_n(\Delta t_n)^2 \\
 & + (I_{d \times d} - U_n^\top U_n) A(t)U_n^\top U_n \left( \sum_{k=1}^m B_k(t_n)X_n\Delta W_n^k \right) \Delta t_n,
 \end{aligned} \tag{77}$$

which is not affected by the smallest singular value (see (11)) and whose second moment can be bounded in the following way

$$\begin{aligned}
 \mathbb{E}[|X_{n+1}|^2] \leq & \mathbb{E}[|X_n|^2] \left( 1 + \lambda_{\max}(A(t_n) + A^\top(t_n))\Delta t_n + \sigma_{\max}^2(A(t_n))(\Delta t_n)^2 \right. \\
 & + \lambda_{\max} \left( A^\top(t_n) (I - U_n^\top U_n) A(t_n)U_n^\top U_n A(t_n) \right. \\
 & \left. \left. + A^\top(t_n)U_n^\top U_n A^\top(t_n) (I - U_n^\top U_n) A(t_n) \right) (\Delta t_n)^3 \right. \\
 & \left. + \sigma_{\max}^2(A(t_n))^4(\Delta t_n)^4 + \sigma_{\max}^2(A(t)) \sum_{k=1}^m |B_k(t_n)|^2(\Delta t_n)^3 + \sum_{k=1}^m |B_k(t_n)|^2\Delta t_n \right).
 \end{aligned} \tag{78}$$

However, it is not immediately clear how to interpret (78) and how to compare it with the stability conditions of the other two schemes. In addition, further investigation should be conducted to obtain sharper results concerning the convergence of the DLR Projector Splitting for EM.

To conclude this paper, we note that all the analyses done in this first part always assumes exact expectations for Algorithms 1, 2, and 3. In the second part of this work [19] these three procedures will be analyzed with a focus of discretizing the probability measure using a Monte Carlo method.

## Acknowledgements

FN and FZ were supported by the Swiss National Science Foundation under the Project n. 2000518 “Dynamical low rank methods for uncertainty quantification and data assimilation”.

## References

- [1] Edward Allen. *Modeling with Itô stochastic differential equations*. Vol. 22. Springer Science & Business Media, 2007.
- [2] Ludwig Arnold. *Stochastic differential equations*. John Wiley, New York (NY), 1974.
- [3] Markus Bachmayr, Henrik Eisenmann, Emil Kieri, and André Uschmajew. “Existence of dynamical low-rank approximations to parabolic problems”. In: *Mathematics of Computation* 90.330 (2021), pp. 1799–1830.
- [4] Benjamin Carrel, Daniel Kressner, Hei Yin Lam, and Bart Vandereycken. “Interpolatory Dynamical Low-Rank Approximation: Theoretical Foundations and Algorithms”. In: *arXiv preprint arXiv:2510.19518* (2025).
- [5] Gianluca Ceruti, Jonas Kusch, and Christian Lubich. “A rank-adaptive robust integrator for dynamical low-rank approximation”. In: *BIT Numerical Mathematics* (2022), pp. 1–26.
- [6] Gianluca Ceruti and Christian Lubich. “An unconventional robust integrator for dynamical low-rank approximation”. In: *BIT Numerical Mathematics* 62.1 (2022), pp. 23–44.
- [7] Giuseppe Da Prato and Jerzy Zabczyk. *Stochastic equations in infinite dimensions*. Vol. 152. Cambridge university press, 2014.
- [8] Lukas Einkemmer and Christian Lubich. “A low-rank projector-splitting integrator for the Vlasov–Poisson equation”. In: *SIAM Journal on Scientific Computing* 40.5 (2018), B1330–B1360.
- [9] Lukas Einkemmer, Alexander Ostermann, and Carmela Scalzone. “A robust and conservative dynamical low-rank algorithm”. In: *Journal of Computational Physics* 484 (2023), p. 112060.
- [10] Antonio Falcó, Wolfgang Hackbusch, and Anthony Nouy. “On the Dirac–Frenkel variational principle on tensor Banach spaces”. In: *Foundations of computational mathematics* 19 (2019), pp. 159–204.
- [11] Christian Franzke, Andrew J Majda, and Eric Vanden-Eijnden. “Low-order stochastic mode reduction for a realistic barotropic model climate”. In: *Journal of the atmospheric sciences* 62.6 (2005), pp. 1722–1745.
- [12] Tobias Grafke and Eric Vanden-Eijnden. “Non-equilibrium transitions in multiscale systems with a bifurcating slow manifold”. In: *Journal of Statistical Mechanics: Theory and Experiment* 2017.9 (2017), p. 093208.
- [13] Jan S Hesthaven, Gianluigi Rozza, Benjamin Stamm, et al. *Certified reduced basis methods for parametrized partial differential equations*. Vol. 590. Springer.
- [14] Desmond J Higham. “A-stability and stochastic mean-square stability”. In: *BIT Numerical Mathematics* 40 (2000), pp. 404–409.
- [15] Roger A Horn and Charles R Johnson. *Matrix analysis*. Cambridge university press, 2012.
- [16] Yoshihito Kazashi and Fabio Nobile. “Existence of dynamical low rank approximations for random semi-linear evolutionary equations on the maximal interval”. In: *Stochastics and Partial Differential Equations: Analysis and Computations* 9.3 (2021), pp. 603–629.
- [17] Yoshihito Kazashi, Fabio Nobile, and Eva Vidličková. “Stability properties of a projector-splitting scheme for dynamical low rank approximation of random parabolic equations”. In: *Numerische Mathematik* 149 (2021), pp. 973–1024.
- [18] Yoshihito Kazashi, Fabio Nobile, and Fabio Zoccolan. “Dynamical low-rank approximation for stochastic differential equations”. In: *Mathematics of Computation* 94.353 (2025), pp. 1335–1375. DOI: [10.1090/mcom/3999](https://doi.org/10.1090/mcom/3999).
- [19] Yoshihito Kazashi, Fabio Nobile, and Fabio Zoccolan. “Numerical Methods for Dynamical Low-Rank Approximations of Stochastic Differential Equations - Part II: Stochastic discretization”. In preparation. 2025.

[20] Rafaïl Khasminskii. *Stochastic stability of differential equations*. Vol. 66. Springer Science & Business Media, 2011.

[21] Emil Kieri, Christian Lubich, and Hanna Walach. “Discretized dynamical low-rank approximation in the presence of small singular values”. In: *SIAM Journal on Numerical Analysis* 54.2 (2016), pp. 1020–1038.

[22] Emil Kieri and Bart Vandereycken. “Projection methods for dynamical low-rank approximation of high-dimensional problems”. In: *Computational Methods in Applied Mathematics* 19.1 (2019), pp. 73–92.

[23] Peter E Kloeden and Eckhard Platen. *Numerical Solution of Stochastic Differential Equations*. Vol. 23. Springer, Berlin, Heidelberg, New York, 1992.

[24] Othmar Koch and Christian Lubich. “Dynamical low-rank approximation”. In: *SIAM Journal on Matrix Analysis and Applications* 29.2 (2007), pp. 434–454.

[25] Jonas Kusch, Gianluca Ceruti, Lukas Einkemmer, and Martin Frank. “Dynamical Low-Rank Approximation for Burgers’ Equations with Uncertainty”. In: *International Journal for Uncertainty Quantification* 12.5 (2022).

[26] Kody Law, Andrew Stuart, and Kostas Zygalakis. *Data assimilation*. Vol. 214. Springer, Cham, Switzerland, 2015, p. 52.

[27] Christian Lubich and Ivan V Oseledets. “A projector-splitting integrator for dynamical low-rank approximation”. In: *BIT Numerical Mathematics* 54.1 (2014), pp. 171–188.

[28] Andrew J Majda, Ilya Timofeyev, and Eric Vanden Eijnden. “Models for stochastic climate prediction”. In: *Proceedings of the National Academy of Sciences* 96.26 (1999), pp. 14687–14691.

[29] Xuerong Mao. *Stochastic differential equations and applications*. Elsevier, 2007.

[30] Grigori N Milstein and Michael V Tretyakov. *Stochastic numerics for mathematical physics*. Vol. 39. Springer, 2004.

[31] Eleonora Musharbash, Fabio Nobile, and Tao Zhou. “Error analysis of the dynamically orthogonal approximation of time dependent random PDEs”. In: *SIAM Journal on Scientific Computing* 37.2 (2015), A776–A810.

[32] Grigorios A Pavliotis. *Stochastic processes and applications*. Springer, New York, NY, 2014.

[33] Donya Ramezanian, Arash G Nouri, and Hessam Babaee. “On-the-fly reduced order modeling of passive and reactive species via time-dependent manifolds”. In: *Computer Methods in Applied Mechanics and Engineering* 382 (2021), p. 113882.

[34] Martin Redmann, Christian Bayer, and Pawan Goyal. “Low-dimensional approximations of high-dimensional asset price models”. In: *SIAM Journal on Financial Mathematics* 12.1 (2021), pp. 1–28.

[35] Yoshihiro Saito and Taketomo Mitsui. “Mean-square stability of numerical schemes for stochastic differential systems”. In: *Vietnam J. Math* 30 (2002), pp. 551–560.

[36] Yoshihiro Saito and Taketomo Mitsui. “Stability Analysis of Numerical Schemes for Stochastic Differential Equations”. In: *SIAM J. Numer. Anal.* 33.6 (1996), pp. 2254–2267.

[37] Themistoklis P Sapsis and Henk A Dijkstra. “Interaction of additive noise and nonlinear dynamics in the double-gyre wind-driven ocean circulation”. In: *Journal of physical oceanography* 43.2 (2013), pp. 366–381.

[38] Themistoklis P Sapsis and Pierre FJ Lermusiaux. “Dynamically orthogonal field equations for continuous stochastic dynamical systems”. In: *Physica D: Nonlinear Phenomena* 238.23-24 (2009), pp. 2347–2360.

[39] Themistoklis P Sapsis and Andrew J Majda. “Blending modified Gaussian closure and non-Gaussian reduced subspace methods for turbulent dynamical systems”. In: *Journal of Nonlinear Science* 23 (2013), pp. 1039–1071.

[40] René L Schilling. *Brownian Motion: A Guide to Random Processes and Stochastic Calculus*. 3rd ed. De Gruyter, 2021.

- [41] Steven E Shreve et al. *Stochastic calculus for finance II: Continuous-time models*. Vol. 11. Springer, 2004.
- [42] T Tyranowski. “Data-driven structure-preserving model reduction for stochastic Hamiltonian systems”. In: *Journal of Computational Dynamics* 11.2 (2024), pp. 220–255.
- [43] Yuxiao Wen, Eric Vanden-Eijnden, and Benjamin Peherstorfer. “Coupling parameter and particle dynamics for adaptive sampling in Neural Galerkin schemes”. In: *Physica D: Nonlinear Phenomena* 462 (2024), p. 134129.